ISSN 1831-9424

European Commission

EU harmonised test method: polarisation curve measurement of high-temperature fuel cell and steam electrolyser

Current-voltage characteristics of solid oxide and proton-conducting ceramic cell/stack assembly units

Malkow, T., Pilenga, A.

2025

Contact information
Name: Thomas Malkow
Address: European Commission, Joint Research Centre, Westerduinweg 3, 1755 LE Petten, The Netherlands
Email: Thomas.Malkow@ec.europa.eu
Tel.: +31 224 56 56 56

EU Science Hub
https://joint-research-centre.ec.europa.eu

JRC134834

EUR 40115 EN

PDF	ISBN 978-92-68-22168-6	ISSN 1831-9424	doi:10.2760/0463992	KJ-01-24-150-EN-N
Print	ISBN 978-92-68-22169-3	ISSN 1018-5593	doi:10.2760/4494305	KJ-01-24-150-EN-C

Luxembourg: Publications Office of the European Union, 2025

How to cite this report: Malkow, T., Pilenga, A., *EU harmonised test method: polarisation curve measurement of high-temperature fuel cell and steam electrolyser*, Publications Office of the European Union, Luxembourg, 2025, https://data.europa.eu/doi/10.2760/0463992, JRC134834.

Contents

Abstract

This document outlines a test method for determining the current-voltage (I-U) characteristics of solid oxide cells and proton-conducting ceramic cells and stacks, operating in either fuel cell mode or electrolysis mode. The primary objective is to establish a commonly accepted method for characterising the performance of such cells and stacks using polarisation curve measurements.

The primary objective of this method is to establish a widely accepted protocol for characterising the performance of such cells and stacks using polarisation curve measurements.

The application of this test method enables an objective evaluation of the performance of various cells and stacks, facilitating meaningful technology comparison. It serves as a benchmark measurement for qualifying a cell or stack in a given application. Furthermore, it may play a role in quality control and quality assurance of cell and stack assembly units.

This test method is intended for use by both the research community and industry. Its application extends to evaluating research and development advancements, establishing priorities in research and innovation, encompassing cost objectives, developmental milestones, and technological benchmarks. Moreover, it empowers stakeholders to make informed decisions concerning technology selection.

Foreword

This report is an update of the Test Module (TM) 03 "Current-Voltage Characteristics" (de Marco *et al.*, 2017) orginally developed by the Solid Oxide Cell and Stack Testing, Safety and Quality Assurance (SOCTES^{QA}) research project (DLR, 2014), which was funded by the Fuel Cells and Hydrogen Joint Undertaking (FCHJU). It combines the test method for polarisation curve measurements of cell/stack assembly units in a single coherent document applicable to high-temperature fuel cells (HTFCs) of solid oxide type and proton-conducting ceramic type, and high-temperature steam electrolysers (HTSEs) of solid oxide electrolyser (SOE) type and protonic ceramic electrolyser (PCE) type.

The drafting of this report was carried out under the framework contract between the Directorate-General Joint Research Centre (JRC) of the European Commission (EC) and the Clean Hydrogen Joint Undertaking (Clean H_2 JU). The JRC contractual activities are summarised in the strategic research and innovation agenda 2021-2027 (SRIA) of the Clean Hydrogen Partnership (CH2P) for Europe (CH2P, 2022, page 103). This report constitutes Deliverable B.1 of the Rolling Plan 2024 contained in the Clean H_2 JU annual work programme 2024 (Clean H_2 JU, 2024a, page 134).

It is the result of a collaborative effort between partners from research and technology organisations in industry and academia participating in European Union (EU) funded research and development (R&D) projects (Clean H_2 JU, 2024b).

Acknowledgements

We would like to express our sincere gratitude to all participants and their respective organisations (see below) for valuable contributions in developing this report. In addition, we appreciate the opportunity to update the SOCTES^{QA} TM 03 ([1]). We also thank Mr Nohl and Mr Steen for reviewing two earlier drafts and the Clean H_2 JU for financial support.

Authors: Malkow, T., Pilenga, A.

Note: Contributors are listed in alphabetical order according to the name of their participating organisation.

	Organisation	**Contributor(s)**
	Commissariat à l'énergie atomique et aux énergies alternatives	Julie Mougin Marie Petitjean Karine Couturier
	Danmarks Tekniske Universitet	Xiufu Sun
	Deutsches Zentrum für Luft- und Raumfahrt e. V.	Michael Lang Rémi Costa
	Agenzia Nazionale per le Nuove tecnologie, l'Energia e lo Sviluppo economico sostenibile	Davide Pumiglia
	Institute of Electrochemistry and Energy Systems Acad. Evgeni Budevski ([2])	Daria Vladikova
	Materials Mates Italia Srl	Paolo Lupotto
	Stiftelsen for industriell og teknisk forskning	Marie-Laure Fontaine Einar Vøllestad
	Solydera SpA	Stefan Diethelm
	Università degli Studi di Genova	Fiammetta Rita Bianchi Barbara Bosio

([1]) The SOCTES^{QA} research project was coordinated by the Deutsches Zentrum für Luft- und Raumfahrt e. V. (DLR) with Commissariat à l'énergie atomique et aux énergies alternatives (CEA), Danmarks Tekniske Universitet (DTU), Agenzia Nazionale per le Nuove tecnologie, l'Energia e lo Sviluppo economico sostenibile (ENEA), JRC and Europäisches Institut für Energieforschung (EIfER) as partners (DLR, 2014).

([2]) Институтът по електрохимия и енергийни системи Акад. Евгени Будевски

1 Introduction

Polarisation curve measurement (**3.1.24**) is the most common test method for the characterisation of the performance (**3.1.22**) of electrochemical cells (**3.1.12**) and stacks, including high-temperature fuel cells (HTFCs) as well as electrolysis cells and stacks, whether of solid oxide cell (SOC) (**3.1.33**) or proton-conducting ceramic (PCC) cell (**3.1.26**) type. Two international standards developed by the Technical Committee (TC) 105 of the International Electrotechnical Commission (IEC) (IEC, 2021a, IEC, 2020c) contain basic test method descriptions on polarisation curve measurements of cell/stack assembly units (**3.1.4**).

HTFCs and electrolysis cells of SOC type are respectively known as solid oxide fuel cells (SOFCs) (**3.1.37**) and solid oxide electrolysis cells (SOECs) (**3.1.34**), while those cells of PCC type are known as protonic ceramic fuel cells (PCFCs) (**3.1.30**) and protonic ceramic electrolysis cells (PCECs) (**3.1.28**). Accordingly, SOC type high-temperature electrolysers (HTEs) performing solid oxide steam electrolysis (SOEL) (**3.1.36**) are known as solid oxide electrolyser (SOE) (**3.1.35**), and PCC type HTE performing proton-conducting ceramic steam electrolysis (PCCEL) (**3.1.27**) are known as protonic ceramic electrolyser (PCE) (**3.1.29**).

HTFCs invariably produce heat regardless of the voltage, using hydrogen (H_2) as fuel. ([3]) In contrast, high-temperature steam electrolysers (HTSEs) consume heat when operated below the temperature-dependent thermo-neutral voltage (U_{tn}), ([4]) whereas they produce heat when operated above this voltage. The fact that HTSEs have a lower thermo-neutral voltage compared to low-temperature water electrolysers (LTWEs) makes the utilisation of waste heat available, for example, from power generation and other industrial processes an attractive option for efficient hydrogen generation.

A reversible solid oxide electrolyser (rSOE) containing reversible solid oxide electrolysis cells (rSOCs) in a single device can operate at a given time in either fuel cell (FC) mode (SOFC mode) or electrolysis mode (SOEC mode). Similarly, a reversible protonic ceramic electrolyser (rPCE) containing reversible proton-conducting ceramic electrolysis cells (rPCCs) in a single device can operate in FC mode (PCFC mode) and electrolysis mode (PCEC mode).

As a widely accepted method in research and development (R&D) within academia and industry, polarisation curve measurements serve to evaluate the performance of cell/stack assembly units through their current-voltage (I-U) characteristics or current density-voltage (J-U) characteristics, jointly referred to as polarisation curves. These curves depict voltage versus current or current density, enabling comparisons between cell/stack assembly units with different configurations, such as electric power, active electrode areas, layout, dimension, and geometry, as well as material selection and manufacturing methods.

Often, polarisation curves are recorded as part of a test run or a test programme to assess performance at specified intervals and determine deviations in the behaviour of a cell/stack assembly unit. In addition to polarisation curves, performance curves of cell/stack assembly units, such as electrical efficiency (η_{el}) (**3.1.10**) versus electric power density ($P_{el,d}$) (**3.1.11**) characteristics (η_{el}-$P_{el,d}$ curves), derived from polarisation curves, can facilitate the comparison of cell/stack assembly units utilising different configurations and technologies.

The current density of a cell/stack assembly unit is calculated as follows:

$$J\ (\mathrm{A/cm^2}) = \frac{I_{dc}\ (\mathrm{A})}{A_{act}\ (\mathrm{cm^2})}, \tag{1.0.1}$$

where I_{dc} is the direct current, A_{act} is the active electrode area (**3.1.2**) of the cell or repeating unit (RU) with the smallest surface electrode area of the cells/RUs within the cell/stack assembly unit, where all cells/RUs are electrically connected in series.

The electric power ($P_{el,dc}$) of a cell/stack assembly unit is calculated as follows:

$$P_{el,dc}\ (\mathrm{kW}) = U_{dc}\ (\mathrm{V}) \cdot I_{dc}\ (\mathrm{A}) \cdot 10^{-3}\ (\mathrm{kW/W}), \tag{1.0.2}$$

where U_{dc} is the DC voltage. The electric power density ($P_{el,d}$) of a cell/stack assembly unit is calculated as follows:

$$P_{el,d}\ (\mathrm{W/cm^2}) = \frac{U_{dc}\ (\mathrm{V}) \cdot J\ (\mathrm{A/cm^2})}{N_{cells}}, \tag{1.0.3}$$

where N_{cells} is the number of cells or repeating units electrically connected in series in the cell/stack assembly unit.

Polarisation curves are determined either in galvanostatic mode or potentiostatic mode. In galvanostatic mode, the input current, which corresponds to a given input current density of the cell/stack assembly unit, is set to a non-zero value (positive in FC mode and negative in electrolysis mode) while the output voltage (U) is

([3]) No distinction is made between the different hydrogen isotopes in this document.

([4]) At standard ambient pressure (p^0 = 100 kPa) and standard ambient temperature (T^0 = 298,15 K), the thermo-neutral voltage is 1,481 V. This voltage is 1.286 V at 1073,15 K (800°C).

concomitantly measured. That is, the current is a test input parameter (TIP), and the voltage is a test output parameter (TOP). In potentiostatic mode, the voltage is set above the open circuit voltage (OCV) ($U_{I=0}$) (**3.1.21**) of the cell/stack assembly unit ([5]), and the current is measured. In this mode, the voltage is a TIP, and the current is a TOP. For HTFCs, whether SOFC or PCFC, and HTSEs, whether SOE or PCE, three main regions are usually distinguished in polarisation curves:

- At very low current densities, the voltage of the cell/stack assembly unit decreases in FC mode (voltage loss) and increases in electrolysis mode (voltage gain) due to electrode (anode and cathode) reaction rate losses (sluggish reaction kinetics) or activation polarisation (**3.1.1**) ([6]).
- At moderate current densities, the voltage of the cell/stack assembly unit decreases in FC mode and increases in electrolysis mode linearly with current due to ohmic resistance losses or ohmic polarisation (**3.1.20**).
- At very high current densities, the voltage of the cell/stack assembly unit decreases in FC mode and increases in electrolysis mode further, departing from the linear relationship with current density due to more pronounced gas transport losses (mass transfer limitations) or concentration polarisation (**3.1.5**) ([7]).

Note that these regions are influenced by the gas composition at the electrodes, and overlapping between the regions is common.

Post-processing the measured current and voltage data enables plotting of performance curves for cell/stack assembly units, including electric power versus current density ($P_{\mathrm{el,dc}}$-J curves) and efficiency (η) (**3.1.9**) versus electric power density (η-$P_{\mathrm{el,d}}$ curves), to assess the optimum working point of the cell/stack assembly unit under specified conditions. By efficiency, we specifically mean the electrical efficiency and the thermal efficiency (η_{th}) (**3.1.48**) for HTFCs and the energy efficiency (η_{e}) (**3.1.15**) for HTSEs (electric power, heat demand, and pneumatic power), based on the higher heating value (HHV) of hydrogen ($\mathrm{HHV}_{\mathrm{H_2}}$ = 79,4 Wh/mol) or the lower heating value (LHV) of hydrogen ($\mathrm{LHV}_{\mathrm{H_2}}$ = 67,2 Wh/mol) (Tsotridis and Pilenga, 2018). This refers to standard ambient temperature and pressure (SATP) (**3.1.40**) (IUPAC, 2019). The selection of SATP conditions for the input streams of fuel and oxidant facilitates the comparison of low-temperature and high-temperature fuel cells. It also facilitates the comparison of hydrogen generation by LTWEs and HTSEs.

In the remainder of this report, we present the objectives and scope in section 2, provide terms and definitions in section 3, and give an overview on the relevant technologies in section 4. In section 5, we give a description of the items to be tested in accordance with the procedure presented in section 6. This is followed by section 7, which provides information on the data post-processing and presentation of the test results. The conclusions are given in section 8. The annexes complement this report.

([5]) Note that OCV refers to the voltage across a complete electrochemical cell (**3.1.12**), whereas open circuit potential (OCP) refers to the potential measured between a half cell and a suitable reference electrode (del Olmo *et al.*, 2021).

([6]) The activation polarisation voltage of a cell/stack assembly unit (U_{act}) can be calculated using equation (7.1.5).

([7]) The concentration polarisation voltage of a cell/stack assembly unit (U_{conc}) can be calculated using equation (7.1.6).

2 Objective and scope of this document

The aim of this document is to describe the test method for performing polarisation curve measurements on HTFCs and HTSEs, encompassing cell/stack assembly units of SOC, including rSOC, and PCC, including rPCC, which are currently considered for use in demonstration projects, first industrial deployment (FID), and eventual commercialisation.

The use of hybrid or mixed oxide ion and proton conductors as electrolyte in HTFCs is not considered in this document.

Although the test method can, in principle, also be applied to cell/stack assembly units using hydrogen containing gas mixtures as fuel and oxygen (O_2) containing gases other than air as oxidants in FC mode, this report only considers the use of hydrogen as fuel and air as oxidant for HTFCs to generate electricity, heat, and water vapour (steam) (steam or $H_2O_{(g)}$).

Similarly, the test method can, in principle, be applied to cell/stack assembly units using, in addition to electricity, steam, and available heat in electrolysis mode, carbon dioxide (CO_2) for co-electrolysis to generate syngas containing carbon monoxide (CO) and possibly hydrocarbon compounds, as well as hydrogen, oxygen, and heat in HTEs. However, this report does not consider operating cell/stack assembly units for co-electrolysis.

Unless specified otherwise, the parameter values, and their respective ranges, including uncertainties, specified in this document are indicative and not mandatory. In addition, the use of the symbols as used in this document for the respective parameters is not obligatory.

3 Terminology

Terms and definitions used in this document are given below, as well as in two Joint Research Centre (JRC) reports (Tsotridis and Pilenga, 2018, Malkow *et al.*, 2021). In addition, International Organization for Standardization (ISO) and IEC maintain terminological databases at the following websites:

- Online browsing platform available at `https://www.iso.org/obp`.
- International Electrotechnical Vocabulary (IEV), also known as electropedia, available at `http://www.electropedia.org`.

The verbal forms used in this document have the following meaning:

- "shall" indicates a requirement,
- "should" indicates a recommendation,
- "may" indicates a permission and
- "can" indicates a possibility or a capability.

Reference to Système International d'Unités (SI) coherent (derived) units include metric prefixes as appropriate. Following clause 9.1 of ISO/IEC Directives, Part 2 (ISO and IEC, 2021), decimal fractions are denoted by comma. Alongside SI units, non-SI units may be used as customary. For example, degree Celsius (°C) is used as unit of temperature (T) alongside Kelvin (K) and kilo Watt hours (kWh) is used as unit of energy (E) instead of Joule (J).

3.1 Terms and definitions

3.1.1 activation polarisation
part of the electrode polarisation (**3.1.14**) arising from a charge-transfer step of the electrode reaction

[Source: IEV 482-03-05]

Note 1 to entry: The electrode reactions are given in equation (4.1.2) for SOFC (**3.1.37**), equation (4.1.3) for PCFC (**3.1.30**), equation (4.2.2) for SOEC (**3.1.34**) and equation (4.2.3) for PCEC (**3.1.28**).

3.1.2 active electrode area (A_{act})
geometric electrode area upon which an electrochemical reaction occurs

Note 1 to entry: Usually this is the smaller of the anode and cathode areas.

[Source: IEC 62282-7-2, 3.1.2 (IEC, 2021a)]

Note 2 to entry: The active electrode area is expressed in square centimetre (cm^2).

3.1.3 average repeating unit voltage ($\bar{U}_{\mathrm{RU}}$)
cell/stack assembly unit voltage divided by the number of the cells in a series connection in the unit

[Source: IEC 62282-7-2, 3.1.4 (IEC, 2021a)]

Note 1 to entry: The average repeating unit voltage is calculated by equation (E.3.1).
Note 2 to entry: The average repeating unit voltage is expressed in volt (V).

3.1.4 cell/stack assembly unit
unit including a single cell or stack, as well as gas supply parts, current collector (**3.1.6**) parts, and any other required peripherals

3.1.5 concentration polarisation
part of the electrode polarisation (**3.1.14**) arising from concentration gradients of electrode reactants and products

[Source: IEV 482-03-08]

Note 1 to entry: Concentration polarisation (mass transfer limitation) increases at high current density (**3.1.7**). In fuel cells, this can lead to a sharp decrease in voltage, potentially dropping below positive values. In electrolysis cells, it may cause a more than proportional increase in voltage.

3.1.6 current collector

electronically conductive material in a cell/stack assembly unit (**3.1.4**) that collects/conducts electrons from/to the electrodes

[Source: IEC 62282-8-101, 3.1.10 (IEC, 2020c)]

3.1.7 current density (J)

electric current divided by the active electrode area (**3.1.2**)

Note 1 to entry: The current density is given by equation (1.0.1).
Note 2 to entry: The current density is expressed in ampere per square centimetre (A/cm^2).

3.1.8 current sweep ($\Delta I/\Delta t$)

current change at a specified constant rate from zero to maximum current (I_{max}) or *vice versa*

Note 1 to entry: Current sweep is pertinent for polarisation curve measurements conducted under galvanostatic conditions and can be either positive or negative.
Note 2 to entry: Unless specified by the manufacturer, maximum current may be determined through preliminary testing or by considering a cut-off voltage ($U_{\text{cut-off}}$), which may depend on temperature and the size of the cell/stack assembly unit. In fuel cell mode, 0,7 V per RU is recommended as cut-off voltage to prevent re-oxidation of Ni-based cermets, while in electrolysis mode, a cut-off voltage of 1,5 V per RU is suggested. For single repeating unit (SRU) of SOE type, the cut-off voltage may be selected between 1,6 and 1,7 V. The voltage of the worst-performing RU should be taken into account.
Note 3 to entry: Current sweep is expressed in ampere per second (A/s).

3.1.9 efficiency (η)

ratio of output power to input power of a device

[Source: IEV 151-15-25]

Note 1 to entry: The efficiency is generally expressed in percentage (%).

3.1.10 electrical efficiency (η_{el})

ratio of output electric power to input power of a fuel cell

Note 1 to entry: The input power is the sum of input power of hydrogen, input thermal power, and input pneumatic power.
Note 2 to entry: The electrical efficiency is generally expressed in percentage (%).

3.1.11 electric power density ($P_{\text{el,d}}$)

ratio of the electric power to the active electrode area (**3.1.2**) of a cell/stack assembly unit (**3.1.4**)

[Source: IEC 62282-7-2, 3.1.16 (IEC, 2021a)]

Note 1 to entry: The electric power density is given by equation (1.0.3).
Note 2 to entry: The electric power density is expressed in watt per square centimetre (W/cm^2).

3.1.12 electrochemical cell

system in which the supplied electric energy (see equation (5.2.1)) produces chemical reactions or, conversely, in which the energy released by chemical reactions is delivered by the system as electric energy

[Source: IEV 114-03-01]

Note 1 to entry: In case that electric energy produces chemical reactions, an electrochemical cell is also known as an electrolytic cell.

3.1.13 electrode gas

gas in one electrode of an electrochemical cell (**3.1.12**) where it reacts while flowing through the cell or is produced while leaving the cell

3.1.14 electrode polarisation

accumulation or depletion of electric charges at an electrode, resulting in a difference between the electrode potential with current flow, and the potential without current flow or equilibrium electrode potential

[Source: IEV 114-02-15]

3.1.15 energy efficiency (η_e)
ratio of output power of hydrogen to input power of a high-temperature electrolyser

Note 1 to entry: The input power is the sum of input power of hydrogen, input thermal power, and input pneumatic power.
Note 2 to entry: The energy efficiency is generally expressed in percentage (%).

3.1.16 Faradaic efficiency (η_F)
fraction of the electric current passing through an electrochemical cell which accomplishes the desired chemical reaction

[Source: IEV 114-03-07]

Note 1 to entry: Faradaic efficiency is also known as current efficiency.
Note 2 to entry: The chemical reactions are specified in equation (4.1.1) for HTFCs and in equation (4.2.1) for HTSEs.
Note 3 to entry: Faradaic efficiency is generally expressed in percentage (%).

3.1.17 gas utilisation (λ^{-1})
inverse of stoichiometric ratio (**3.1.42**)

Note 1 to entry: Considering under SATP conditions (**3.1.40**) the overall HTFC reaction (4.1.1) as well as the overall HTSE reaction (4.2.1), the gas utilisation is calculated as follows:

$$\lambda^{-1} = \frac{I_{\text{dc}}\ (\text{A}) \cdot N_{\text{cells}} \cdot V_{\text{m}}\ (\text{m}^3/\text{mol})}{z \cdot F\ (\text{C/mol}) \cdot q_{\text{V}}\ (\text{m}^3/\text{s})} \approx \frac{I_{\text{dc}}\ (\text{A}) \cdot N_{\text{cells}}}{77,84 \cdot 10^5\ (\text{A s/m}^3) \cdot q_{\text{V}}\ (\text{m}^3/\text{s})}; \tag{3.1.1}$$

V_{m} is the molar volume at SATP conditions, z=2 is the number of electrons exchanged in the electrode reactions (4.1.2) and (4.1.3) in FC mode and the electrode reactions (4.2.2) and (4.2.3) in electrolysis mode, F = 96485,3321 C/mol is the Faraday constant, and q_{V} is the inlet volumetric flow rate of the reactant concerned.
Note 2 to entry: Gas utilisation is generally known as reactant utilisation. Specifically, in FC mode, gas utilisation is known as hydrogen (fuel) gas utilisation and air utilisation. In electrolysis mode, gas utilisation is known as steam conversion.

3.1.18 minimum cell/stack assembly unit voltage (U_{min})
lowest cell/stack assembly unit voltage specified by the manufacturer

[Source: IEC 62282-7-2, 3.1.14 (IEC, 2021a)]

Note 1 to entry: Minimum cell/stack assembly unit voltage applies to FC mode.
Note 2 to entry: The minimum cell/stack assembly unit voltage is expressed in volt (V).

3.1.19 negative electrode
electrode at which fuel (hydrogen) gas is consumed (fuel cell mode) or produced (electrolysis mode)

Note 1 to entry: The negative electrode is also referred to as the fuel (hydrogen) electrode. In fuel cell mode, it is termed the anode, whereas in electrolysis mode, it is called cathode (negatrode).
Note 2 to entry: In fuel cell mode, the gas at the negative electrode is typically hydrogen or a mixture where hydrogen is the principal component. For safety purposes, an inert gas may be added to the fuel gas.
Note 3 to entry: In electrolysis mode, the gas at the negative electrode primarily consists of steam, with small additions of hydrogen to control the partial pressure of oxygen and prevent the oxidation of the electrode materials.

3.1.20 ohmic polarisation
polarisation (**3.1.23**) caused by the resistance to the flow of ions in the electrolyte and of electrons in the electrodes, bipolar plates (biPs), and current collectors (**3.1.6**)

Note 1 to entry: The term "ohmic" refers to the fact that the voltage drop follows Ohm's law proportional to

the current with an ohmic resistance (called "internal resistance" of the cell) as the proportionality constant.

[Source: IEV 485-15-03]

3.1.21 open circuit voltage (OCV) ($U_{I=0}$)
voltage across the electrode terminals of an electrochemical cell (**3.1.12**) with the electrode gases (**3.1.13**) present and in the absence of external current flow

Note 1 to entry: OCV is also known as "no-load voltage".
Note 2 to entry: The open circuit voltage is expressed in volt (V).

3.1.22 performance
ability of a test item (**3.1.46**) to operate as intended, under given conditions of use and maintenance

3.1.23 polarisation
change of an electrode potential caused by current flow

Note 1 to entry: Current flow results in concentration polarisation (**3.1.5**) and activation polarisation (**3.1.1**).

[Source: ISO 22426:2020, 3.3 (ISO, 2020)]

3.1.24 polarisation curve
plot of the voltage of a cell/stack assembly unit (**3.1.4**) as a function of current or current density under defined reaction conditions

Note 1 to entry: In galvanostatic polarisation curve measurements, current is the TIP (**3.1.45**) that is set, and voltage is the measured TOP (**3.1.47**). Conversely, in potentiostatic polarisation curve measurements, voltage is the set TIP, and current is the measured TOP.
Note 2 to entry: The polarisation curve is expressed in volt (V) versus ampere (A) or in volt (V) versus ampere per square centimetre (A/cm^2).

3.1.25 positive electrode
electrode at which oxygen is consumed (fuel cell mode) or produced (electrolysis mode)

Note 1 to entry: The positive electrode is also referred to as the oxygen (oxygen) or air electrode. In fuel cell mode, it is termed the cathode, whereas in electrolysis mode, it is called anode (positrode).
Note 2 to entry: In fuel cell mode, the gas at the positive electrode is typically oxygen or air.
Note 3 to entry: In electrolysis mode, the gas at the positive electrode primarily consists of air in SOE and steam in PCE, in addition to the oxygen generated.

3.1.26 proton-conducting ceramic (PCC) cell
electrochemical cell (**3.1.12**) that uses a proton-conducting oxide as solid electrolyte

3.1.27 proton-conducting ceramic steam electrolysis (PCCEL)
steam electrolysis that employs one or more proton-conducting ceramic cells (**3.1.26**) to generate hydrogen

3.1.28 protonic ceramic electrolysis cell (PCEC)
electrolysis cell that uses a proton-conducting oxide as the electrolyte

3.1.29 protonic ceramic electrolyser (PCE)
proton-conducting ceramic cell (**3.1.26**) based electrolyser used in high-temperature steam electrolysis

3.1.30 protonic ceramic fuel cell (PCFC)
fuel cell that uses a proton-conducting oxide as the electrolyte

3.1.31 quality assurance (QA)
part of quality management focused on continually providing confidence that requirements are being fulfilled

[Source: ISO/IEC/IEEE 32675:2022 (IEEE, 2022)].

3.1.32 quality control (QC)
part of quality management focused on fulfilling quality requirements

[Source: ISO 16559:2022, 3.162 (ISO, 2022)].

3.1.33 solid oxide cell (SOC)
electrochemical cell (**3.1.12**) that uses an ion-conducting oxide as solid electrolyte

3.1.34 solid oxide electrolysis cell (SOEC)
electrolysis cell that uses an ion-conducting oxide as the electrolyte

3.1.35 solid oxide electrolyser (SOE)
solid oxide cell (**3.1.33**) based electrolyser used in high-temperature steam electrolysis

3.1.36 solid oxide steam electrolysis (SOEL)
steam electrolysis that employs one or more solid oxide cells (**3.1.33**) to generate hydrogen

3.1.37 solid oxide fuel cell (SOFC)
fuel cell that uses an ion-conducting oxide as the electrolyte

[Source: IEV 485-08-10]

3.1.38 stable state
condition of a cell/stack assembly unit (**3.1.4**) at which the unit is stable enough for the controlling test parameter(s) to remain within the specified tolerance range(s) of variation

Note 1 to entry: In polarisation curve measurements, the controlling parameter includes stack temperature (**3.1.39**) in addition to current and voltage.

3.1.39 stack temperature (T_{stack})
operating temperature of the cell/stack assembly unit (**3.1.4**), measured or estimated following the manufacturer's instructions

Note 1 to entry: Stack temperature is typically represented as an average temperature $\bar{T}_{\text{stack}}$ (see equation (E.3.2a)), with a standard variance $s^2\left(T_{\text{stack}}\right)$ (see equation (E.4.1a)).
Note 2 to entry: For a compact cell/stack assembly unit of small dimension, consisting of a single cell or a small number of cells or repeating units electrically connected in series in the cell/stack assembly unit, the stack temperature may be measured at a representative location near the unit, such as the centre of the electrode gas (**3.1.13**) flow channel. For larger cell/stack assembly units, whether due to greater dimension or a higher number of cells or RUs, the stack temperature may be estimated using a method devised by the manufacturer. This involves a number of individual temperature measurements at representative locations on and inside the unit to account for spatial and temporal temperature distributions. These distributions arise from the differing thermal properties of materials used in various unit components and the varying fluid properties (composition, pressure, and temperature) of the gases flowing within the unit, given its configuration, geometry, and structure. Temperature measurements should allow sufficient time for spatial and temporal equilibration of induced changes in heat demand (*e. g.* , unit heating/cooling, especially upon start-up, shut-down, or reversal of operation), acknowledging that large cell/stack assembly units typically possess a high thermal mass. The estimation of stack temperature may be aided by computation (integration and gradient calculations), modelling (analytical or numerical), and simulations, including the use of machine learning (ML) or other artificial intelligence (AI) techniques.

3.1.40 SATP conditions
standard ambient temperature, T^0 = 298,15 K (25 °C) and standard ambient pressure, p^0 = 100 kPa (1 bar)

3.1.41 step duration
time interval between the first data acquisition (DAQ) and the last DAQ

Note 1 to entry: Step duration is only relevant for polarisation curve measurements when applying method (**A**); refer to section 6.3.2.
Note 2 to entry: This duration excludes the time required to achieve a stable state (**3.1.38**).
Note 3 to entry: Step duration is expressed in seconds (s).

3.1.42 stoichiometric ratio (λ)

ratio between the number of moles of reactant gas flowing per unit time to that needed by the electrochemical reaction

[Source: IEC 62282-7-2, 3.1.19 (IEC, 2021a)]

Note 1 to entry: The terms "stoichiometric ratio" and "gas utilisation" (**3.1.17**) are related; the stoichiometric ratio is the reciprocal of gas utilisation.
Note 2 to entry: The electrochemical reactions are specified in equation (4.1.1) for HTFCs and in equation (4.2.1) for HTSEs.

3.1.43 sweep gas

gas primarily used to carry away heat from a cell/stack assembly unit (**3.1.4**), flowing through an electrode compartment during operation

Note 1 to entry: In FC mode, air is typically used as a sweep gas for heat removal. An inert sweep gas may also be employed to remove electrode gas (**3.1.13**) from a cell/stack assembly unit. Small amounts of hydrogen (or oxygen or air) might be added to the inert sweep gas to prevent electrode oxidation (or reduction).
Note 2 to entry: In electrolysis mode, the use of a sweep gas may not be necessary.

3.1.44 test environment

space in which the test is carried out, described by a set of parameters

Note 1 to entry: A test environment commonly contains facilities, hardware, software, firmware, procedures, documentation, needed to conduct a test.

[Source: ISO 14644-14:2016, 3.7 (ISO, 2016)]

3.1.45 test input parameter (TIP)

parameter whose value can be set to define the test conditions of the test system, including the operating conditions of the test item (**3.1.46**)

Note 1 to entry: TIPs must be both controllable and measurable. Their values are known prior to conducting the test. TIPs can be either static or variable; static TIPs remain constant during the test, while variable TIPs are adjusted.

3.1.46 test item

cell/stack assembly unit (**3.1.4**) of the type high-temperature fuel cell or high-temperature electrolyser

3.1.47 test output parameter (TOP)

parameter that reflects the response of the test item (**3.1.46**) as a result of variations in test input parameters (**3.1.45**)

Note 1 to entry: The values of TOPs are not known prior to the test and are measured during the test or calculated afterwards.

3.1.48 thermal efficiency (η_{th})

ratio of output thermal power to input power of a fuel cell

Note 1 to entry: The input power is the sum of input power of hydrogen, input thermal power, and input pneumatic power.
Note 2 to entry: The thermal efficiency is generally expressed in percentage (%).

3.1.49 voltage sweep ($\Delta U/\Delta t$)

voltage change at a specified constant rate, generally from OCV (**3.1.21**) to a cut-off voltage, or *vice versa*

Note 1 to entry: Voltage sweep is relevant for polarisation curve measurements conducted under potentiostatic conditionsa and can be either positive or negative.
Note 2 to entry: The cut-off voltage should be specified prior to testing. In fuel cell mode, a cut-off voltage of 0,7 V per RU is recommended to prevent re-oxidation of Ni-based cermets, while in electrolysis mode, a cut-off voltage of 1,5 V per RU is advised. For SRU of the SOE type, the cut-off voltage may be selected between 1,6 and 1,7 V per RU. The voltage of the worst-performing RU should be taken into account.
Note 3 to entry: Voltage sweep is expressed in volt per second (V/s).

3.2 Abbreviations and acronyms used

A list of abbreviations and acronyms used in this report is appended; please refer to the list beginning on page 39.

3.3 Symbols used

A list of symbols used in this report is appended; please refer to the list beginning on page 43.

4 Overview of high-temperature fuel cells and steam electrolysis

4.1 Electrode reactions in high-temperature fuel cells

In a HTFC, whether of SOFC type or PCFC type, one mole of gaseous hydrogen ($H_{2\,(g)}$) is utilised as fuel alongside half a mol of gaseous oxygen ($O_{2\,(g)}$) from the air. This combinatio produces one mole of water vapour (steam), direct current (DC) electricity, and heat in the overall fuel cell reaction:

$$\text{HTFC:}\quad H_{2\,(g)} + \frac{1}{2}\,O_{2\,(g)} \rightarrow H_2O_{(g)}. \tag{4.1.1}$$

Traditionally, SOFCs operate at temperatures between 600°C and 1000°C, primarily to ensure that the solid oxide electrolyte exhibits sufficient ionic conductivity. Currently, most SOFCs function at temperatures around and below 800°C, depending on the thickness of the electrolyte and the materials used. This adjustments results in improved thermo-mechanical stability, reduced degradation, and enhanced durability, while maintaining adequate performance.

In the future, it may become feasible for intermediate-temperature to low-temperature SOFC to operate below 584,85°C, the auto-ignition temperature of hydrogen in air (ISO, 2015), and as low as 300°C, outside of laboratory environments. PCFCs currently function at temperatures between 400°C and 650°C, with the most common ranges being from 500°C to 650°C. In addition to the primary charge carrier - oxide ions in SOFC and protons in PCFC - and the operating temperatures, other characteristics are used to classify HTFCs; see section 4.3 for details. The two principal HTFC technologies are as follows:

- **SOFC** operates as an electrochemical cell where one mole of gaseous hydrogen is oxidised by an oxide ion (O^{2-}) to form one mole of water vapour (steam), while concurrently releasing two electrons (e^-) at the negative electrode (hydrogen/fuel electrode or anode) (**3.1.25**) through the hydrogen oxidation reaction (HOR):

$$\text{Negative electrode:}\quad H_{2\,(g)} + O^{2-}{}_{(el)} \xrightarrow{\text{HOR}} H_2O_{(g)} + 2e^-{}_{(ed)}. \tag{4.1.2a}$$

Simultaneously, at the positive electrode (oxygen electrode or cathode) (**3.1.19**), half a mole of gaseous oxygen from the air is reduced to an oxide ion by utilising two electrons through the oxygen reduction reaction (ORR):

$$\text{Positive electrode:}\quad \frac{1}{2}\,O_{2\,(g)} + 2e^-{}_{(ed)} \xrightarrow{\text{ORR}} O^{2-}{}_{(el)}. \tag{4.1.2b}$$

The electrons are conducted via the electrodes (denoted by subscript $_{(ed)}$) connected to an external circuit (DC power consumer),which presents an ohmic resistance. Upon drawing current, oxide ions diffuse under the potential difference between the positive and negative electrodes along grain boundaries - two-dimensional crystalline planar defects between lattices of differing crystalline orientations - and through doubly positively charged oxide ion lattice vacancies ($V_O^{\bullet\bullet}$) within the grains (lattices with same crystal orientation) of the polycrystalline solid oxide ceramic electrolyte membrane (denoted by subscript $_{(el)}$). This diffusion introduces an ionic resistance, additional to the ohmic resistance. Using Kröger–Vink notation (Kröger and Vink, 1956, Kröger and Vink, 1958), the reactions (4.1.2) are described by the reactions (C.1.1) in Annex C.

- **PCFC** operates as an electrochemical cell where one mole of gaseous hydrogen is oxidised to produce two protons (H^+) and two electrons at the negative electrode through the HOR:

$$\text{Negative electrode:}\quad H_{2\,(g)} \xrightarrow{\text{HOR}} 2\,H^+{}_{(el)} + 2e^-{}_{(ed)}. \tag{4.1.3a}$$

Simultaneously, at the positive electrode, half a mole of gaseous oxygen from the air is reduced to form one mole of water vapour (steam) by utilising two protons and two electrons in the ORR:

$$\text{Positive electrode:}\quad \frac{1}{2}\,O_{2\,(g)} + 2\,H^+{}_{(el)} + 2e^-{}_{(ed)} \xrightarrow{\text{ORR}} H_2O_{(g)}. \tag{4.1.3b}$$

While electrons are conducted via the electrodes connected to an external circuit, protons are conveyed alongside dissociative adsorption and rotational diffusion, primarily through Grotthuss-type diffusion (proton hopping) (Kreuer *et al.*, 2004, Kreuer, 2000). This occurs via protonic defects such as hydroxide ions at singly positively charged oxide ion lattice sites ($OH_O^{\bullet}$) within the disordered or sub-stoichiometric oxides that make up the electrolyte membrane of the PCC (Duan *et al.*, 2020). In Kröger–Vink notation, the reactions (4.1.3) are described by the reactions (C.1.2) in Annex C.

4.2 Electrode reactions in high-temperature steam electrolyser

In HTSE, whether of SOE type or PCE type, one mole of steam is utilised alongside DC electricity and any available heat to produce one mole of gaseous hydrogen, half a mole of gaseous oxygen, and additional heat([8]) through the overall steam electrolysis reaction:

$$\text{HTSE:}\quad \mathrm{H_2O_{(g)}} \rightarrow \mathrm{H_{2\,(g)}} + \frac{1}{2}\,\mathrm{O_{2\,(g)}}. \tag{4.2.1}$$

In principle, SOECs can function at temperatures ranging from 600°C to 950°C. Currently, most SOECs operate between 650°C and 850°C, contingent upon the thickness and materials of the electrolyte to prevent excessive degradation. In the future, SOECs may be able to function at temperatures significantly below 600°C. PCECs can operate within a temperatures range of 400°C to 700°C, primarily dictated by the materials used for the electrolyte. Today, PCECs generally operate at temperatures at or above 500°C, although in the future, they may function at temperatures as low as 350°C. The two primary HTSE technologies are as follows:

- **SOE** operate as an electrochemical system where gaseous hydrogen is produced by reducing steam and employing two electrons at the negative electrode (hydrogen electrode or cathode) through the hydrogen evolution reaction (HER):

$$\text{Negative electrode:}\quad \mathrm{H_2O_{(g)}} + 2e^-_{\text{(ed)}} \xrightarrow{\text{HER}} \mathrm{H_{2\,(g)}} + \mathrm{O^{2-}_{(el)}}. \tag{4.2.2a}$$

  Electrons are conducted via the electrodes connected to an external circuit (DC power supply), which presents an ohmic resistance. The oxide ions diffuse under the potential difference between negative and positive electrode along grain boundaries and through doubly positively charged oxide ion lattice vacancies within the grains of the polycrystalline solid oxide ceramic electrolyte membrane of the SOC. This diffusion contributes an additional ionic resistance. Simultaneously, at the positive electrode (oxygen electrode or anode), gaseous oxygen is formed when the potential (voltage) between the negative and positive electrode exceeds the OCV, achieved by oxidising oxide ions ($\mathrm{O^{2-}}$) in the oxygen evolution reaction (OER):

$$\text{Positive electrode:}\quad \mathrm{O^{2-}_{(el)}} \xrightarrow{\text{OER}} \frac{1}{2}\,\mathrm{O_{2\,(g)}} + 2e^-_{\text{(ed)}} \tag{4.2.2b}$$

  Note that the potential difference results from the supplied DC (galvanostatic operation) or applied DC voltage (potnetiostatic operation) and the resistance of the cell/stack assembly unit.

  In a rSOE operated in FC mode, also known as SOFC mode, the electrode reactions (4.2.2) proceed in the reverse direction from right to left by drawing current, resulting in reactions (4.1.2). That is, the reverse of reaction (4.2.2b) corresponds to the ORR (4.1.2b) at the FC cathode, while the reverse of reaction (4.2.2a) corresponds to the HOR (4.1.2a) at the FC anode. In SOFC mode, heat is produced, whereas in PCEC mode, a rSOE, like an ordinary SOE, consumes heat when operated below the theoretical thermo-neutral voltage and produces heat when operated above such voltage. In Kröger–Vink notation, the reactions (4.2.2) are described by the reactions (C.2.1) in Annex C.

- **PCE** operate as an electrochemical system where gaseous hydrogen is produced by the reduction of protons ($\mathrm{H^+}$) at the negative electrode, aslo known as the cathode, through the HER:

$$\text{Negative electrode:}\quad 2\,\mathrm{H^+_{(el)}} + 2e^-_{\text{(ed)}} \xrightarrow{\text{HER}} \mathrm{H_{2\,(g)}}. \tag{4.2.3a}$$

  While electrons are conducted via the electrodes connected to an external circuit, protons are primarily conducted through Grotthuss-type diffusion, proton hopping, via protonic defects such as hydroxide ions at singly positively charged oxide ion lattice sites ($\mathrm{OH^{\bullet}_O}$) present in the electrolyte membrane of the PCC, which is composed of disordered or sub-stoichiometric oxides (Duan *et al.*, 2020). Simultaneously, at the positive electrode, known as the anode, gaseous oxygen is generated under an applied DC potential exceeding the OCV by oxidising steam in the OER:

$$\text{Positive electrode:}\quad \mathrm{H_2O_{(g)}} \xrightarrow{\text{OER}} 2\,\mathrm{H^+_{(el)}} + 2e^-_{\text{(ed)}} + \frac{1}{2}\,\mathrm{O_{2\,(g)}} \tag{4.2.3b}$$

  In a rPCE operating in FC mode, also referred to as PCFC mode, the electrode reactions (4.2.3) proceed in the reverse direction, from right to left, by drawing current resulting in reactions (4.1.3). Specifically, the reverse of reaction (4.2.3b) corresponds to the ORR at the PCFC cathode, while the reverse of reaction (4.2.3a) corresponds to the HOR at the PCFC anode. In PCFC mode, heat is produced, whereas in PCEC mode, a rPCE, similar to a conventional PCE, consumes heat when operated below the theoretical thermo-neutral

([8]) In a HTSE, heat is not always generated; refer to section 4.4 below.

voltage and generates heat when operated above this voltage. It is important to note that the electrolyte materials in PCEs are practically mixed conductors, exhibiting both proton and electronic conduction, typically through electron holes and electrons. This results in a heat-generating leakage current, which consequently reduces the Faradaic efficiency (η_F) (**3.1.16**) of the cell/stack assembly unit. Consequently, the practical thermo-neutral voltage is lower than the theoretical thermo-neutral voltage (Herradon *et al.*, 2022, Rand *et al.*, 2024), and PCEs effectively operate in an exothermic mode; refer to section 4.4 for further details. In Kröger–Vink notation, the reactions (4.2.3) are described by the reactions (C.2.2) in Annex C.

4.3 Materials, configurations and technology readiness levels

While rSOE have currently achieved a technology readiness level (TRL) of 5-6, SOEs that utilise SOECs as their constituent units are more advanced, with a TRL of 7-8, benefiting from decades of research on SOFCs. The least mature are PCEs, which have a TRL below 5 and are currently in the early stages of development. This phase includes research on suitable stack designs and manufacturing processes, as well as investigations into the most appropriate combinations of electrode and electrolyte materials for PCECs as constituent units.

In SOCs, the most common electrolyte is yttria-stabilised zirconia (YSZ). The positive electrode often consists of strontium-doped lanthanum cobalt iron oxide (LSCF) or strontium-doped lanthanum cobalt oxide (LSC) combined with ceria-doped gadolinium oxide (CGO), while the negative electrode is typically made of a nickel-cermet. In PCCs, common electrolyte materials include yttrium-doped barium zirconate (BZY), yttrium-doped barium cerate (BCY), and scandia-stabilised zirconia (ScSZ). These materials exhibit high proton conductivity and stability under operating conditions. Among these, BZY is the most extensively used and researched, given its compatibility with the electrodes typically made of nickel-YSZ cermet for the negative electrode and nickel-barium zirconate (BZ) cermet or nickel-BZY cermet for the positive electrode. These cermets offer high catalytic activity, electrical conductivity, and a high triple-phase boundary (TPB) density. Additionally, they provide mechanical strength and stability, supporting the cell or RU components.

The geometry of SOC/PCC devices can be either tubular or planar. Planar SOCs/PCCs devices are generally circular, square, or rectangular. The mechanical support of planar SOCs/PCCs devices can be provided by one of the electrodes, the electrolyte, or a metal interconnect. ([9]) In planar SOCs/PCCs devices, the interconnect also serves as the current collector/conductor. The geometry of planar stacks, which constitute several RUs sandwiched between gas flow channel-containing interconnects that are electrically connected in series, is often rectangular or square.

4.4 Operation modes of HTSE cell/stack assembly units

Under galvanostatic conditions, an input current is supplied to the HTSE cell/stack assembly unit, resulting in a voltage generated for each RU. These voltages collectively contribute to the overall voltage of the cell/stack assembly unit when all RUs are electrically connected in series. Under potentiostatic conditions, an input voltage is applied to the stack, which generates a current flowing through the stack perpendicular to the active electrode area. Depending on the supplied current or applied voltage, as well as the input temperature of steam transferring heat to the HTSE cell/stack assembly unit, the stack primarily operates in endothermic, isothermal, or exothermic modes.

The operation mode of the stack influences both its energy efficiency and degradation in performance. Under galvanostatic conditions, performance degradation manifests as an increase in voltage within the cell/stack assembly unit, whereas under potentiostatic conditions, performance degradation, it results in a decrease in current. Degradation occurs with the accumulation of operating hours, regardless of whether operation is continuous or intermittent.

Additionally, degradation is exacerbated by high and variable input power to the cell/stack assembly unit. The operation modes of an HTSE cell/stack assembly unit are as follows:

- *Endothermic operation*: In this mode, the steam temperature decreases from the input to the output of the cell/stack assembly unit, and its voltage remains below the thermo-neutral voltage. Among the three modes of operation, this results in the highest energy efficiency for the cell/stack assembly unit. However, this efficiency is achieved at the cost of a lower hydrogen output rate. Under presumed adiabatic conditions, the heat required for the high-temperature steam electrolysis (HTSEL) reactions (4.2.2) and (4.2.3) is derived primarily from the supplied gases, especially steam, rather than from ohmic (Joule) heating, which is limited by an insufficient supply of electricity, whether current or voltage.

([9]) In metal-supported cells (MSCs), porous metal supports - sometimes coated with suitable materials - are utilised to enhance gas transport, particularly in PCC devices, which typically operate at lower temperatures than SOC devices. As a result, PCCs devices are generally less susceptible to excessive degradation caused by oxidation during operation. Oxidation-related materials degradation is especially characterised by a reduction in pore size and decreased electrical conductivity due to the formation of metal oxides.

- *Isothermal (thermal-neutral) operation*: In this mode, the stack temperature remains virtually unchanged from the input to the output of the stack, with the voltage maintained at approximately the thermo-neutral voltage. The energy efficiency of the stack under this mode is superior to that in exothermic operation, although this increase in efficiency is often counterbalanced by higher cost. The additional heat required to sustain the equilibrium of the HTSEL reactions (4.2.2) and (4.2.3) generally originates from Joule heating attributable to the externally supplied electricity, which is also necessary to establish the reversible potential (U_{rev}). ([10]) Given the voltage difference between the thermo-neutral voltage and the reversible potential (voltage) at the operating temperature and pressure of an HTSE cell/stack assembly unit, Joule heating within stacks can advantageously be replaced by supplementary heat supplied to the stack when available. ([11]) This is particularly relevant for (waste) heat from energy conversion and other industrial processes where heat is generated by methods other than electricity. It is also applicable to heat sourced from natural resources such as geothermal and solar energy. Given the same electricity input in a HTSEL system, the utilisation of high-temperature heat in HTSE cell/stack assembly units makes hydrogen generation by HTSEL potentially more energy-efficient compared to LTWE with the same hydrogen output rate and quality.

- *Exothermic operation*: In this mode, the stack voltage exceeds the thermo-neutral voltage, and the steam temperature rises from the input to the output of the stack. Consequently, the energy efficiency of the cell/stack assembly unit in this mode is the lowest among the three operation modes. This is because more heat is generated through Joule heating from the supplied electricity than necessary to sustain the HTSEL reactions (4.2.2) and (4.2.3). A significant advantage of this mode is that increasing the electricity supply to the cell/stack assembly unit enhances its hydrogen output rate. However, this benefit is offset by an increase in performance degradation. To mitigate excessive stack degradation, a voltage limit of typically no more than 1,5 V per RU is applied, whether operating under potentiostatic or galvanostatic conditions. At the system level, the heat generated by the cell/stack assembly unit can be recovered to enhance the overall system energy efficiency.

([10]) At SATP conditions, the reversible potential is 1,230 V, while this potential decreases to 0,978 V at 1073,15 K (800 °C).

([11]) The continuous availability of heat, along with the steam pressure and temperature, typically dictates the dimensions (size, input power range, hydrogen output rate), configuration, and technology of the HTSE cell/stack assembly unit(s) used in a HTSEL system.

5 Description of test items

For polarisation curve measurements, the test items of interest are HTFC cell/stack assembly units and HTSE cell/stack assembly units. These units are schematically described, along with their inputs and outputs, in section 5.1 for HTFC and in section 5.1 for HTSE units.

5.1 HTFC cell/stack assembly unit

Figure 1 provides a schematic representation of the input and output streams of energy forms and substances in a HTFC cell/stack assembly unit.

Figure 1: Schematic illustration of the input and output streams (indicated by directional arrows) of energy forms (depicted in diamond shape) and substances (depicted in circular shape) in a HTFC cell/stack assembly unit (represented by a rectangular shape); q and p denote flow rate and pressure, respectively. The thick line surrounding the grey-shaded box outlines the boundary of the cell/stack assembly unit.

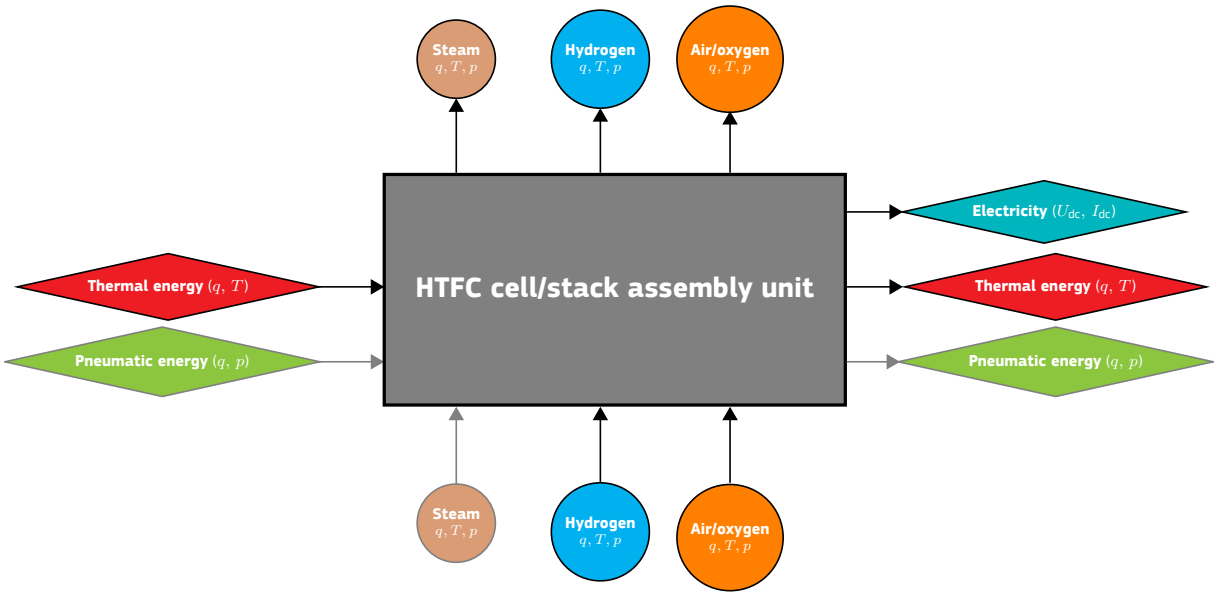

Note: Steam is employed to regulate the partial pressure of oxygen at the negative electrode. Sweep gas (**3.1.43**), used to remove electrode gas (**3.1.13**), is not depicted. Hydrogen that is not utilised is either exhausted or recirculated back into the cell/stack assembly unit, which is also not shown.

Source: JRC, 2024.

The input energy streams to a HTFC cell/stack assembly unit include:

- **Chemical energy** in the form of hydrogen, used as fuel, with a molar flow rate ($q_{\mathrm{n,H_2,in}}$) calculated as follows:

$$q_{\mathrm{n,H_2,in}}\ (\mathrm{mol/s}) = x_{\mathrm{n,H_2,in}}\ (\mathrm{mol/mol}) \cdot \frac{q_{\mathrm{V,in}}\ (\mathrm{m^3/s})}{V_{\mathrm{m,H_2}}\ (\mathrm{m^3/mol})}; \tag{5.1.1}$$

$x_{\mathrm{n,H_2,in}}$ represents the molar concentration of hydrogen in the inlet electrode gas, $V_{\mathrm{m,H_2}}$ is the molar volume of hydrogen, and $q_{\mathrm{V,in}}$ is the inlet volumetric flow rate of the electrode gas. Under SATP conditions, the molar volume of hydrogen is 24,789 $\mathrm{m^3/mol}$. For the negative electrode reactions (4.1.2a) and (4.1.3a) to occur at a specified current, the minimum inlet molar flow rate of hydrogen ($q_{\mathrm{n,H_2,in,min}}$) is calculated as follows:

$$q_{\mathrm{n,H_2,in,min}}\ (\mathrm{mol/s}) = \lambda_{\mathrm{H_2}} \cdot \frac{I\ (\mathrm{A}) \cdot N_{\mathrm{cells}}}{z \cdot F\ (\mathrm{C/mol})} \approx \lambda_{\mathrm{H_2}} \cdot \frac{I\ (\mathrm{A}) \cdot N_{\mathrm{cells}}}{1,93 \cdot 10^5\ (\mathrm{A\ s/mol})}; \tag{5.1.2}$$

$\lambda_{\mathrm{H_2}}$ is the stoichiometric ratio (**3.1.42**) of hydrogen. The input power of hydrogen based on HHV ($P^{\mathrm{HHV}}_{\mathrm{H_2,in}}$), and the input power of hydrogen based on LHV ($P^{\mathrm{LHV}}_{\mathrm{H_2,in}}$), are calculated as follows:

$$P^{\mathrm{HHV}}_{\mathrm{H_2,in}}\ (\mathrm{kW}) = q_{\mathrm{n,H_2,in}}\ (\mathrm{mol/s}) \cdot 79,4 \cdot 10^{-3}\ (\mathrm{kWh/mol}) \cdot 3600\ (\mathrm{s/h}) \quad \text{and} \tag{5.1.3a}$$

$$P^{\mathrm{LHV}}_{\mathrm{H_2,in}}\ (\mathrm{kW}) = q_{\mathrm{n,H_2,in}}\ (\mathrm{mol/s}) \cdot 67,2 \cdot 10^{-3}\ (\mathrm{kWh/mol}) \cdot 3600\ (\mathrm{s/h}). \tag{5.1.3b}$$

- **Thermal energy** (E_{th}) is supplied to the cell/stack assembly unit using one or more heat transfer fluids (input substance streams), ([12]) such as hydrogen and air/oxygen, as detailed in Table 3:

$$E_{\text{th}}\ \text{(kWh)} = P_{\text{th}}\ \text{(kW)} \cdot t\ \text{(h)}; \tag{5.1.4a}$$

t represents time, and the thermal power (P_{th}) is calculated as follows:

$$P_{\text{th}}\ \text{(kW)} = \sum_{\text{i}} q_{\text{m}}^{\text{i}}\ \text{(kg/s)} \cdot c_{\text{p}}^{\text{i}}\left(T^{\text{i}}\right)\ \text{(kJ/(kg K))} \cdot \left(T^{\text{i}}\ \text{(K)} - T^{0}\ \text{(K)}\right); \tag{5.1.4b}$$

q_{m}^{i}, c_{p}^{i}, and T^{i} represent the mass flow rate, the specific heat capacity at constant pressure (p^{i}), and the temperature of component (constituent) i in the electrode gas (see Table 3), respectively, while t is the duration for which heat is supplied to the cell/stack assembly unit. In practical terms, c_{p}^{i} is estimated for a given fluid temperature and pressure according to the manufacturer's instructions. The temperature of component i corresponds to that of the electrode gas, while the pressure of the electrode gas is the sum of the partial pressures of all constituent components i. The mass flow rate of fluid i (q_{m}^{i}) is calculated as follows:

$$q_{\text{m}}^{\text{i}}\ \text{(kg/s)} = x_{\text{n,i}}\ \text{(mol/mol)} \cdot M_{\text{i}}\ \text{(kg/mol)} \cdot q_{\text{n}}\ \text{(mol/s)}; \tag{5.1.4c}$$

$x_{\text{n,i}}$ and M_{i} represent the molar concentration and the molar mass of component i in the electrode gas (see Table 3), respectively, while q_{n} denotes the molar flow rate of the electrode gas under SATP conditions.

- **Pneumatic energy** (E_{p}), which is relevant for a cell/stack assembly unit using pressurised electrode gas (pressurised cell/stack assembly unit), is calculated as follows:

$$E_{\text{p}}\ \text{(kWh)} = P_{\text{p}}\ \text{(kW)} \cdot t\ \text{(h)}. \tag{5.1.5a}$$

The pneumatic power (P_{p}) is calculated using the following expression:

$$P_{\text{p}}\ \text{(kW)} = \sum_{\text{j}} \left(\frac{\gamma^{\text{j}}}{\gamma^{\text{j}}-1}\right) \frac{\bar{Z}^{\text{j}}\left(p^{\text{j}},\, T^{\text{j}}\right) \cdot R_{\text{g}}\ \text{(kJ/(mol K))} \cdot T^{0}\ \text{(K)} \cdot q_{\text{n}}^{\text{j}}\ \text{(mol/h)}}{3600\ \text{(s/h)}} \cdot$$

$$\left(\left(\frac{p^{\text{j}}\ \text{(kPa)}}{p^{0}\ \text{(kPa)}}\right)^{\frac{\gamma^{\text{j}}-1}{\gamma^{\text{j}}}} - 1\right) \approx \sum_{\text{j}} \left(\frac{\gamma^{\text{j}}}{\gamma^{\text{j}}-1}\right) \bar{Z}^{\text{j}}\left(p^{\text{j}},\, T^{\text{j}}\right) \cdot 6,88 \cdot 10^{-4}\ \text{(kWh/mol)} \cdot$$

$$q_{\text{n}}^{\text{j}}\ \text{(mol/h)} \cdot \left(\left(\frac{p^{\text{j}}\ \text{(kPa)}}{p^{0}\ \text{(kPa)}}\right)^{\frac{\gamma^{\text{j}}-1}{\gamma^{\text{j}}}} - 1\right); \tag{5.1.5b}$$

$\bar{Z}^{\text{j}}$, p^{j} and T^{j} are the average compressibility factor, the pressure and the temperature of component j in the electrode gas (see Table 3), respectively, while R_{g}=8,3445 J/(mol K^{-1}) is the universal gas constant. The temperature of component j is that of the electrode gas while the pressure of the electrode gas is the sum of the partial pressures of all components j. The isentropic expansion factor of fluid j (γ^{j}) is calculated as follows:

$$\gamma^{\text{j}}(p^{\text{j}},\, T^{\text{j}}) = \frac{c_{\text{p}}^{\text{j}}\left(T^{\text{j}}\right)\ \text{(kJ/(kg K))}}{c_{\text{V}}^{\text{j}}\left(p^{\text{j}},\, T^{\text{j}}\right)\ \text{(kJ/(kg K))}} \neq 1; \tag{5.1.5c}$$

c_{p}^{j} and c_{V}^{j} are the specific heat capacity at constant pressure and at constant volume of component j, respectively. Practically, $\bar{Z}^{\text{j}}$ and γ^{j} are estimated for a given fluid temperature and pressure according to the manufacturer's instructions. For a pressurised cell/stack assembly unit, the pneumatic fluids j (input substance streams) are primarily hydrogen and air/oxygen, as outlined in Table 3. The molar flow rate of fluid j (q_{n}^{j}) is calculated as follows:

$$q_{\text{n}}^{\text{j}}\ \text{(mol/s)} = x_{\text{n,j}}\ \text{(mol/mol)} \cdot q_{\text{n}}\ \text{(mol/s)}; \tag{5.1.5d}$$

$x_{\text{n,j}}$ denotes the molar concentration of component j in the electrode gas.

In addition to reaction products such as water vapour (steam) and heat, the output of a HTFC cell/stack assembly unit includes **electricity**, specifically in the form of DC power ($P_{\text{el,dc}}$), as described in equation (1.0.2).

([12]) Radiative heat transfer to the cell/stack assembly unit, such as that provided by an electric furnace enclosing the unit to maintain the stack temperature, is indirectly accounted as it also contributes to the heating of the electrode gases.

5.2 HTSE cell/stack assembly unit

Figure 2 provides a schematic representation of the input and output streams of energy forms and substances in a HTSE cell/stack assembly unit.

Figure 2: Schematic illustration of the input and output streams (indicated by directional arrows) of energy forms (depicted in diamond shape) and substances (depicted in circular shape) in a HTSE cell/stack assembly unit (represented by a rectangular shape). The thick line surrounding the grey-shaded box outlines the boundary of the cell/stack assembly unit.

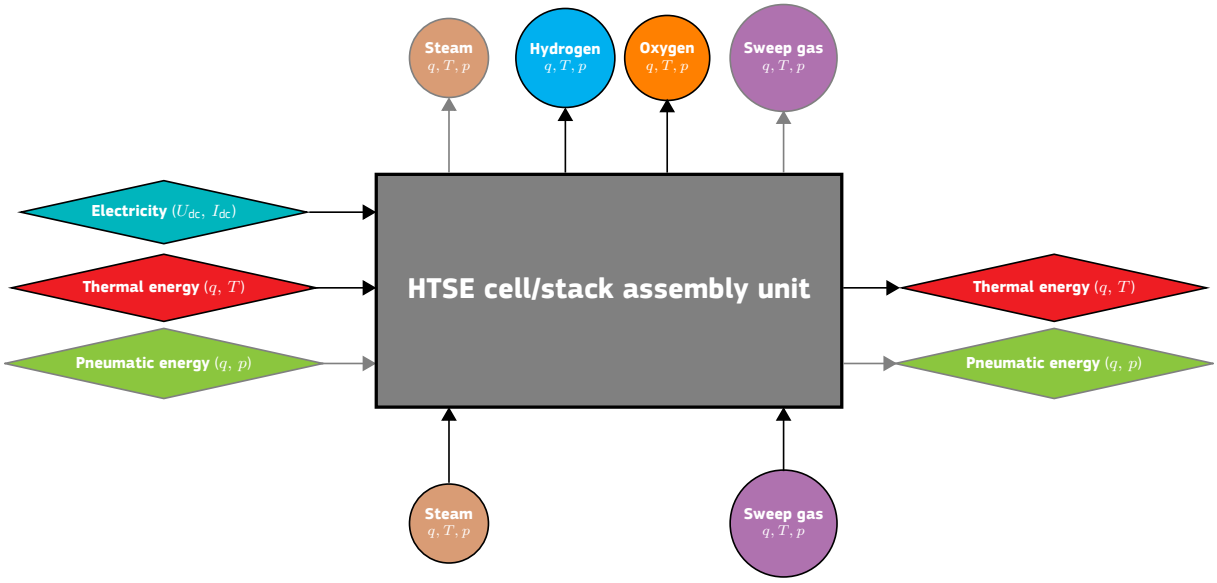

Note: For heat removal in SOE, air is primarily employed as a positrode sweep gas, while steam can, in principle, also serve as a negatrode sweep gas. In PCE, steam is used as a positrode sweep gas.

Source: JRC, 2024.

The input energy streams to a HTSE cell/stack assembly unit include:

- **Electricity** in the form of electric energy (E_{el}):

$$E_{\text{el}}\ (\text{kWh}) = P_{\text{el, dc}}\ (\text{kW}) \cdot t\ (\text{h}). \tag{5.2.1}$$

- **Thermal energy**, as described in equation (5.1.4a), in the form of heat supplied to the cell/stack assembly unit using one or more heat transfer fluids (input substance streams), rimarily steam and air, as detailed in Table 3 ([13]).

- **Pneumatic energy**, as described in equation (5.1.5a), is relevant only for a pressurised cell/stack assembly unit. For such units, the pneumatic component j of the electrode gas (input substance stream) is primarily steam.

The primary output gas stream of a HTSE cell/stack assembly unit is:

- **Hydrogen** with a molar flow rate ($q_{\text{n, H}_2\text{, out}}$) calculated as follows:

$$q_{\text{n, H}_2\text{, out}}\ (\text{mol/s}) = x_{\text{n, H}_2\text{, out}}\ (\text{mol/mol}) \cdot \frac{q_{\text{V, out}}\ (\text{m}^3/\text{s})}{V_{\text{m, H}_2}\ (\text{m}^3/\text{mol})}; \tag{5.2.2}$$

$x_{\text{n, H}_2\text{, out}}$ is the molar concentration of hydrogen in the outlet electrode gas, and $q_{\text{V, out}}$ is the product gas volumetric flow rate. The molar concentration of hydrogen can be estimated through gas analysis. Practically, the outlet molar concentration of hydrogen is determined as an average value $\bar{x}_{\text{n, H}_2\text{, out}}$, with standard variance $s^2\,(x_{\text{n, H}_2\text{, out}})$; for the calculations, refer to equation (E.3.2d) and equation (E.4.1d). In

([13]) Similar to HTFCs, radiative heat transfer to the cell/stack assembly unit - such as that provided by an electric furnace used to maintain the stack temperature - is indirectly accounted for as the electrode gases also receive heat in this manner. Additional heat may be generated within the cell/stack assembly unit via Joule heating, utilising a portion of the DC power supplied to maintain the stack temperature.

the absence of measurements of the outlet molar flow rate of hydrogen, this flow rate can be calculated as follows:

$$q_{\mathrm{n,H_2,out}}\ (\mathrm{mol/s}) = \frac{\eta_{\mathrm{F}}\ \%}{100\ \%} \cdot \frac{I\ (\mathrm{A}) \cdot N_{\mathrm{cells}}}{z \cdot F\ (\mathrm{C/mol})} \approx \frac{\eta_{\mathrm{F}}\ \%}{100\ \%} \cdot \frac{I\ (\mathrm{A}) \cdot N_{\mathrm{cells}}}{1,93 \cdot 10^5\ (\mathrm{A\ s/m^3})}, \tag{5.2.3}$$

where the Faradaic efficiency may be determined through preliminary testing, as detailed in Annex D. The output power of hydrogen based on HHV ($P^{\mathrm{HHV}}_{\mathrm{H_2,out}}$), and the output power of hydrogen based on LHV ($P^{\mathrm{LHV}}_{\mathrm{H_2,out}}$), are calculated as follows:

$$P^{\mathrm{HHV}}_{\mathrm{H_2,out}}\ (\mathrm{kW}) = q_{\mathrm{n,H_2,out}}\ (\mathrm{mol/s}) \cdot 79,4 \cdot 10^{-3}\ (\mathrm{kWh/mol}) \cdot 3600\ (\mathrm{s/h}) \quad \text{and} \tag{5.2.4a}$$

$$P^{\mathrm{LHV}}_{\mathrm{H_2,out}}\ (\mathrm{kW}) = q_{\mathrm{n,H_2,out}}\ (\mathrm{mol/s}) \cdot 67,2 \cdot 10^{-3}\ (\mathrm{kWh/mol}) \cdot 3600\ (\mathrm{s/h}). \tag{5.2.4b}$$

6 Test procedure

6.1 Test set-up, instrumentation and equipment

Figure 3 shows schematically the test system configuration for a cell/stack assembly unit in the test environment (**3.1.44**).

Figure 3: Schematic of the test system configuration for a cell/stack assembly unit, encompassing all subsystems. The dashed line encircling the green-shaded box indicates the boundary of the test environment, while the thick line surrounding the grey-shaded box delineates the perimeter of the cell/stack assembly unit.

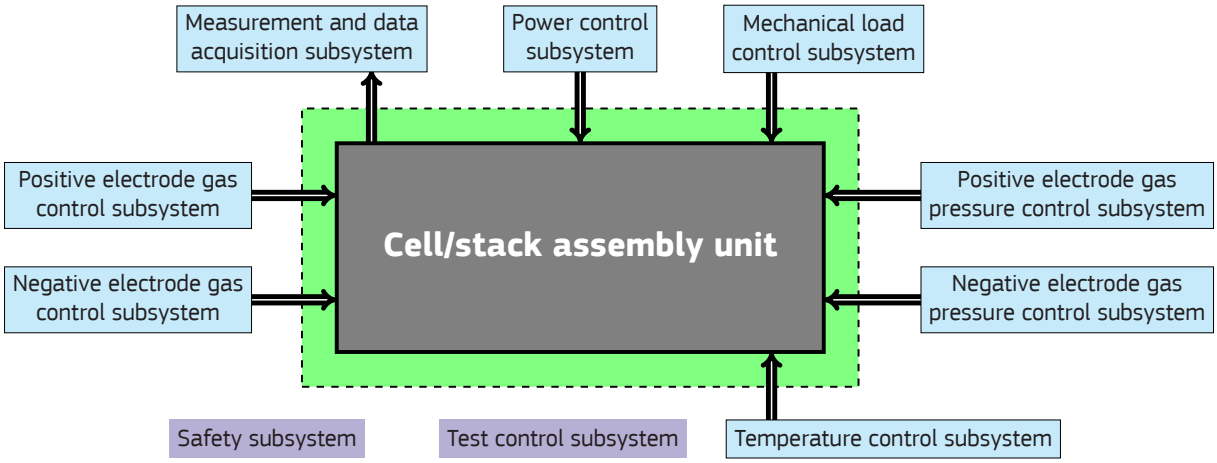

Source: JRC, 2024.

The functions of the individual test subsystems are as follows:

- The **measurement and DAQ** subsystem is responsible for acquiring and recording the test parameters of the cell/stack assembly unit, and optionally the environmental conditions of the test environment. THis is conducted in accordance with the specified measurement methods using appropriate instrumentation that meets the designated uncertainties and permissible variation ranges, as detailed in Table 2.
- The **power control** subsystem regulates the output current or voltage of the cell/stack assembly unit when in fuel cell mode, and the input current or voltage supplied to the unit during electrolysis mode.
- The optional **mechanical load control** subsystem applies and maintains a mechanical load that enhances contacts among components in the cell/stack assembly unit through compression during testing.
- The **electrode gas control** subsystems manage the composition, flow rate, and temperature of the respective electrode gases delivered to the cell/stack assembly unit.
- The optional **electrode gas pressure control** subsystems regulate the pressure of the respective electrode gases of the cell/stack assembly unit, for example, by employing back pressure control valves (PCVs).
- The **temperature control** subsystem maintains the temperature of the cell/stack assembly unit, including the interior temperature of the electric furnace housing the unit, to ensure its operating temperature remains within the specified tolerances.
- The **safety** subsystem functions as an automated detection and alarm system for hazards arising within the test environment and malfunctions of the test system. It operates based on defined parameters and criteria to mainatain a safe state for the test system and environment.
- The **test control** subsystem provides oversees the test environment by providing integrated control and regulation of each subsystem, including the monitoring of relevant test parameters, as listed in Table 1.

The actual test set-up employed, as well as the cell/stack assembly unit tested, should be detailed in the test report, including a description of the instruments and test equipment used; refer to Annex B for further information.

6.2 Test parameters

6.2.1 Test input parameters

Table 1 enumerates the static and variable TIPs used in the polarisation curve measurements conducted during the tests outlined in section 6.3.2 (Test 6.3.2) and section 6.3.3 (Test 6.3.3).

Table 1: Static and variable test input parameters

Parameter	Symbol	non-SI unit [a]	SI unit	Test 6.3.2	Test 6.3.3
Sweep rate(s) of current [b]	$\Delta I/\Delta t$		A/s	static	static
Sweep rate(s) of voltage [c]	$\Delta U/\Delta t$		V/s	static	static
Maximum current [b]	I_{max}		A	static	static
Cut-off voltage [b,c]	$U_{\text{cut-off}}$		V	static	static
Step duration [d]	t_{step}		s	static (variable)	static (variable)
Step sampling rate [d]	f_{step}	Hz	s^{-1}	static (variable)	static (variable)
Sweep sampling rate [e]	f_{sweep}	Hz	s^{-1}	static (variable)	static (variable)
		High-temperature fuel cell			
Inlet volumetric flow rate of positive electrode gas	$q_{\text{V, pos, in}}$	Nlpm, slpm [f]	m^3/s	static	variable
Utilisation of positive electrode gas	$\lambda^{-1}_{\text{gas, pos}}$	-	-	variable	static
Inlet molar concentration of component i in positive electrode gas [g]	$x_{\text{i, pos, in}}$		mol/mol	static	static
Inlet pressure of positive electrode gas	$p_{\text{pos, in}}$	mbar, kPa	N/m^2	static [h]	static [h]
Inlet temperature of positive electrode gas	$T_{\text{pos, in}}$	°C	K	static	static
Inlet volumetric flow rate of negative electrode gas	$q_{\text{V, neg, in}}$	Nlpm, slpm [f]	m^3/s	static	variable
Inlet molar concentration of component i in negative electrode gas [f]	$x_{\text{i, neg, in}}$		mol/mol	static	static
Utilisation of negative electrode gas	$\lambda^{-1}_{\text{gas, neg}}$	-	-	variable	static
Inlet pressure of negative electrode gas	$p_{\text{neg, in}}$	mbar, kPa	N/m^2	static [g]	static [h]
Inlet temperature of negative electrode gas	$T_{\text{neg, in}}$	°C	K	static	static
		High-temperature steam electrolyser			
Inlet volumetric flow rate of positive electrode gas	$q_{\text{V, pos, in}}$	Nlpm, slpm [f]	m^3/s	static	variable
Utilisation of positive electrode gas	$\lambda^{-1}_{\text{gas, pos}}$	-	-	variable	static
Inlet molar concentration of component i in positive electrode gas [f]	$x_{\text{i, pos, in}}$		mol/mol	static	static
Inlet pressure of positive electrode gas	$p_{\text{pos, in}}$	mbar, kPa	N/m^2	static [h]	static [h]
Inlet temperature of positive electrode gas	$T_{\text{pos, in}}$	°C	K	static	static
Inlet volumetric flow rate of negative electrode gas	$q_{\text{V, neg, in}}$	Nlpm, slpm [f]	m^3/s	static	variable
Inlet molar concentration of component i in negative electrode gas [g]	$x_{\text{i, neg, in}}$		mol/mol	static	static
Utilisation of negative electrode gas	$\lambda^{-1}_{\text{gas, neg}}$	-	-	variable	static
Inlet pressure of negative electrode gas	$p_{\text{neg, in}}$	mbar, kPa	N/m^2	static [h]	static [h]
Inlet temperature of negative electrode gas	$T_{\text{neg, in}}$	°C	K	static	static

Note: Under galvanostatic (potentiostatic) conditions, current (voltage) serves as a TIP. Accordingly, current density is a TIP under galvanostatic conditions.

[a] These units are frequently used.
[b] This parameter is pertinent for measurements under galvanostatic conditions.
[c] This parameter is pertinent for measurements under potentiostatic conditions.
[d] This parameter is only relevant when current or voltage is adjusted incrementally.
[e] Relevant solely for current sweep (**3.1.8**) or voltage sweep (**3.1.49**).
[f] Normal litre per minute, standard litre per minute.
[g] Refer to Table 3 for the inlet electrode gas components.
[h] For automated gas pressure regulation using a back PCV at the outlet of the cell/stack assembly unit, this TIP is variable.

Source: JRC, 2024.

Table 2 provides the instrument standard uncertainties for generic TIPs and TOPs, indicating whether these standard uncertainties are rated (nominal) or full scale (FS).

Table 2: Instrument standard uncertainties of generic test input parameters and generic test output parameters

Parameter	Symbol	Instrument uncertainty
Current	I	± 1 % of rated
Voltage	U	$\pm$0,5 % of rated
Flow rate	q	± 3 % of FS
Molar concentration	x_{n}	± 2 % of FS
Pressure	p	± 3 % of rated
Temperature	T	$\pm$0,5 K

Source: JRC, 2024.

Table 3 details the constituents of the electrode gases at the inlet and outlet of HTFCs and HTSEs.

Table 3: Electrode gas composition at the inlet and outlet of cell/stack assembly units

cell/stack	Type of electrode	port	Electrode gas composition: Hydrogen	Air	Oxygen	Steam	Nitrogen
			High-temperature fuel cell				
SOFC [a]	Positive electrode	inlet	✓			✓ [b]	(✓) [c]
		outlet	(✓) [d]			✓	(✓) [c]
	Negative electrode	inlet		✓ [e]	(✓) [f]		(✓) [c]
		outlet		✓	✓		(✓) [c]
PCFC [g]	Positive electrode	inlet	✓			(✓) [b]	(✓) [c]
		outlet	✓ [d]			(✓) [b]	(✓) [c]
	Negative electrode	inlet		✓	(✓) [e]		(✓) [c]
		outlet		✓	✓	✓	(✓) [c]
			High-temperature steam electrolyser				
SOEC [h]	Positive electrode	inlet		✓ [e]			(✓) [c]
		outlet		✓ [e]	✓		(✓) [c]
	Negative electrode	inlet	✓ [i]			✓	
		outlet	✓			✓	
PCEC [j]	Positive electrode	inlet				✓	(✓) [c]
		outlet			✓	✓	(✓) [c]
	Negative electrode	inlet	✓				
		outlet	✓				

Note: For testing and operation purposes, the use of ✓ indicates the mandatory presence of components in the electrode gas, while (✓) signifies an optional inclusion of components in the electrode gas.
[a] This includes rSOCs operated in fuel cell mode.
[b] Small additions of water vapour (steam) may be used to adjust the partial pressure of oxygen in the electrode gas, thereby establishing a defined OCV.
[c] Nitrogen may be utilised as a diluent or inert gas and may also be employed for test safety, particularly during pressure operation.
[d] Cell/stack assembly units in a dead-ended configuration do not have a fuel (hydrogen) gas outlet.
[e] Typically, air is used for heat removal.
[f] Using oxygen instead of air enhnaces the performance of the cell/stack assembly unit by reducing mass transfer limitations.
[g] This includes rPCCs operated in fuel cell mode.
[h] This includes rSOCs operated in electrolysis mode.
[i] Small additions of hydrogen may be used to adjust the partial pressure of oxygen in the electrode gas to prevent metal (*i. e.* Ni) oxidation in the cermet.
[j] This includes rPCCs operated in electrolysis mode.
Source: JRC, 2024.

6.2.2 Test output parameters

Table 4 enumerates the TOPs obtained from polarisation curve measurements conducted under galvanostatic or potentiostatic conditions, as well as the parameters derived from post-processing the test results.

Table 4: Test output parameters

Parameter	Symbol	non-SI unit	(derived) SI unit
Current	I_{dc}		A
Current density	J	A/cm^2	A/m^2
Cell voltage(s)	U_{cell}		V ([c])
Voltage	U_{dc}		V
Average repeating unit voltage	$\bar{U}_{\text{RU}}$		V
Reversible voltage ([b])	U_{rev}		V ([a])
Activation polarisation voltage	U_{act}		V ([a])
Concentration polarisation voltage	U_{conc}		V ([a])
Ohmic resistance	R		Ω
Area-specific resistance	R_{ASR}	Ω.cm^2	Ω.m^2
Electric power	$P_{\text{el, dc}}$		kW
Electric power density	$P_{\text{el, d}}$	W/cm^2	W/m^2
Operating temperature ([c])	T_{stack}	°C	K
	High-temperature fuel cell		
Fuel cell repeating unit voltage	$U_{\text{RU, FC}}$		V
Outlet volumetric flow rate of positive electrode gas	$q_{\text{V, pos, out}}$	Nlpm, slpm	m^3/s
Outlet molar concentration of component i in positive electrode gas ([d])	$x_{\text{i, pos, out}}$		mol/mol
Outlet pressure of positive electrode gas	$p_{\text{pos, out}}$	mbar, kPa	N/m^2
Outlet temperature of positive electrode gas	$T_{\text{pos, out}}$	°C	K
Outlet volumetric flow rate of negative electrode gas	$q_{\text{V, neg, out}}$	Nlpm, slpm	m^3/s
Outlet molar concentration of component i in negative electrode gas	$x_{\text{i, neg, out}}$		mol/mol
Outlet pressure of negative electrode gas	$p_{\text{neg, out}}$	mbar, kPa	N/m^2
Outlet temperature of negative electrode gas	$T_{\text{neg, out}}$	°C	K
Fuel cell electric efficiency based on HHV	$\eta_{\text{el, FC}}^{\text{HHV}}$	%	
Output thermal power	$P_{\text{th, out}}$		kW
Fuel cell thermal efficiency based on HHV	$\eta_{\text{th, FC}}^{\text{HHV}}$	%	
Fuel cell electric efficiency based on LHV	$\eta_{\text{el, FC}}^{\text{LHV}}$	%	
Fuel cell thermal efficiency based on LHV	$\eta_{\text{th, FC}}^{\text{LHV}}$	%	
	High-temperature steam electrolyser		
Electrolyser repeating unit voltage	$U_{\text{RU, EL}}$		V
Outlet volumetric flow rate of positive electrode gas	$q_{\text{V, pos, out}}$	Nlpm, slpm	m^3/s
Outlet molar concentration of component i in positive electrode gas ([d])	$x_{\text{i, pos, out}}$		mol/mol
Outlet pressure of positive electrode gas	$p_{\text{pos, out}}$	mbar, kPa	N/m^2
Outlet temperature of positive electrode gas	$T_{\text{pos, out}}$	°C	K
Outlet volumetric flow rate of negative electrode gas	$q_{\text{V, neg, out}}$	Nlpm, slpm	m^3/s
Outlet molar concentration of component i in negative electrode gas ([d])	$x_{\text{i, neg, out}}$		mol/mol
Outlet pressure of negative electrode gas	$p_{\text{neg, out}}$	mbar, kPa	N/m^2
Outlet temperature of negative electrode gas	$T_{\text{neg, out}}$	°C	K
Electrolyser energy efficiency based on HHV	$\eta_{\text{e, EL}}^{\text{HHV}}$	%	
Electrolyser energy efficiency based on LHV	$\eta_{\text{e, EL}}^{\text{LHV}}$	%	

Note: Under galvanostatic (potentiostatic) conditions, voltage (current) is a TOP. Accordingly, current density is a TOP under potentiostatic conditions. The uncertainties of these TOPs and those of the TIPs (see Table 1) are not listed in this table.

([a]) The metric prefix 'm' stands for 'milli' $\left(10^{-3}\right)$ and 'k' represents 'kilo' $\left(10^{3}\right)$. These prefixes may also be used.

([b]) In fuel cell mode, this TOP serves as a control parameter for stable state (**3.1.38**) of the cell/stack assembly unit, refer to section 6.3.1. The theoretical value is calculated in accordance with equation (7.1.3a).

([c]) This is a control parameter for the stable state (**3.1.38**) of the cell/stack assembly unit, refer to section 6.3.1

([d]) Refer to Table 3 for details on the outlet electrode gases.

Source: JRC, 2024.

6.3 Measurement of current-voltage characteristics

6.3.1 Test parameter control for stable state

Testing of the fully conditioned cell/stack assembly unit begins by gradually adjusting the static TIPs (as outlined in Table 1) usually stepwise to their specified values (test conditions) in accordance with the manufacturer's instructions. The cell/stack assembly unit should be operated until the stable state is achieved under OCV

conditions (I = 0) in fuel cell mode, with the stack temperature and DC voltage serving as the initial controlling parameters.

The stable state of the cell/stack assembly unit, including its tolerance range and observation duration, should be defined prior to testing. It is recommended that the variation in stack temperature does not exceed $\pm$**5** K for a minimum duration of **30** seconds. During this period, the DC voltage of the cell/stack assembly unit should not vary by more than **5** mV for any RU in FC mode and **10** mV in electrolysis mode.

Once stable state of the fully conditioned cell/stack assembly unit is achieved, the measurement of current-voltage (I-U) characteristics can proceed. This can be done by incrementally changing the current under galvanostatic conditions or the voltage under potentiostatic conditions, as in method (**A**), or by sweeping the current or voltage at a constant speed, as in method (**B**); refer to Figure 4. Each step should ensure that the cell/stack assembly unit reaches a stable state after each incremental change in current or voltage. Specifically, each step must allow sufficient time for the unit to equilibrate. The duration of each step depends on several factors, including the unit's architecture, technology, materials, operating history, and state. Typically, the number of steps will result in 20 to 40 data points for the polarisation curve, measured in either direction:

- Ascending from zero current (I = 0) to the maximum current ($I = I_{\text{max}}$), and
- Descending from the maximum current to zero current in FC mode.

In electrolysis mode, where the current is conventionally negative, the term 'maximum current' is replaced by 'minimum current'. The maximum and minimum current should be:

- Recommended by the manufacturer of the cell/stack assembly unit, or
- Selected based on the following criteria:
  - The minimum/maximum voltage should be 0,6 V multiplied by the number of cells or repeating units electrically connected in series in the cell/stack assembly unit, or
  - The absolute power of the cell/stack assembly unit should be at its highest.

When using a current sweep or voltage sweep, the rate must be set so that the maximum width of the resultant voltage hysteresis ([14]) does not exceed **10** mV for any RU. Unless specified by the manufacturer of the cell/stack assembly unit, this may necessitate preliminary testing.

In addition to specifying the gas compositions, flow rates, temperatures and pressures, the actual steps for method (**A**) and the actual sweep rate for method (**B**) should also be outlined as part of the test program.

6.3.2 Determination of polarisation curves under constant gas flow rate

The term 'constant gas flow rate' may refer to a consistent volumetric flow rate of the positive electrode gas, the negative electrode gas, or both. The gas flow rate should be set to correspond to that required to achieve the maximum current of the cell/stack assembly unit.

(**A**) When the current or voltage is adjusted stepwise, at a minimum, the current, voltage, and temperature of the cell/stack assembly unit, as well as the flow rate and pressure of the electrode gases, should be recorded for the entire step duration (**3.1.41**) at the specified sampling rate. The average value, along with the standard uncertainty (u) or combined standard uncertainty (u_c) of these measurements, should represent the values of the polarisation curve and their variations for that step; refer to Annex E. The average value should be calculated from at least the last five recorded data points.

(**B**) When a current sweep or voltage sweep is emploed, at least the current, voltage, and temperature of the cell/stack assembly unit should be measured at the specified sweep sampling rate. The measured instantaneous values will be used as the values for the polarisation curve.

Additional test parameters may also be measured, as outlined in Table 1 and Table 4.

6.3.3 Determination of polarisation curves under constant stoichiometric ratio or constant gas utilisation

Constant stoichiometric ratio (λ) or gas utilisation (λ^{-1}) (**3.1.17**) may refer to that of positive electrode gas, of negative electrode gas, or of both gases.

([14]) This refers to the maximum difference in voltage when sweeping from OCV to maximum current and back to OCV, or *vice versa*.

(**A**) When current or voltage is changed stepwise, at least current, voltage, and temperature of the cell/stack assembly unit, as well as flow rate and pressure of the electrode gases are recorded for the entire step duration at the specified sampling rate. The average value along with its standard uncertainty or combined standard uncertainty of these measurements shall be the polarisation curve values and their variations for that step; see Annex E. The average value shall be calculated from at least the last five recorded values.

(**B**) When a current sweep or voltage sweep is used, at least current, voltage, and temperature of the cell/stack assembly unit are measured at the specified sweep sampling rate. The measured instantaneous values shall be the polarisation curve values.

Additional test parameters may also be measured, as outlined in Table 1 and Table 4.

7 Data post-processing and presentation of test results

7.1 Data post-processing

Voltage breakdown analysis (VBA) (Lang *et al.*, 2017, Ma *et al.*, 2021, Falcão and Pinto, 2020, Gerhardt *et al.*, 2021, Dizon *et al.*, 2022) provides a method to estimate voltage losses in HTFCs. This techniques involves fitting the measured data from the polarisation curve measurements of the cell/stack assembly unit to an empirical formula using non-linear least squares (NLS) fitting. The formula is as follows:

$$U_{\mathrm{RU,FC}}\ (\mathrm{V}) \;=\; \frac{U_{\mathrm{dc}}}{N_{\mathrm{cells}}} \;=\; U_{\mathrm{rev}}\ (\mathrm{V}) \;-\; U_{\mathrm{act}}\ (\mathrm{V}) \;-\; I\ (\mathrm{A}) \cdot R\ (\Omega) \;-\; U_{\mathrm{conc}}\ (\mathrm{V}); \tag{7.1.1}$$

$U_{\mathrm{RU,FC}}$ is the voltage of a RU in the cell/stack assembly unit operated in fuel cell mode, U_{rev} is the reversible voltage, given by equation (7.1.3a), U_{act} is the activation polarisation voltage in the electrodes of the cell/stack assembly unit, given by equation (7.1.5), I is the current flowing perpendicular to the active electrode area of each cell in the cell/stack assembly unit, R is the resistance of the cell/stack assembly unit, and U_{conc} is the concentration polarisation voltage in the cell/stack assembly unit, given by equation (7.1.6).

For HTSEs, voltage gains can be estimated by fitting the measured data of the polarisation curve measurements of the cell/stack assembly unit to an empirical formula using NLS fitting, as follows:

$$U_{\mathrm{RU,EL}}\ (\mathrm{V}) \;=\; \frac{U_{\mathrm{dc}}}{N_{\mathrm{cells}}} \;=\; U_{\mathrm{rev}}\ (\mathrm{V}) \;+\; U_{\mathrm{act}}\ (\mathrm{V}) \;+\; I\ (\mathrm{A}) \cdot R\ (\Omega) \;+\; U_{\mathrm{conc}}\ (\mathrm{V}) \tag{7.1.2}$$

$U_{\mathrm{RU,EL}}$ is the voltage of a RU in the cell/stack assembly unit operated in electrolysis mode.

In equation (7.1.1) and equation (7.1.2), the R is estimated from the slopes of the measured polarisation curves, for instance, through curve fitting. Alternatively, R can be determined over a suitably wide interval of the measured polarisation curves by calculating the ratio of differences in voltage to the corresponding current of the cell/stack assembly unit. An interval is deemed suitable if the associated section of the polarisation curve graph is linear, thereby ensuring that voltage and current are practically directly proportional throughout the interval. Ideally, this interval should be centred between the minimum and maximum current of the the measured polarisation curve.

In the absence of gas crossover across the electrodes and other non-ideal conditions, the temperature-dependent reversible voltage is calculated as follows (Jia and Taheri, 2021):

$$\begin{aligned} U_{\mathrm{rev}}(T)\ (\mathrm{V}) \;&=\; 1,253\ \mathrm{V} \;-\; 2,4516 \cdot 10^{-4}\ (\mathrm{V/K}) \cdot T\ (\mathrm{K}) \\ &\pm\; U_{\mathrm{th}}\ (\mathrm{V})\ \log\left(\frac{p_{\mathrm{H_2}}\ (\mathrm{kPa})}{p^0\ (\mathrm{kPa})} \cdot \left(\frac{p_{\mathrm{O_2}}\ (\mathrm{kPa})}{p^0\ (\mathrm{kPa})}\right)^{0,5} \cdot \left(\frac{p_{\mathrm{H_2O}}\ (\mathrm{kPa})}{p^0\ (\mathrm{kPa})}\right)^{-1}\right); \end{aligned} \tag{7.1.3a}$$

$$U_{\mathrm{th}}\ (\mathrm{V}) \;=\; \frac{R_{\mathrm{g}}\ (\mathrm{J/(mol\ K)}) \cdot T\ (\mathrm{K})}{z \cdot F\ (\mathrm{C/mol})} \;\approx\; 43,09 \cdot 10^{-6}\ (\mathrm{V/K}) \cdot T\ (\mathrm{K}), \tag{7.1.3b}$$

where U_{th} is the thermal voltage (positive for FC mode and negative for electrolysis mode), $p_{\mathrm{H_2}}$, $p_{\mathrm{O_2}}$, and $p_{\mathrm{H_2O}}$ are the partial pressure of hydrogen, oxygen and steam in the concerned electrode gases, respectively, and T is the operating temperature of the cell/stack assembly unit (T_{stack}). The use of 0,5 as power exponent arises because half a mole of oxygen is involved in both the HTFC reaction (4.1.1) and the HTSE reaction (4.2.1). In cases where the pressure of a respective electrode gas exceeds the standard ambient pressure, the standard ambient pressure in equation (7.1.3a) must be replaced by the pressure of the concerned electrode gas. Note that the sum of the partial pressure of all constituents within an electrode gas equals the pressure of that gas. The activation polarisation voltage is depict in the Butler-Volmer equation (Hernández-Gómez *et al.*, 2020):

$$I\ (\mathrm{A}) \;=\; I_0 \cdot \left[\exp\left(\alpha^{\mathrm{neg}} \frac{U_{\mathrm{act}}\ (\mathrm{V})}{U_{\mathrm{th}}\ (\mathrm{V})}\right) - \exp\left(-\left(1-\alpha^{\mathrm{pos}}\right) \frac{U_{\mathrm{act}}\ (\mathrm{V})}{U_{\mathrm{th}}\ (\mathrm{V})}\right)\right]; \tag{7.1.4}$$

I_0, α^{neg}, and α^{pos} denote the exchange current, the negative electrode charge transfer coefficient, and the positive electrode charge transfer coefficient, respectively. The exchange current is an indicator of the electrode reaction kinetics (Fukumoto *et al.*, 2022). Assuming $\alpha^{\mathrm{neg}} = \alpha^{\mathrm{pos}} = 0,5$ in equation (7.1.4), the temperature-dependent activation polarisation voltage is calculated as follows:

$$U_{\mathrm{act}}(T)\ (\mathrm{V}) \;=\; 2U_{\mathrm{th}}\ (\mathrm{V}) \cdot \sinh^{-1}\left(\frac{I\ (\mathrm{A})}{2I_0\ (\mathrm{A})}\right). \tag{7.1.5}$$

The temperature-dependent concentration polarisation voltage is calculated as follows (Hernández-Gómez *et al.*, 2020):

$$U_{\mathrm{conc}}(T)\ (\mathrm{V}) \;=\; \pm U_{\mathrm{th}}\ (\mathrm{V}) \cdot \log\left(\frac{c^0_{\mathrm{O_2}}\ (\mathrm{mol/m^3})}{c^{\mathrm{TPB}}_{\mathrm{O_2}}\ (\mathrm{mol/m^3})} \cdot \frac{c^0_{\mathrm{H_2}}\ (\mathrm{mol/m^3})}{c^{\mathrm{TPB}}_{\mathrm{H_2}}\ (\mathrm{mol/m^3})} \cdot \left(\frac{c^0_{\mathrm{H_2O}}\ (\mathrm{mol/m^3})}{c^{\mathrm{TPB}}_{\mathrm{H_2O}}\ (\mathrm{mol/m^3})}\right)^{-1}\right); \tag{7.1.6a}$$

$c^{\mathsf{TPB}}_{\mathsf{O}_2}$, $c^{\mathsf{TPB}}_{\mathsf{H}_2}$, and $c^{\mathsf{TPB}}_{\mathsf{H}_2\mathsf{O}}$ are the concentrations of oxygen, hydrogen, and steam at the respective electrode gas-electrolyte-electrode interface (triple-phase boundary), respectively, while $c^{0}_{\mathsf{O}_2}$, $c^{0}_{\mathsf{H}_2}$, and $c^{0}_{\mathsf{H}_2\mathsf{O}}$ are their equilibrium concentrations in the respective electrode gases. Note that equation (7.1.6a) applies in the absence of steam in the negative electrode gas of both PCFC and PCEC. When the concentration of a reactant approaches zero at the TPB, equation (7.1.6a) simplifies to:

$$U_{\mathsf{conc}}(T)\ (\mathsf{V}) \;=\; -U_{\mathsf{th}}\ (\mathsf{V}) \cdot \log\left(1 - \frac{I\ (\mathsf{A})}{I_{\mathsf{L}}\ (\mathsf{A})}\right); \tag{7.1.6b}$$

I_{L} is the limiting current, representing the mass transfer (diffusion) limitation of the reactant at the TPB in the concerned electrode.

The area-specific resistance (ASR) (R_{ASR}) is calculated as follows:

$$R_{\mathsf{ASR}}\ (\Omega.\mathsf{cm}^2) \;=\; R\ (\Omega) \cdot A_{\mathsf{act}}\ (\mathsf{cm}^2); \tag{7.1.7}$$

R is the resistance used in equation (7.1.1) for HTFCs and equation (7.1.2) for HTSEs.

For a HTFC, electrical efficiency is generally of interest, and in combined heat and power (CHP) applications, thermal efficiency is also relevant. For a HTSE, the focus is on energy efficiency.

The electrical efficiency of a HTFC is determined through the fuel cell electric efficiency based on HHV ($\eta^{\mathsf{HHV}}_{\mathsf{el,FC}}$), and fuel cell electric efficiency based on LHV ($\eta^{\mathsf{LHV}}_{\mathsf{el,FC}}$), calculated as follows:

$$\eta^{\mathsf{HHV}}_{\mathsf{el,FC}}\ (\%) \;=\; \frac{P_{\mathsf{el,dc}}\ (\mathsf{kW})}{P^{\mathsf{HHV}}_{\mathsf{H_2,in}}\ (\mathsf{kW}) \;+\; P_{\mathsf{th,in}}\ (\mathsf{kW}) \;+\; P_{\mathsf{p,in}}\ (\mathsf{kW})} \cdot 100\ \%\ \text{ and} \tag{7.1.8a}$$

$$\eta^{\mathsf{LHV}}_{\mathsf{el,FC}}\ (\%) \;=\; \frac{P_{\mathsf{el,dc}}\ (\mathsf{kW})}{P^{\mathsf{LHV}}_{\mathsf{H_2,in}}\ (\mathsf{kW}) \;+\; P_{\mathsf{th,in}}\ (\mathsf{kW}) \;+\; P_{\mathsf{p,in}}\ (\mathsf{kW})} \cdot 100\ \%, \tag{7.1.8b}$$

respectively; in principle, $P_{\mathsf{el,dc}}$ is given by equation (1.0.2), $P^{\mathsf{HHV}}_{\mathsf{H_2,in}}$ is given by equation (5.1.3a), $P_{\mathsf{th,in}}$ is given by equation (5.1.4b), $P_{\mathsf{p,in}}$ is given by equation (5.1.5b), and $P^{\mathsf{LHV}}_{\mathsf{H_2,in}}$ is given by equation (5.1.3b).

The thermal efficiency of a HTFC is determined as the fuel cell thermal efficiency based on HHV ($\eta^{\mathsf{HHV}}_{\mathsf{th,FC}}$), and fuel cell thermal efficiency based on LHV ($\eta^{\mathsf{LHV}}_{\mathsf{th,FC}}$), calculated as follows:

$$\eta^{\mathsf{HHV}}_{\mathsf{th,FC}}\ (\%) \;=\; \frac{P_{\mathsf{th,out}}\ (\mathsf{kW})}{P^{\mathsf{HHV}}_{\mathsf{H_2,in}}\ (\mathsf{kW}) \;+\; P_{\mathsf{th,in}}\ (\mathsf{kW}) \;+\; P_{\mathsf{p,in}}\ (\mathsf{kW})} \cdot 100\ \%\ \text{ and} \tag{7.1.9a}$$

$$\eta^{\mathsf{LHV}}_{\mathsf{th,FC}}\ (\%) \;=\; \frac{P_{\mathsf{th}}\ (\mathsf{kW})}{P^{\mathsf{LHV}}_{\mathsf{H_2,in}}\ (\mathsf{kW}) \;+\; P_{\mathsf{th,in}}\ (\mathsf{kW}) \;+\; P_{\mathsf{p,in}}\ (\mathsf{kW})} \cdot 100\ \%, \tag{7.1.9b}$$

respectively; in principle, $P_{\mathsf{th,out}}$ is given by equation (5.1.4b). Note that, in equation (7.1.8) and equation (7.1.9), pure hydrogen gas (H_2) is considered as the input fuel.

The energy efficiency for a HTSE is determined through the electrolyser energy efficiency based on HHV ($\eta^{\mathsf{HHV}}_{\mathsf{e,EL}}$), and electrolyser energy efficiency based on LHV ($\eta^{\mathsf{LHV}}_{\mathsf{e,EL}}$), calculated as follows:

$$\eta^{\mathsf{HHV}}_{\mathsf{e,EL}}\ (\%) \;=\; \frac{P^{\mathsf{HHV}}_{\mathsf{H_2,out}}\ (\mathsf{kW})}{P_{\mathsf{el,dc}}\ (\mathsf{kW}) \;+\; P_{\mathsf{th,in}}\ (\mathsf{kW}) \;+\; P_{\mathsf{p,in}}\ (\mathsf{kW})} \cdot 100\ \%\ \text{ and} \tag{7.1.10a}$$

$$\eta^{\mathsf{LHV}}_{\mathsf{e,EL}}\ (\%) \;=\; \frac{P^{\mathsf{LHV}}_{\mathsf{H_2,out}}\ (\mathsf{kW})}{P_{\mathsf{el,dc}}\ (\mathsf{kW}) \;+\; P_{\mathsf{th,in}}\ (\mathsf{kW}) \;+\; P_{\mathsf{p,in}}\ (\mathsf{kW})} \cdot 100\ \%, \tag{7.1.10b}$$

respectively; in principle, $P^{\mathsf{HHV}}_{\mathsf{H_2,out}}$ is given by equation (5.2.4a), and $P^{\mathsf{LHV}}_{\mathsf{H_2,out}}$ is given by equation (5.2.4b). When hydrogen is used in addition to steam as the negative electrode inlet gas in SOE, $P^{\mathsf{HHV}}_{\mathsf{H_2,out}}$ in equation (7.1.10a) and $P^{\mathsf{LHV}}_{\mathsf{H_2,out}}$ in equation (7.1.10b) should be replaced by the differences, $P^{\mathsf{HHV}}_{\mathsf{H_2,out}}$ - $P^{\mathsf{HHV}}_{\mathsf{H_2,in}}$ and $P^{\mathsf{LHV}}_{\mathsf{H_2,out}}$ - $P^{\mathsf{LHV}}_{\mathsf{H_2,in}}$, respectively. The same substitution applies when hydrogen is used, in addition to steam, as the negative electrode inlet gas in PCE.

Unless the inlet gases are introduced to the cell/stack assembly unit at pressures above atmospheric pressure, the input pneumatic power is not considered in equation (7.1.8), equation (7.1.9), and equation (7.1.10) (P_{p} = 0). In these three equations, the input thermal power of the cell/stack assembly unit is the sum of the individual input thermal power of both electrode gases. The same principle applies to the input pneumatic power of the cell/stack assembly unit.

7.2 Presentation of test results

Figure 4 displays polarisation curves (average repeating unit voltage versus current density) alongside the evolution of stack temperature for an 84 cm^2 solid oxide 5-cell/stack assembly unit operated in both FC (SOFC)

mode and electrolysis (SOEC) mode. Additionally, performance curves (power density versus current density), derived from the polarisation curves, are presented. The figure also illustrates the progression of gas utilisation, specifically focusing on hydrogen gas utilisation in SOFC mode and steam conversion in SOFC mode.

Figure 4: Polarisation curves (depicting average repeating unit voltage and stack temperature versus current density) (top) and performance curves (illustrating average power density and gas utilisation versus current density) (bottom) for an 84 cm^2 solid oxide 5-cell/stack assembly unit (designation: CSZ-10-05-043) operated in fuel cell (SOFC) mode (a) and electrolysis (SOEC) mode (b).

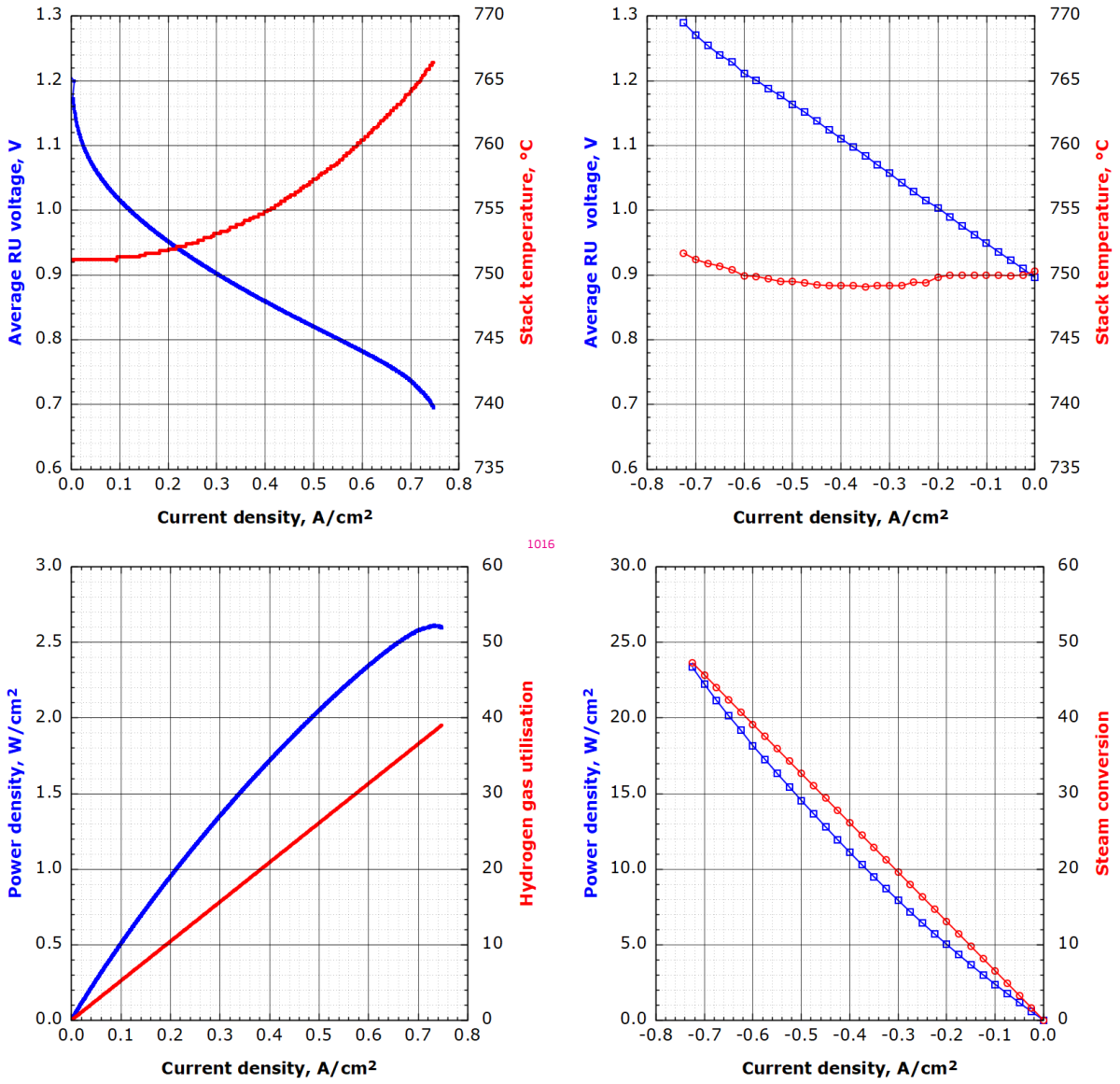

(a) SOFC mode: 2.5 Nlpm H_2 (negative electrode) and 2.5 Nlpm N_2 / 20 Nlpm air (positive electrode)

(b) SOEC mode: 0.63 Nlpm H_2 / 2 Nlpm $H_2O_{(g)}$ (negative electrode) and 5 Nlpm air (positive electrode)

Note: By convention, values of current density are displayed as positive numbers in SOFC mode and as negative numbers in SOEC mode.
Source: JRC, 2024.

In addition to presenting the test results as polarisation curves, which include the current-voltage characteristics (I-U curves) and the current density-electric power characteristics (J-P_{el} curves) or current density-power density characteristics (J-P_d curves) of the cell/stack assembly unit, and showcasing the evolution of the stack temperature, performance curves can also be plotted. These performance curves may comprise the electrical efficiency-electric power density characteristics (η_{el}-$P_{el,d}$ curves) for HTFCs and the energy efficiency-electric power density characteristics (η_e-$P_{el,d}$ curves) for HTSEs.

When method (**A**) is employed in polarisation curve measurements (refer to section 6.3.2 and section 6.3.3), the standard variances (s^2) or standard deviations (s) of the measured test parameters, along with the combined standard variances (u_c^2) or combined standard uncertainties (u_c) of the calculated (derived) test parameters,

may be multiplied by the coverage factor (k) (see Annex E) and indicated appropriately in the plots, such as with error bars.

8 Conclusions

This report outlines a testing procedure for conducting polarisation curve measurements applicable to HTFCs and HTSEs. It is equally suitable for cell/stack assembly units of SOC, including rSOC, and PCC, including rPCC. As a fundamental characterisation technique, polarisation curve measurements evaluate the performance of cell/stack assembly units based on their current-voltage characteristics (I-U curves) or current density-electric power characteristics (J-P_{el} curves) as well as efficiency-electric power density characteristics (η-$P_{\mathrm{el,d}}$ curves).

This testing method serves a dual purpose in both R&D and in the realm of quality assurance (QA) (**3.1.31**) and quality control (QC) (**3.1.32**) for manufactured cell/stack assembly units. Additionally, it serves as a general test method for qualifying cell/stack assembly units in a given application.

References

CH2P, 'Strategic Research and Innovation Agenda 2021-2027 of the Clean Hydrogen Joint Undertaking', 2022. URL https://www.clean-hydrogen.europa.eu/about-us/key-documents/strategic-research-and-innovation-agenda_en.

Clean H_2 JU, 'Clean Hydrogen JU Annual Work Programmes', 2024a. URL https://www.clean-hydrogen.europa.eu/about-us/key-documents/annual-work-programmes_en.

Clean H_2 JU, 'Projects repository'. 2024b. URL https://www.clean-hydrogen.europa.eu/projects-dashboard/projects-repository_en.

del Olmo, D., Pavelka, M. and Kosek, J., 'Open-circuit voltage comes from non-equilibrium thermodynamics', *Journal of Non-Equilibrium Thermodynamics*, Vol. 46, No 1, 2021, pp. 91–108. doi:10.1515/jnet-2020-0070.

Fukumoto, T., Endo, N., Natsukoshi, K., Tachikawa, Y., Harrington, G. F., Lyth, S. M., Matsuda, J. and Sasaki, K., 'Exchange current density of reversible solid oxide cell electrodes', *International Journal of Hydrogen Energy*, Vol. 47, No 37, 2022, pp. 16626–16639. doi:10.1016/j.ijhydene.2022.03.164.

DLR, 'Solid Oxide Cell and Stack Testing, Safety and Quality Assurance', Project information, Community Research and Development Information Service (CORDIS), 2014. URL https://cordis.europa.eu/project/id/621245.

JCGM, 'Evaluation of measurement data - Guide to the expression of uncertainty in measurement', GUM: Guide to the Expression of Uncertainty in Measurement JCGM 100:2008, Joint Committee for Guides in Metrology, 2008. URL https://www.bipm.org/utils/common/documents/jcgm/JCGM_100_2008_E.pdf.

Herradon, C., Le, L., Meisel, C., Huang, J., Chmura, C., Kim, Y. D., Cadigan, C., O'Hayre, R. and Sullivan, N. P., 'Proton-conducting ceramics for water electrolysis and hydrogen production at elevated pressure', *Frontiers in Energy Research*, Vol. 10, 2022. doi:10.3389/fenrg.2022.1020960.

Kröger, F. A. and Vink, H. J., 'Relations between the Concentrations of Imperfections in Crystalline Solids', *Solid State Physics*, Vol. 3, No C, 1956, pp. 307–435. doi:10.1016/S0081-1947(08)60135-6.

Kröger, F. A. and Vink, H. J., 'Relations between the concentrations of imperfections in solids', *Journal of Physics and Chemistry of Solids*, Vol. 5, No 3, 1958, pp. 208–223. doi:10.1016/0022-3697(58)90069-6.

Dizon, A., Schuler, T., Weber, A. Z., Danilovic, N. and Bender, G., 'Advanced voltage break down analysis by statistical open-source tool case study based on polymer electrolyte water electrolysis', *ECS Meeting Abstracts*, Vol. MA2022-02, No 39, 2022, p. 1400. doi:10.1149/MA2022-02391400mtgabs.

IUPAC, 'standard conditions for gases', online version 3.0.1, International Union of Pure and Applied Chemistry, 2019. doi:10.1351/goldbook.S05910. URL https://doi.org/10.1351/goldbook.S05910.

Gerhardt, M. R., Pant, L. M., Bui, J. C., Crothers, A. R., Ehlinger, V. M., Fornaciari, J. C., Liu, J. and Weber, A. Z., 'Method - practices and pitfalls in voltage breakdown analysis of electrochemical energy-conversion systems', *Journal of the Electrochemical Society*, Vol. 168, No 7, 2021, p. 074503. doi:10.1149/1945-7111/abf061.

EP and Council, 'Approximation of the laws of the Member States concerning equipment and protective systems intended for use in potentially explosive atmospheres', Directive 94/9/EC, Publications Office of the European Union, Brussels (BE), 23 March 1994. URL http://data.europa.eu/eli/dir/1994/9/oj. OJ L 100 of 19.4.1994.

EP and Council, 'General Product Safety', Directive 2001/95/EC, Publications Office of the European Union, Brussels (BE), 3 December 2001. URL http://data.europa.eu/eli/dir/2001/95/oj. OJ L 11 of 15.1.2002.

EP and Council, 'Machinery, and amending Directive 95/16/EC', Directive 2006/42/EC, Publications Office of the European Union, Brussels (BE), 17 May 2006. URL http://data.europa.eu/eli/dir/2006/42/oj. OJ L 157 of 9.6.2006.

EP and Council, 'Harmonisation of the laws of the Member States relating to electromagnetic compatibility', Directive 2014/30/EU, Publications Office of the European Union, Brussels (BE), 26 February 2014a. URL http://data.europa.eu/eli/dir/2014/30/oj. OJ L 96 of 29.3.2014.

EP and Council, 'Harmonisation of the laws of the Member States relating to equipment and protective systems intended for use in potentially explosive atmospheres', Directive 2014/34/EU, Publications Office of the European Union, Brussels (BE), 26 February 2014b. URL http://data.europa.eu/eli/dir/2014/34/oj. OJ L 96 of 29.3.2014.

EP and Council, 'Harmonisation of the laws of the Member States relating to the making available on the market of electrical equipment designed for use within certain voltage limits', Directive 2014/35/EU, Publications Office of the European Union, Brussels (BE), 26 February 2014c. URL http://data.europa.eu/eli/dir/2014/35/oj. OJ L 96 of 29.3.2014.

EP and Council, 'Harmonisation of the laws of the Member States relating to the making available on the market of pressure equipment', Directive 2014/68/EU, Publications Office of the European Union, Brussels (BE), 15 May 2014d. URL http://data.europa.eu/eli/dir/2014/68/oj. OJ L 189 of 27.6.2014.

IEC, 'Possible safety and health hazards in the use of alkaline secondary cells and batteries - Guide to equipment manufacturers and users', Technical Report IEC TR 61438:1996, International Electrotechnical Commission, Geneva (CH), 1996. URL https://webstore.iec.ch/publication/5455.

IEC, 'Explosive atmospheres - Part 17: Electrical installations inspection and maintenance', International Standard IEC 60079-17:2013, International Electrotechnical Commission, Geneva (CH), 2013. URL https://webstore.iec.ch/publication/631.

IEC, 'Explosive atmospheres - Part 14: Electrical installations design, selection and erection', International Standard IEC 60079-14:2013, International Electrotechnical Commission, Geneva (CH), 2014. URL https://webstore.iec.ch/publication/628.

IEC, 'Explosive atmospheres - Part 0: Equipment - General requirements', International Standard IEC 60079-0:2017, International Electrotechnical Commission, Geneva (CH), 2017. URL https://webstore.iec.ch/publication/32878.

IEC, 'Safety of machinery - Electrical equipment of machines - Part 11: Requirements for equipment for voltages above 1 000 V AC or 1 500 V DC and not exceeding 36 kV', International Standard IEC 60204-11:2018 RLV, International Electrotechnical Commission, Geneva (CH), 2018. URL https://webstore.iec.ch/publication/63667.

IEC, 'Fuel cell technologies - Part 3-100: Stationary fuel cell power systems - Safety', International Standard IEC 62282-3-100:2019, International Electrotechnical Commission, Geneva (CH), 2019. URL https://webstore.iec.ch/publication/59780.

IEC, 'Explosive atmospheres – Part 10-1: Classification of areas – Explosive gas atmospheres', International Standard IEC 60079-10-1:2020, International Electrotechnical Commission, Geneva (CH), 2020a. URL https://webstore.iec.ch/publication/63327.

IEC, 'Fuel cell technologies - Part 2-100: Fuel cell modules - Safety', International Standard IEC 62282-2-100:2020, International Electrotechnical Commission, Geneva (CH), 2020b. URL https://webstore.iec.ch/publication/59780.

IEC, 'Fuel cell technologies - Part 8-101: Energy storage systems using fuel cell modules in reverse mode - Test procedures for the performance of solid oxide single cells and stacks, including reversible operation', International Standard IEC 62282-8-101:2020, International Electrotechnical Commission, Geneva (CH), 2020c. URL https://webstore.iec.ch/publication/33278.

IEC, 'Fuel cell technologies - Part 7-2: Test methods - Single cell and stack performance tests for solid oxide fuel cells (SOFCs)', International Standard IEC 62282-7-2:2021, International Electrotechnical Commission, Geneva (CH), 2021a. URL https://webstore.iec.ch/publication/66455.

IEC, 'Safety of machinery - Electrical equipment of machines - Part 1: General requirements', International Standard IEC 60204-1:2016+AMD1:2021 CSV, International Electrotechnical Commission, Geneva (CH), 2021b. URL https://webstore.iec.ch/publication/71256.

IEEE, 'Information technology - DevOps - Building reliable and secure systems including application build, package and deployment', Standard ISO/IEC/IEEE 32675:2022, International Organization for Standardization, International Electrotechnical Commission, Institute of Electrical and Electronics Engineers, Geneva (CH), New York (NY), 2022. URL https://www.iso.org/standard/83670.html.

ISO, 'Basic considerations for the safety of hydrogen systems', Technical Report ISO/TR 15916:2015, International Organization for Standardization, Geneva (CH), 2015. URL https://www.iso.org/standard/69212.html.

ISO, 'Cleanrooms and associated controlled environments - Part 14: Assessment of suitability for use of equipment by airborne particle concentration', International Standard ISO 14644-14:2016, International Organization for Standardization, Geneva (CH), 2016. URL https://www.iso.org/standard/60970.html.

ISO, 'Occupational health and safety management systems - Requirements with guidance for use', International Standard ISO 45001:2018, International Organization for Standardization, Geneva (CH), 2018. URL https://www.iso.org/standard/63787.html.

ISO, 'Gas analysis - Analytical methods for hydrogen fuel - Proton exchange membrane (PEM) fuel cell applications for road vehicles', International Standard ISO 21087:2019, International Organization for Standardization, Geneva (CH), 2019a. URL https://www.iso.org/standard/69909.html.

ISO, 'Hydrogen generators using water electrolysis - Industrial, commercial, and residential applications', International Standard ISO 22734:2019, International Organization for Standardization, Geneva (CH), 2019b. URL https://www.iso.org/standard/69212.html.

ISO, 'Assessment of the effectiveness of cathodic protection based on coupon measurements', International Standard ISO 22426:2020, International Organization for Standardization, Geneva (CH), 2020. URL https://www.iso.org/standard/73167.html.

ISO, 'Solid biofuels - Vocabulary', International Standard ISO 16559:2022, International Organization for Standardization, Geneva (CH), 2022. URL https://www.iso.org/standard/75261.html.

ISO, 'Hydrogen generators using water electrolysis - Part 1: General requirements, test protocols and safety requirements', Draft International Standard ISO/DIS 22734-1:2024, International Organization for Standardization, Geneva (CH), 2024. URL https://www.iso.org/standard/82766.html.

ISO and IEC, 'Principles and rules for the structure and drafting of ISO and IEC documents', ISO/IEC Directives, Part 2, Ninth edition, International Organization for Standardization, International Electrotechnical Commission, Geneva (CH), 2021. URL https://www.iso.org/sites/directives/current/part2/index.xhtml.

Duan, C., Huang, J., Sullivan, N., and O'Hayre, R., 'Proton-conducting oxides for energy conversion and storage', *Applied Physics Review*, Vol. 7, 2020, p. 011314. doi:10.1063/1.5135319.

Ma, Z., Witteman, L., Wrubel, J. A. and Bender, G., 'A comprehensive modeling method for proton exchange membrane electrolyzer development', *International Journal of Hydrogen Energy*, Vol. 46, No 34, 2021, pp. 17627–17643. doi:10.1016/j.ijhydene.2021.02.170.

Hernández-Gómez, Á., Ramirez, V. and Guilbert, D., 'Investigation of pem electrolyzer modeling: Electrical domain, efficiency, and specific energy consumption', *International Journal of Hydrogen Energy*, Vol. 45, No 29, 2020, pp. 14625–14639. doi:10.1016/j.ijhydene.2020.03.195.

Falcão, D. S. and Pinto, A. M. F. R., 'A review on PEM electrolyzer modelling: Guidelines for beginners', *Journal of Cleaner Production*, Vol. 261, 2020, p. 121184. doi:10.1016/j.jclepro.2020.121184.

Tsotridis, G. and Pilenga, A., 'EU harmonised terminology for low temperature water electrolysis for energy storage applications', JRC112082, EUR 29300 EN, KJ-NA-29300-EN-N (online), KJ-NA-29300-EN-C (print). Publications Office of the European Union, Luxembourg (L), 2018. ISBN 978-92-79-90387-8 (online), 978-92-79-90388-5 (print). doi:10.2760/138987(online),10.2760/014448(print). URL http://publications.jrc.ec.europa.eu/repository/handle/JRC112082.

Fu, Q., Brisse, A., Iorio, S. D., Karine Couturier, Michael Lang, Auer, C., Wenz, F., Braniek, G., Broß, S., Nygaard, F., Veltzé, S., Nielsen, E. R., McPhail, S. J., Muñoz, C. B., Pumiglia, D., Malkow, T., de Marco, G., Kotsionopoulos, N. and Liu, Q., 'General SOC testing guidelines, version 2.5', SOCTESQA Test Module 00, Europäisches Institut für Energieforschung, Commissariat à l'énergie atomique et aux énergies alternatives, Deutsches Zentrum für Luft- und Raumfahrt e. V., Danmarks Tekniske Universitet, Agenzia Nazionale per le Nuove tecnologie, l'Energia e lo Sviluppo economico sostenibile, Joint Research Centre, Nanyang Technological University, 09 May 2017. URL https://elib.dlr.de/119897.

de Marco, G., Kotsionopoulos, N., Malkow, T., Couturier, K. and Lang, M., 'Current-voltage characteristics', SOCTESQA Test Module 03, Joint Research Centre, Commissariat à l'énergie atomique et aux énergies alternatives, Deutsches Zentrum für Luft- und Raumfahrt e. V.„ 15 May 2017. URL https://elib.dlr.de/119895.

Lang, M., Bohn, C., Henke, M., Schiller, G., Willich, C. and Hauler, F., 'Understanding the current-voltage behavior of high temperature solid oxide fuel cell stacks', *Journal of the Electrochemical Society*, Vol. 164, No 13, 2017, pp. F1460–F1470. doi:10.1149/2.1541713jes.

Malkow, K. T., Pilenga, A. and Blagoeva, D., 'EU harmonised terminology for hydrogen generated by electrolysis', EUR 30324 EN, KJ-NA-30324-EN-N (online), KJ-NA-30324-EN-C (print). Publications Office of the European Union, Luxembourg (L), 2021. ISBN 978-92-76-21042-9 (online), 978-92-76-21041-2 (print). doi:10.2760/293538(print),10.2760/732809(online). URL https://publications.jrc.ec.europa.eu/repository/handle/JRC120120.

Jia, H. and Taheri, B., 'Model identification of solid oxide fuel cell using hybrid Elman neural network/quantum pathfinder algorithm', *Energy Reports*, Vol. 7, 2021, pp. 3328–3337. doi:10.1016/j.egyr.2021.05.070.

Kreuer, K.-D., 'On the complexity of proton conduction phenomena', *Solid State Ionics*, Vol. 136-137, 2000, pp. 149–160. doi:10.1016/S0167-2738(00)00301-5.

Kreuer, K.-D., Paddison, S. J., Spohr, E. and Schuster, M., 'Transport in proton conductors for fuel-cell applications: Simulations, elementary reactions, and phenomenology', *Chemical Reviews*, Vol. 104, No 10, 2004, pp. 4637–4678. doi:10.1021/cr020715f.

Rand, P. W., Huang, J. D., Kim, Y.-D., Meisel, C., Hernandez, C. H., Chmura, C., O'Hayre, R. P. and Sullivan, N. P., 'Statistical design of experiments for efficient performance characterization of protonic-ceramic electrolysis cells', *Journal of Physics: Energy*, Vol. 7, No 1, 2024, p. 015003. doi:10.1088/2515-7655/ad92ab.

List of abbreviations and acronyms

Abbreviation	Description
AI	artificial intelligence
ASR	area-specific resistance
ATEX	Appareils destinés à être utilisés en atmosphères explosibles
BCY	yttrium-doped barium cerate
biP	bipolar plate
BZ	barium zirconate
BZY	yttrium-doped barium zirconate
CC BY 4.0	Creative Commons Attribution 4.0 International
CEA	Commissariat à l'énergie atomique et aux énergies alternatives
CGO	ceria-doped gadolinium oxide
CH	Switzerland
CH2P	Clean Hydrogen Partnership
CHP	combined heat and power
Clean H_2 JU	Clean Hydrogen Joint Undertaking
CORDIS	Community Research and Development Information Service
DAQ	data acquisition
DC	direct current
DIS	draft international standard
DLR	Deutsches Zentrum für Luft- und Raumfahrt e. V.
doi	digital object identifier
DTU	Danmarks Tekniske Universitet
e. V.	eingetragener Verein
EC	European Commission
ec	electrochemical cell
EEA	European Economic Area
EIfER	Europäisches Institut für Energieforschung
EMC	electromagnetic compatibility
EN	English
ENEA	Agenzia Nazionale per le Nuove tecnologie, l'Energia e lo Sviluppo economico sostenibile
ES	energy storage
EU	European Union
EUR	European Union Report
FC	fuel cell

Abbreviation	Description
FCHJU	Fuel Cells and Hydrogen Joint Undertaking
FID	first industrial deployment
FS	full scale
GLP	good laboratory practice
HER	hydrogen evolution reaction
HHV	higher heating value
HOR	hydrogen oxidation reaction
HTE	high-temperature electrolyser
HTFC	high-temperature fuel cell
HTSE	high-temperature steam electrolyser
HTSEL	high-temperature steam electrolysis
IEC	International Electrotechnical Commission
IEEE	Institute of Electrical and Electronics Engineers
IEES	Institute of Electrochemistry and Energy Systems Acad. Evgeni Budevski
IEV	International Electrotechnical Vocabulary
ISBN	international standard book number
ISO	International Organization for Standardization
ISSN	international standard serial number
IUPAC	International Union of Pure and Applied Chemistry
JCGM	Joint Committee for Guides in Metrology
JRC	Joint Research Centre
L	Luxembourg
LHS	left hand side
LHV	lower heating value
LSC	strontium-doped lanthanum cobalt oxide
LSCF	strontium-doped lanthanum cobalt iron oxide
LTWE	low-temperature water electrolyser
LVD	Low-Voltage Directive
ML	machine learning
MSC	metal-supported cell
Nlpm	normal litre per minute
NLS	non-linear least squares
NY	New York
OCP	open circuit potential
OCV	open circuit voltage

Abbreviation	Description
OER	oxygen evolution reaction
OHS	occupational health and safety
OJ	Official Journal
ORR	oxygen reduction reaction
PCC	proton-conducting ceramic
PCCEL	proton-conducting ceramic steam electrolysis
PCE	protonic ceramic electrolyser
PCEC	protonic ceramic electrolysis cell
PCFC	protonic ceramic fuel cell
PCV	pressure control valve
PDF	portable document format
PED	Pressure Equipment Directive
QA	quality assurance
QC	quality control
R&D	research and development
R&I	research and innovation
RHS	right hand side
RLV	redline version
rPCC	reversible proton-conducting ceramic electrolysis cell
rPCE	reversible protonic ceramic electrolyser
rSOC	reversible solid oxide electrolysis cell
rSOE	reversible solid oxide electrolyser
RU	repeating unit
SATP	standard ambient temperature and pressure
ScSZ	scandia-stabilised zirconia
SI	Système International d'Unités
SINTEF	Stiftelsen for industriell og teknisk forskning
slpm	standard litre per minute
SOC	solid oxide cell
SOCTES^{QA}	Solid Oxide Cell and Stack Testing, Safety and Quality Assurance
SOE	solid oxide electrolyser
SOEC	solid oxide electrolysis cell
SOEL	solid oxide steam electrolysis
SOFC	solid oxide fuel cell
SpA	Società per azioni

Abbreviation	Description
SRIA	strategic research and innovation agenda 2021-2027
Srl	Società a responsabilità limitata
SRU	single repeating unit
TC	Technical Committee
TIP	test input parameter
TM	Test Module
TOP	test output parameter
TPB	triple-phase boundary
TR	Technical Report
TRL	technology readiness level
URL	uniform resource locator
VBA	voltage breakdown analysis
WE	water electrolyser
WG	Working Group
YSZ	yttria-stabilised zirconia

List of symbols

Symbol	Description
(ed)	subscript denoting electrode
(el)	subscript denoting electrolyte
(g)	subscript denoting gaseous phase
A_{act}	active electrode area
α^{neg}	negative electrode charge transfer coefficient
α^{pos}	positive electrode charge transfer coefficient
$c^{0}_{\text{H}_2}$	equilibrium hydrogen concentration
$c^{0}_{\text{H}_2\text{O}}$	equilibrium steam concentration
$c^{0}_{\text{O}_2}$	equilibrium oxygen concentration
c	concentration
CO	carbon monoxide
CO_2	carbon dioxide
c_{p}	specific heat capacity at constant pressure
c^{i}_{p}	specific heat capacity at constant pressure of fluid i
c^{j}_{p}	specific heat capacity at constant pressure of fluid j
$c^{\text{TPB}}_{\text{H}_2\text{O}}$	water vapour concentration at the triple-phase boundary
$c^{\text{TPB}}_{\text{H}_2}$	hydrogen concentration at the triple-phase boundary
$c^{\text{TPB}}_{\text{O}_2}$	oxygen concentration at the triple-phase boundary
c^{j}_{V}	specific heat capacity at constant volume of fluid j
E	energy
e'	electron (in Kröger-Vink notation)
e^{-}	electron
E_{el}	electric energy
E_{p}	pneumatic energy
U_{rev}	voltage under reversible (equilibrium) conditions
η	efficiency
η_{e}	energy efficiency
$\eta^{\text{HHV}}_{\text{e, EL}}$	electrolyser energy efficiency based on HHV
$\bar{\eta}^{\text{HHV}}_{\text{e, EL}}$	average value of electrolyser energy efficiency based on HHV
$\eta^{\text{LHV}}_{\text{e, EL}}$	electrolyser energy efficiency based on LHV
$\bar{\eta}^{\text{LHV}}_{\text{e, EL}}$	average value of electrolyser energy efficiency based on LHV
η_{el}	electrical efficiency
$\eta^{\text{HHV}}_{\text{el, FC}}$	fuel cell electrical efficiency based on HHV
$\bar{\eta}^{\text{HHV}}_{\text{el, FC}}$	average value of fuel cell electrical efficiency based on HHV
$\eta^{\text{LHV}}_{\text{el, FC}}$	fuel cell electrical efficiency based on LHV
$\bar{\eta}^{\text{LHV}}_{\text{el, FC}}$	average value of fuel cell electrical efficiency based on LHV
η_{F}	Faradaic efficiency
η_{th}	thermal efficiency
$\bar{\eta}^{\text{HHV}}_{\text{th, FC}}$	average value of fuel cell thermal efficiency based on HHV
$\eta^{\text{HHV}}_{\text{th, FC}}$	fuel cell thermal efficiency based on HHV
$\eta^{\text{LHV}}_{\text{th, FC}}$	fuel cell thermal efficiency based on LHV
$\bar{\eta}^{\text{LHV}}_{\text{th, FC}}$	average value of fuel cell thermal efficiency based on LHV
E_{th}	thermal energy
F	Faraday constant
f_{step}	step sampling rate
f_{sweep}	sweep sampling rate
γ^{j}	isentropic expansion factor of fluid j
H	hydrogen
H^{+}	proton
$\text{h}^{\bullet}$	electron hole
H_2	molecular hydrogen or dihydrogen
$\text{H}_2\text{O}_{\text{(g)}}$	water vapour
HHV_{H_2}	HHV of hydrogen
I_{L}	limiting current
I	current
$\Delta I/\Delta t$	sweep rate of current

Symbol	Description
I_0	current
I_{dc}	direct current
$\bar{I}_{dc}$	average value of direct current
$I_{dc,l}$	instantaneous value of direct current
I_{in}	input current
I_{max}	maximum current
J	current density
$\bar{J}$	average value of current density
J_l	instantaneous value of current density
k	coverage factor
L	number of measurements
λ^{-1}	gas utilisation
λ	stoichiometric ratio
$\lambda^{-1}_{gas,neg}$	utilisation of negative electrode gas
$\lambda^{-1}_{gas,pos}$	utilisation of positive electrode gas
λ_{H_2}	stoichiometric ratio of hydrogen
LHV_{H_2}	LHV of hydrogen
M	molar mass
M_i	molar mass of component i
N_2	nitrogen
N_{cells}	number of cells or RUs electrically connected in series in the cell/stack assembly unit
O	oxygen
O_2	molecular oxygen or dioxygen
O^{2-}	oxide ion
$OH^{\bullet}_O$	hydroxide ion at singly positively charged oxygen lattice site
O^{x}_O	oxygen on neutral oxide ion lattice site
P	power
p	pressure
p^0	standard ambient pressure
P_d	power density
P_{el}	electric power
$P_{el,d}$	electric power density
$\bar{P}_{el,d}$	average value of electric power density
$P_{el,dc}$	DC power
$\bar{P}_{el,dc}$	average value of DC power
$P_{el,dc,l}$	instantaneous value of DC power
$\tilde{P}_{el,dc}$	pseudo-average of DC power
$P_{el,d,l}$	instantaneous value of electric power density
$\tilde{P}_{el,d}$	pseudo-average of electric power density
p_{H_2}	partial pressure of hydrogen
$P_{H_2,in}$	input power of hydrogen
$P^{HHV}_{H_2,in}$	input power of hydrogen based on HHV
$\bar{P}^{HHV}_{H_2,in}$	average value of input power of hydrogen based on HHV
$P^{HHV}_{H_2,in,l}$	instantaneous value of input power of hydrogen based on HHV
$\tilde{P}^{HHV}_{H_2,in}$	pseudo-average of input power of hydrogen based on HHV
$P^{LHV}_{H_2,in}$	input power of hydrogen based on LHV
$\bar{P}^{LHV}_{H_2,in}$	average value of input power of hydrogen based on LHV
$P^{LHV}_{H_2,in,l}$	instantaneous value of input power of hydrogen based on LHV
$\tilde{P}^{LHV}_{H_2,in}$	pseudo-average of input power of hydrogen based on LHV
p_{H_2O}	partial pressure of water vapour (steam)
$P_{H_2,out}$	output power of hydrogen
$P^{HHV}_{H_2,out}$	output power of hydrogen based on HHV
$\bar{P}^{HHV}_{H_2,out}$	average value of output power of hydrogen based on HHV
$P^{HHV}_{H_2,out,l}$	instantaneous value of output power of hydrogen based on HHV
$\tilde{P}^{HHV}_{H_2,out}$	pseudo-average of output power of hydrogen based on HHV
$P^{LHV}_{H_2,out}$	output power of hydrogen based on LHV
$\bar{P}^{LHV}_{H_2,out}$	average value of output power of hydrogen based on LHV
$P^{LHV}_{H_2,out,l}$	instantaneous value of output power of hydrogen based on LHV
$\tilde{P}^{LHV}_{H_2,out}$	pseudo-average of output power of hydrogen based on LHV

Symbol	Description
p^{i}	pressure of fluid i
$\bar{p}^{\mathrm{i}}$	average value of pressure of fluid i
$p_{\mathrm{l}}^{\mathrm{i}}$	instantaneous value of pressure of fluid i
P_{in}	input power
p^{j}	pressure of fluid j
$\bar{p}^{\mathrm{j}}$	average value of pressure of fluid j
$p_{\mathrm{l}}^{\mathrm{j}}$	instantaneous value of pressure of fluid j
$p_{\mathrm{neg,\,in}}$	inlet pressure of negative electrode gas
$p_{\mathrm{neg,\,out}}$	outlet pressure of negative electrode gas
$p_{\mathrm{O_2}}$	partial pressure of oxygen
P_{out}	output power
P_{p}	pneumatic power
$P_{\mathrm{p,\,in}}$	input pneumatic power
$\bar{P}_{\mathrm{p,\,in}}$	average value of input pneumatic power
$P_{\mathrm{p,\,in,\,l}}$	instantaneous value of input pneumatic power
$\tilde{P}_{\mathrm{p,\,in}}$	pseudo-average of input pneumatic power
$p_{\mathrm{pos,\,in}}$	inlet pressure of positive electrode gas
$p_{\mathrm{pos,\,out}}$	outlet pressure of positive electrode gas
P_{th}	thermal power
$P_{\mathrm{th,\,in}}$	input thermal power
$\bar{P}_{\mathrm{th,\,in}}$	average value of input thermal power
$P_{\mathrm{th,\,in,\,l}}$	instantaneous value of input thermal power
$\tilde{P}_{\mathrm{th,\,in}}$	pseudo-average of input thermal power
$P_{\mathrm{th,\,out}}$	output thermal power
$\bar{P}_{\mathrm{th,\,out}}$	average value of output thermal power
$P_{\mathrm{th,\,out,\,l}}$	instantaneous value of output thermal power
$\tilde{P}_{\mathrm{th,\,out}}$	pseudo-average of output thermal power
q	flow rate
q_{m}	mass flow rate
$q_{\mathrm{m}}^{\mathrm{i}}$	mass flow rate of fluid i
$\bar{q}_{\mathrm{m}}^{\mathrm{i}}$	average value of mass flow rate of fluid i
$q_{\mathrm{m,\,l}}^{\mathrm{i}}$	instantaneous value of mass flow rate of fluid i
q_{n}	molar flow rate
$q_{\mathrm{n,\,H_2}}$	molar flow rate of hydrogen
$q_{\mathrm{n,\,H_2,\,in}}$	inlet molar flow rate of hydrogen
$\bar{q}_{\mathrm{n,\,H_2,\,in}}$	average value of inlet molar flow rate of hydrogen
$q_{\mathrm{n,\,H_2,\,in,\,l}}$	instantaneous value of inlet molar flow rate of hydrogen
$q_{\mathrm{n,\,H_2,\,in,\,min}}$	minimum inlet molar flow rate of hydrogen
$q_{\mathrm{n,\,H_2,\,net}}$	net molar flow rate of hydrogen
$q_{\mathrm{n,\,H_2,\,out}}$	outlet molar flow rate of hydrogen
$\bar{q}_{\mathrm{n,\,H_2,\,out}}$	average value of outlet molar flow rate of hydrogen
$q_{\mathrm{n,\,H_2,\,out,\,l}}$	instantaneous value of outlet molar flow rate of hydrogen
$q_{\mathrm{n}}^{\mathrm{j}}$	molar flow rate of fluid j
$\bar{q}_{\mathrm{n}}^{\mathrm{j}}$	average value of molar flow rate of fluid j
$q_{\mathrm{n,\,l}}^{\mathrm{j}}$	instantaneous value of molar flow rate of fluid j
$q_{\mathrm{n,\,l}}$	instantaneous value of molar flow rate
q_{V}	volumetric flow rate
$q_{\mathrm{V,\,in}}$	inlet volumetric flow rate
$\bar{q}_{\mathrm{V,\,in}}$	average value of inlet volumetric flow rate
$q_{\mathrm{V,\,in,\,l}}$	instantaneous value of inlet volumetric flow rate
$q_{\mathrm{V,\,neg,\,in}}$	inlet volumetric flow rate of negative electrode gas
$q_{\mathrm{V,\,neg,\,out}}$	outlet volumetric flow rate of negative electrode gas
$q_{\mathrm{V,\,out}}$	product gas volumetric flow rate
$\bar{q}_{\mathrm{V,\,out,\,l}}$	average value of product gas volumetric flow rate
$q_{\mathrm{V,\,out,\,l}}$	instantaneous value of product gas volumetric flow rate
$q_{\mathrm{V,\,pos,\,in}}$	inlet volumetric flow rate of positive electrode gas
$q_{\mathrm{V,\,pos,\,out}}$	outlet volumetric flow rate of positive electrode gas
R	resistance
R_{ASR}	area-specific resistance

Symbol	Description
R_{g}	universal gas constant
s	standard deviation
s^2	standard variance
$s^2\left(I_{\mathrm{dc}}\right)$	standard variance of direct current
$s^2\left(J\right)$	standard variance of current density
$s^2\left(P_{\mathrm{H_2,\,in}}^{\mathrm{HHV}}\right)$	standard variance of input power of hydrogen based on HHV
$s^2\left(P_{\mathrm{H_2,\,in}}^{\mathrm{LHV}}\right)$	standard variance of input power of hydrogen based on LHV
$s^2\left(P_{\mathrm{H_2,\,out}}^{\mathrm{HHV}}\right)$	standard variance of output power of hydrogen based on HHV
$s^2\left(P_{\mathrm{H_2,\,out}}^{\mathrm{LHV}}\right)$	standard variance of output power of hydrogen based on LHV
$s^2\left(p^{\mathrm{i}}\right)$	standard variance of pressure of fluid i
$s^2\left(p^{\mathrm{j}}\right)$	standard variance of pressure of fluid j
$s^2\left(q_{\mathrm{m}}^{\mathrm{i}}\right)$	standard variance of mass flow rate of fluid i
$s^2\left(q_{\mathrm{n,\,H_2,\,in}}\right)$	standard variance of inlet molar flow rate of hydrogen
$s^2\left(q_{\mathrm{n}}^{\mathrm{j}}\right)$	standard variance of molar flow rate of fluid j
$s^2\left(q_{\mathrm{V,\,in}}\right)$	standard variance of inlet volumetric flow rate
$s^2\left(q_{\mathrm{V,\,out}}\right)$	standard variance of product gas volumetric flow rate
$s^2\left(T^{\mathrm{i}}\right)$	standard variance of temperature of fluid i
$s^2\left(T^{\mathrm{j}}\right)$	standard variance of temperature of fluid j
$s^2\left(T_{\mathrm{stack}}\right)$	standard variance of stack temperature
$s^2\left(U_{\mathrm{dc}}\right)$	standard variance of DC voltage
$s^2(X)$	standard variance of test parameter X
$s^2\left(x_{\mathrm{n,\,H_2,\,out}}\right)$	standard variance of outlet molar concentration of hydrogen
T	temperature
t	time
T^0	standard ambient temperature
T^{i}	temperature of fluid i
$\bar{T}^{\mathrm{i}}$	average value of temperature of fluid i
$T_{\mathrm{l}}^{\mathrm{i}}$	instantaneous value of temperature of fluid i
T^{j}	temperature of fluid j
$\bar{T}^{\mathrm{j}}$	average value of temperature of fluid j
$T_{\mathrm{l}}^{\mathrm{j}}$	instantaneous value of temperature of fluid j
$T_{\mathrm{neg,\,in}}$	inlet temperature of negative electrode gas
$T_{\mathrm{neg,\,out}}$	outlet temperature of negative electrode gas
$T_{\mathrm{pos,\,in}}$	inlet temperature of positive electrode gas
$T_{\mathrm{pos,\,out}}$	outlet temperature of positive electrode gas
T_{stack}	stack temperature
$\bar{T}_{\mathrm{stack}}$	average value of stack temperature
$T_{\mathrm{stack,\,l}}$	instantaneous value of stack temperature
t_{step}	step duration
U	voltage
u	standard uncertainty
$\Delta U/\Delta t$	sweep rate of voltage
$u_{\mathrm{c}}^2\left(\eta_{\mathrm{e,\,EL}}^{\mathrm{HHV}}\right)$	square of combined standard uncertainty of electrolyser energy efficiency based on HHV
$u_{\mathrm{c}}^2\left(\eta_{\mathrm{e,\,EL}}^{\mathrm{LHV}}\right)$	square of combined standard uncertainty of electrolyser energy efficiency based on LHV
$u_{\mathrm{c}}^2\left(\eta_{\mathrm{el,\,FC}}^{\mathrm{HHV}}\right)$	square of combined standard uncertainty of fuel cell electrical efficiency based on HHV
$u_{\mathrm{c}}^2\left(\eta_{\mathrm{el,\,FC}}^{\mathrm{LHV}}\right)$	square of combined standard uncertainty of fuel cell electrical efficiency based on LHV
$u_{\mathrm{c}}^2\left(\eta_{\mathrm{th,\,FC}}^{\mathrm{HHV}}\right)$	square of combined standard uncertainty of fuel cell thermal efficiency based on HHV
$u_{\mathrm{c}}^2\left(\eta_{\mathrm{th,\,FC}}^{\mathrm{LHV}}\right)$	square of combined standard uncertainty of fuel cell thermal efficiency based on LHV
$u_{\mathrm{c}}^2\left(P_{\mathrm{el,\,d}}\right)$	square of combined standard uncertainty of electric power density
$u_{\mathrm{c}}^2\left(P_{\mathrm{el,\,dc}}\right)$	square of combined standard uncertainty of DC power
$u_{\mathrm{r}}^2\left(I_{\mathrm{dc}}\right)$	square of relative standard uncertainty of direct current
$u_{\mathrm{r}}^2\left(J\right)$	square of relative standard uncertainty of current density
$u_{\mathrm{r}}^2\left(p^{\mathrm{j}}\right)$	of pressure of fluid j
$u_{\mathrm{r}}^2\left(q_{\mathrm{m}}^{\mathrm{i}}\right)$	square of relative standard uncertainty of mass flow rate of fluid i
$u_{\mathrm{r}}^2\left(q_{\mathrm{n,\,H_2,\,in}}\right)$	square of relative standard uncertainty of inlet molar flow rate of hydrogen
$u_{\mathrm{r}}^2\left(q_{\mathrm{n}}^{\mathrm{j}}\right)$	square of relative standard uncertainty of molar flow rate of fluid j
$u_{\mathrm{r}}^2\left(q_{\mathrm{V,\,out}}\right)$	of product gas volumetric flow rate

Symbol	Description
$u_{\mathrm{r}}^2\left(\Delta T^{\mathrm{i}}\right)$	square of relative standard uncertainty of temperature difference between temperature of fluid i and standard ambient temperature
$u_{\mathrm{r}}^2\left(U_{\mathrm{dc}}\right)$	square of relative standard uncertainty of DC voltage
U_{act}	activation polarisation voltage
u_{c}	combined standard uncertainty
u_{c}^2	combined standard variance
U_{cell}	cell voltage
U_{conc}	concentration polarisation voltage
$u_{\mathrm{c}}\left(P_{\mathrm{el,d}}\right)$	combined standard uncertainty of electric power density
$u_{\mathrm{c}}\left(P_{\mathrm{el,dc}}\right)$	combined standard uncertainty of DC power
$U_{\mathrm{cut\text{-}off}}$	cut-off voltage
$u_{\mathrm{c}}^2(Y)$	square of combined standard uncertainty of test parameter Y
$u_{\mathrm{c}}(Y)$	combined standard uncertainty of test parameter Y
U_{dc}	DC voltage
$\bar{U}_{\mathrm{dc}}$	average value of DC voltage
$U_{\mathrm{dc,I}}$	instantaneous value of DC voltage
U_{in}	input voltage
U_{min}	minimum cell/stack assembly unit voltage
$U_{\mathrm{I=0}}$	open circuit voltage
u_{r}	relative standard uncertainty
$u_{\mathrm{r}}\left(\eta_{\mathrm{e,EL}}^{\mathrm{HHV}}\right)$	relative combined standard uncertainty of electrolyser energy efficiency based on HHV
$u_{\mathrm{r}}\left(\eta_{\mathrm{e,EL}}^{\mathrm{LHV}}\right)$	relative combined standard uncertainty of electrolyser energy efficiency based on LHV
$u_{\mathrm{r}}\left(\eta_{\mathrm{el,FC}}^{\mathrm{HHV}}\right)$	relative combined standard uncertainty of fuel cell electrical efficiency based on HHV
$u_{\mathrm{r}}\left(\eta_{\mathrm{el,FC}}^{\mathrm{LHV}}\right)$	relative combined standard uncertainty of fuel cell electrical efficiency based on LHV
$u_{\mathrm{r}}\left(\eta_{\mathrm{th,FC}}^{\mathrm{HHV}}\right)$	relative combined standard uncertainty of fuel cell thermal efficiency based on HHV
$u_{\mathrm{r}}\left(\eta_{\mathrm{th,FC}}^{\mathrm{LHV}}\right)$	relative combined standard uncertainty of fuel cell thermal efficiency based on LHV
U_{rev}	reversible voltage
$u_{\mathrm{r}}\left(I_{\mathrm{dc}}\right)$	relative standard uncertainty of direct current
$u_{\mathrm{r}}(J)$	relative standard uncertainty of current density
$u_{\mathrm{r}}\left(P_{\mathrm{el,d}}\right)$	relative standard uncertainty of electric power density
$u_{\mathrm{r}}\left(P_{\mathrm{el,dc}}\right)$	relative standard uncertainty of DC power
$u_{\mathrm{r}}\left(P_{\mathrm{H_2,in}}^{\mathrm{HHV}}\right)$	relative standard uncertainty of input power of hydrogen based on HHV
$u_{\mathrm{r}}\left(P_{\mathrm{H_2,in}}^{\mathrm{LHV}}\right)$	relative standard uncertainty of input power of hydrogen based on LHV
$u_{\mathrm{r}}\left(P_{\mathrm{H_2,out}}^{\mathrm{HHV}}\right)$	relative standard uncertainty of output power of hydrogen based on HHV
$u_{\mathrm{r}}\left(P_{\mathrm{H_2,out}}^{\mathrm{LHV}}\right)$	relative standard uncertainty of output power of hydrogen based on LHV
$u_{\mathrm{r}}\left(p^{\mathrm{i}}\right)$	relative combined standard uncertainty of pressure of fluid i
$u_{\mathrm{r}}\left(p^{\mathrm{j}}\right)$	relative combined standard uncertainty of pressure of fluid j
$u_{\mathrm{r}}\left(q_{\mathrm{m}}^{\mathrm{i}}\right)$	relative combined standard uncertainty of mass flow rate of fluid i
$u_{\mathrm{r}}\left(q_{\mathrm{n,H_2,in}}\right)$	relative standard uncertainty of inlet molar flow rate of hydrogen
$u_{\mathrm{r}}\left(q_{\mathrm{n}}^{\mathrm{j}}\right)$	relative combined standard uncertainty of molar flow rate of fluid j
$u_{\mathrm{r}}\left(q_{\mathrm{V,in}}\right)$	relative standard uncertainty of inlet volumetric flow rate
$u_{\mathrm{r}}\left(q_{\mathrm{V,out}}\right)$	relative standard uncertainty of product gas volumetric flow rate
$u_{\mathrm{r}}\left(T^{\mathrm{i}}\right)$	relative combined standard uncertainty of temperature of fluid i
$u_{\mathrm{r}}\left(\Delta T^{\mathrm{i}}\right)$	relative standard uncertainty of temperature difference between temperature of fluid i and standard ambient temperature
$u_{\mathrm{r}}\left(T^{\mathrm{j}}\right)$	relative combined standard uncertainty of temperature of fluid j
$u_{\mathrm{r}}\left(T_{\mathrm{stack}}\right)$	relative combined standard uncertainty of stack temperature
$\bar{U}_{\mathrm{RU}}$	average repeating unit voltage
$u_{\mathrm{r}}\left(U_{\mathrm{dc}}\right)$	relative standard uncertainty of DC voltage
$U_{\mathrm{RU,EL}}$	electrolyser repeating unit voltage
$U_{\mathrm{RU,FC}}$	fuel cell repeating unit voltage
$u_{\mathrm{r}}(X)$	relative standard uncertainty of test parameter X
$u_{\mathrm{r}}^2\left(x_{\mathrm{n,H_2,out}}\right)$	of outlet molar concentration of hydrogen
$u_{\mathrm{r}}\left(x_{\mathrm{n,H_2,out}}\right)$	relative standard uncertainty of outlet molar concentration of hydrogen
$u_{\mathrm{r}}(Y)$	relative standard uncertainty of test parameter Y
U_{th}	thermal voltage
U_{tn}	thermo-neutral voltage
$u(X)$	standard uncertainty of test parameter X

Symbol	Description
V	volume
$V_O^{\bullet\bullet}$	doubly positively charged oxide ion lattice vacancy
V_m	molar volume
V_{m,H_2}	molar volume of hydrogen
X	test parameter
$\bar{X}$	average value test parameter X
$x_{i,neg,in}$	inlet molar concentration of component i in negative electrode gas
$x_{i,neg,out}$	outlet molar concentration of component i in negative electrode gas
$x_{i,pos,in}$	inlet molar concentration of component i in positive electrode gas
$x_{i,pos,out}$	outlet molar concentration of component i in positive electrode gas
X_l	instantaneous value of test parameter X
x_n	molar concentration
x_{n,H_2}	molar concentration of hydrogen
$x_{n,H_2,in}$	inlet molar concentration of hydrogen
$x_{n,H_2,out}$	outlet molar concentration of hydrogen
$\bar{x}_{n,H_2,out}$	average value of outlet molar concentration of hydrogen
$x_{n,H_2,out,l}$	instantaneous value of outlet molar concentration of hydrogen
$x_{n,i}$	molar concentration of component i
$x_{n,j}$	molar concentration of component j
Y	test parameter
$\bar{Y}$	average value of test parameter Y
$\tilde{Y}$	pseudo-average of test parameter Y
z	number of electrons exchanged
$\bar{Z}$	average compressibility factor
$\bar{Z}^j$	average compressibility factor of fluid j

List of figures

List of tables

Annex A Test safety

The measurement of polarisation curves of cell/stack assembly units should adhere to fundamental safety considerations (Fu *et al.*, 2017). In HTFC and HTSE cell/stack assembly units, hazards arise due to various factors including:

- The presence of steam, combustible gases (especially hydrogen), oxidising gases (particularly oxygen), and asphyxiating gases (such as nitrogen),
- High temperature,
- High pressure, and
- High voltage.

Throughout the phases of installation, commissioning, operation, quiescence, maintenance, and decommissioning, ensuring the safety of personnel requires diligence and caution from all involved parties. Entities conducting testing and chemical analysis must adhere to the occupational health and safety (OHS) requirements outlined in ISO 45001:2018 (ISO, 2018) and follow good laboratory practices (GLPs). Tests on cell/stack assembly units should comply with applicable legislation, granted licenses, and issued permits to mitigate harm or unacceptable risk to humans, property, and the environment.

Guidance on the safety of electrical equipment (IEC, 2021b, IEC, 2018) and alkaline energy storage (ES) devices (IEC, 1996) has been provided by the IEC, while ISO published guidance on the safety of hydrogen systems (ISO, 2015). ([15]) These guidances should be adhered to when testing water electrolyser (WE) stacks. ([16]) Standards related to FC safety issued by the IEC (IEC, 2019, IEC, 2020b) may be applied by analogy. Additionally, IEC guidance on the classification of areas where explosive atmospheres can occur (IEC, 2014, IEC, 2013, IEC, 2017, IEC, 2020a), should be followed.

In the European Economic Area (EEA), ([17]) directives such as the ATEX Directives 2014/34/EU (EP and Council, 2014b) and 94/9/EC (EP and Council, 1994) apply, alongside other EU legislation including the electromagnetic compatibility (EMC) Directive 2014/30/EU (EP and Council, 2014a), the Low-Voltage Directive (LVD) 2014/35/EU (EP and Council, 2014c), the general product safety Directive 2001/95/EC (EP and Council, 2001), the machinery Directive 2006/42/EC (EP and Council, 2006), and the Pressure Equipment Directive (PED) 2014/68/EU (EP and Council, 2014d) ([18]).

([15]) Working Group (WG) 29 of TC 197 is currently reviewing ISO/Technical Report (TR) 15916:2015.

([16]) Note that ISO 22734:2019 Hydrogen generators using water electrolysis — Industrial, commercial, and residential applications (ISO, 2019b), specifies safety-related aspects of WE. Additionally, WG 34 of TC 197 recently issued ISO/DIS 22734-1:2024 Hydrogen generators using water electrolysis - Part 1: General requirements, test protocols and safety requirements (ISO, 2024), which includes clauses on safety among others, aiming to replace ISO 22734:2019.

([17]) The EEA encompasses the European Union (EU) territory as defined by Article 52 of the Treaty on European Union and Article 355 of the Treaty on the Functioning of the European Union, as well as Island, Norway, and Liechtenstein. Switzerland also adheres to EEA principles under a mutual recognition agreement, and Türkiye under a Customs Union Agreement with the EU.

([18]) The European Commission provides online guidance for various directives and regulations, including:

- The Appareils destinés à être utilisés en atmosphères explosibles (ATEX) Directive (https://single-market-economy.ec.europa.eu/single-market/european-standards/harmonised-standards/equipment-explosive-atmospheres-atex_en),
- The EMC Directive (https://single-market-economy.ec.europa.eu/sectors/electrical-and-electronic-engineering-industries-eei/electromagnetic-compatibility-emc-directive_en),
- The LVD (https://single-market-economy.ec.europa.eu/sectors/electrical-and-electronic-engineering-industries-eei/low-voltage-directive-lvd_en),
- The General product safety Directive (https://single-market-economy.ec.europa.eu/single-market/european-standards/harmonised-standards/general-product-safety_en),
- The Machinery Directive (https://single-market-economy.ec.europa.eu/sectors/mechanical-engineering/machinery_en), and
- The PED (https://single-market-economy.ec.europa.eu/sectors/pressure-equipment-and-gas-appliances/pressure-equipment-sector/pressure-equipment-directive_en).

Annex B Test report

B.1 General

The test report must accurately, clearly, and objectively present all pertinent information to demonstrate the purpose(s) and objective(s) of the test. At a minimum, the test report should include a title page (section B.2) and a summary (section B.3) presenting the measured or calculated TIPs and TOPs, at least as mean values, accompanied by their (combined) standard uncertainties, whether absolute, relative, or both. Calibration records or certificates for the measuring instruments should be documented in the report and made available upon request.

B.2 Title page

The titlepage should include the following information:

(a) Report identification, *i. e.* report number (optional).

(b) Type of report (summary, detailed, or full).

(c) Author(s) of the report.

(d) Entity issuing the report, including name and address.

(e) Date of the report.

(f) Person(s) conducting the test, if different from the reporting author(s).

(g) Organisation conducting the test, if different from the report-issuing entity.

(h) Date and time per test run.

(i) Location per test run, if different from the address of the report-issuing entity.

(j) Descriptive name per test.

(k) Identification (such as model name, serial number, type and specification) of the cell/stack tested, including the manufacturer.

A contents page may follow the title page before the summary.

B.3 Summary report

The summary should include the following information:

(i) Test purpose(s) and objective(s).

(ii) Description of the test(s) with sufficient information on the test conduct and measurement set-up, including test methods, measurement techniques, and test conditions.

(iii) All relevant test parameters, namely TIPs and TOPs with uncertainties.

(iv) Conclusion(s), including a graphical presentation of test results and a discussion with remark(s) and/or observation(s), as appropriate.

Further guidance on reporting test results is available in the Test Module (TM) 00 of the Solid Oxide Cell and Stack Testing, Safety and Quality Assurance (SOCTES^{QA}) project (Fu *et al.*, 2017).

Annex C Electrode reactions in Kröger–Vink notation

C.1 High-temperature fuel cells

In Kröger–Vink notation, the SOFC electrode reactions (4.1.2) read ([19])

$$\text{Negative electrode: } H_{2\,(g)} + O^{x}_{0\,(el)} \xrightarrow{\text{HOR}} H_2O_{(g)} + V^{\bullet\bullet}_{0\,(el)} + 2\,e'_{(ed)} \text{ and} \tag{C.1.1a}$$

$$\text{Positive electrode: } \frac{1}{2}\,O_{2\,(g)} + 2\,e'_{(ed)} + V^{\bullet\bullet}_{0\,(el)} \xrightarrow{\text{ORR}} O^{x}_{0\,(el)}; \tag{C.1.1b}$$

O^{x}_{0} and e' denote oxygen on neutral oxide ion lattice site and electron in the lattice, respectively. The presence of doubly positively charged oxide ion lattice vacancies in the anion lattice structure of the solid oxide ceramic electrolyte is the result of the specific incorporation of foreign metal cations of lower valency into its cation lattice structure.

For PCFC, the electrode reactions (4.1.3) read:

$$\text{Negative electrode: } H_{2\,(g)} + 2\,O^{x}_{0\,(el)} \xrightarrow{\text{HOR}} 2\,OH^{\bullet}_{0\,(el)} + 2\,e'_{(ed)} \text{ and} \tag{C.1.2a}$$

$$\text{Positive electrode: } 2\,OH^{\bullet}_{0\,(el)} + 2\,e'_{(ed)} + \frac{1}{2}\,O_{2\,(g)} \xrightarrow{\text{ORR}} H_2O_{(g)} + 2\,O^{x}_{0\,(el)}. \tag{C.1.2b}$$

C.2 High-temperature steam electrolysers

For SOEC, the electrode reactions (4.2.2) read in this notation as follows:

$$\text{Negative electrode: } H_2O_{(g)} + 2\,e'_{(ed)} + V^{\bullet\bullet}_{0\,(el)} \xrightarrow{\text{HER}} H_{2\,(g)} + O^{x}_{0\,(el)} \text{ and} \tag{C.2.1a}$$

$$\text{Positive electrode: } O^{x}_{0\,(el)} \xrightarrow{\text{OER}} \frac{1}{2}\,O_{2\,(g)} + 2\,e'_{(ed)} + V^{\bullet\bullet}_{0\,(el)} \tag{C.2.1b}$$

while for PCEC, the electrode reactions (4.2.3) read:

$$\text{Negative electrode: } 2\,OH^{\bullet}_{0\,(el)} + 2\,e'_{(ed)} \xrightarrow{\text{HER}} H_{2\,(g)} + 2\,O^{x}_{0\,(el)} \text{ and} \tag{C.2.2a}$$

$$\text{Positive electrode: } H_2O_{(g)} + 2\,O^{x}_{0\,(el)} \xrightarrow{\text{OER}} 2\,OH^{\bullet}_{0\,(el)} + 2\,e'_{(ed)} + \frac{1}{2}\,O_{2\,(g)}; \tag{C.2.2b}$$

Note that intermittent steps and partial pressure-dependent side reactions are possible in the reactions (C.2.1) and (C.2.2).

([19]) Note, with respect to neutral lattice charge, the use of two electrons on the right hand side (RHS) of reaction (C.1.1a) is equivalent to the use of two electron holes ($h^{\bullet}$) on the left hand side (LHS) of this reaction. The same applies to the reactions (C.1.2a), (C.2.1b) and (C.2.2b) and by analogy also to the reactions (C.1.1b), (C.1.2b), (C.2.1a) and (C.2.2a).

Annex D Determination of Faradaic efficiency

In HTSE cell/stack assembly units, electronic leakage can occur in addition to gas leakage through sealing, resulting in a reduction of Faradaic efficiency. This reduction takes place as some of the imposed current is conducted through the dense ceramic electrolyte membrane without contributing to ionic flux and, consequently, hydrogen flux. This phenomenon is particularly pronounced in PCECs, which employ mixed conductors as ceramic electrolyte membranes. These membranes exhibit both electronic and proton conduction, typically through electron hole and electron. Therefore, the Faradaic efficiency of a cell/stack assembly unit depends on the material properties of the ceramic electrolyte membrane, particularly its conductivity. It is also a function of the operating conditions, including current, gas inlet composition, flow rate, pressures and temperature.

In the presence of electrode gases on their respective sides of the ceramic electrolyte membrane, which features an inherently inhomogeneous defect structure, charge carriers (electrons and ionic species) can permeate this membrane (resulting in internal leakage) even at OCV, thereby allowing the determination of the minimum internal leakage current. Nonetheless, Faradaic efficiency is calculated as follows:

$$\eta_{\mathrm{F}}\ \% = \frac{z \cdot F\ (\mathrm{C/mol}) \cdot q_{\mathrm{n,H_2,net}}\ (\mathrm{mol/s})}{I\ (\mathrm{A}) \cdot N_{\mathrm{cells}}} \cdot 100\ \% \approx \frac{1,93 \cdot 10^5\ (\mathrm{A\ s/mol}) \cdot q_{\mathrm{n,H_2,net}}\ (\mathrm{mol/s})}{I\ (\mathrm{A}) \cdot N_{\mathrm{cells}}} \cdot 100\ \%, \qquad \text{(D.0.1)}$$

where $q_{\mathrm{n,H_2,net}}$ is the net molar flow rate of hydrogen defined as the difference between the inlet and outlet molar flow rates of hydrogen measured. The composition of hydrogen in the inlet and outlet gases may be determined by gas analysis in accordance with ISO 21087:2019 (ISO, 2019a).

The Faradaic efficiency of a cell/stack assembly unit at a given pressure and temperature using defined inlet gas compositions and flow rates, is determined for each specified current by performing the following steps:

1. Operate the cell/stack assembly unit at the specified inlet gas compositions, flow rates, and current for a minimum of 20 minutes. Record the current and voltage of the unit at least every 30 seconds to verify stable state conditions.

2. Following attainment of stable state conditions, operate the cell/stack assembly unit further under the same conditions. Measure the current, voltage, and in the presence of hydrogen, the molar flow rates of hydrogen at the specified sampling rate for a minimum of 10 minutes at the gas inlet and outlet. This measurement is performed using flow meters according to the expected range of flow rate and gas analysers according to the range of expected compositions and the required accuracy. Stable state conditions are considered to be achieved when the voltage and temperature of the cell/stack assembly unit remain within their tolerance ranges for a specified duration of not less than 5 minutes. Flow and gas measurements at the inlet and outlet of the cell/stack assembly unit are performed at SATP conditions. Prior to gas outlet measurements, this involves cooling the outlet gas, including steam condensation, and, as necessary, de-pressurisation of the unit.

3. Repeat the previous steps until the last current value within its specified range has been evaluated.

4. Calculate the Faradaic efficiency in accordance with equation (D.0.1) and plot it versus current density. This procedure can be repeated for other pressures and temperatures, as well as inlet gas compositions and flow rates.

Annex E Measurement uncertainties

E.1 General

The average value (arithmetic mean) of test parameter X ($\bar{X}$) is calculated from L equally spaced measurements ([20]) X_l as follows (JCGM, 2008):

$$\bar{X} = \frac{1}{L}\sum_{l=1}^{L} X_l; \tag{E.1.1a}$$

X_l is the instantaneous value of test parameter X. The standard uncertainty of test parameter X is multiplied by the coverage factor as follows (JCGM, 2008):

$$k \cdot u(X) = 3\sqrt{s^2(X)}; \tag{E.1.1b}$$

$s^2(X)$ is the standard variance of test parameter X calculated as follows (JCGM, 2008):

$$s^2(X) = \frac{1}{L-1}\sum_{l=1}^{L}\left(X_l - \bar{X}\right)^2. \tag{E.1.1c}$$

When test parameter Y depends on one or more test parameters X, the combined standard uncertainty of test parameter Y is also multiplied by the coverage factor as follows (JCGM, 2008):

$$k \cdot u_c(Y) = 3\sqrt{u_c^2(Y)}; \tag{E.1.1d}$$

$u_c^2(Y)$ is the square of combined standard uncertainty of test parameter Y as a function of test parameters X calculated as follows (JCGM, 2008):

$$u_c^2(Y) = \left(\frac{\partial Y}{\partial X}\right)^2 \cdot s^2(X). \tag{E.1.1e}$$

The partial derivative $\partial Y/\partial X$ is evaluated at the pseudo-average of test parameter Y using the average value of test parameter X. The relative standard uncertainty (u_r) of test parameter X or Y is calculated as follows (JCGM, 2008):

$$u_r(X) = \frac{u(X)}{\bar{X}} \text{ or } u_r(Y) = \frac{u_c(Y)}{\bar{Y}}; \tag{E.1.1f}$$

$u(X)$ is the positive square root of the standard variance of test parameter X and $u_c(Y)$ is the positive square root of the square of combined standard uncertainty of test parameter Y. It is assumed that all test parameters are uncorrelated. These computations can easily be performed using spreadsheet software.

Where referring to equation (1.0.2), equation (1.0.3), equation (5.1.4b), equation (5.1.4c) and equation (5.1.5b), the quantities used in these equations should be interpreted in the context of either input or output, as applicable.

E.2 Computation of instantaneous values

The instantaneous values for the inlet molar flow rate of hydrogen ($q_{n,H_2,in,l}$), outlet molar flow rate of hydrogen ($q_{n,H_2,out,l}$), mass flow rate of fluid i ($q^i_{m,l}$), and molar flow rate of fluid j ($q^j_{n,l}$) are calculated as follows:

$$q_{n,H_2,in,l}\ \text{(mol/s)} = x_{n,H_2,in}\ \text{(mol/mol)} \cdot \frac{q_{V,in,l}\ \text{(m}^3\text{/s)}}{V_{m,H_2}\ \text{(m}^3\text{/mol)}}, \tag{E.2.1a}$$

$$q_{n,H_2,out,l}\ \text{(mol/s)} = \bar{x}_{n,H_2,out}\ \text{(mol/mol)} \cdot \frac{q_{V,out,l}\ \text{(m}^3\text{/s)}}{V_{m,H_2}\ \text{(m}^3\text{/mol)}}, \tag{E.2.1b}$$

$$q^i_{m,l}\ \text{(kg/s)} = x_{n,i}\ \text{(mol/mol)} \cdot M_i\ \text{(kg/mol)} \cdot q_{n,l}\ \text{(mol/s)} \text{ and} \tag{E.2.1c}$$

$$q^j_{n,l}\ \text{(mol/s)} = x_{n,j}\ \text{(mol/mol)} \cdot q_{n,l}\ \text{(mol/s)}, \tag{E.2.1d}$$

respectively; $q_{V,in,l}$ is the instantaneous value of inlet volumetric flow rate, $\bar{x}_{n,H_2,out}$ is given by equation (E.3.2d), $q_{V,out,l}$ is the instantaneous value of product gas volumetric flow rate and $q_{n,l}$ is the instantaneous value of

([20]) For polarisation curve measurements employing method A (see section 6.3.2 and section 6.3.3), the number of measurements, L, correspond to the number of data points acquired during the step duration, t_{step}. Each data point yields the instantaneous values (denoted by subscript $_l$) of the various measured and calculated test parameters, as detailed in Table 1 and Table 4.

molar flow rate of respectively fluid i and j as regards equation (E.2.1c) and equation (E.2.1d). Note, the molar concentrations $x_{\mathrm{n,H_2,in}}$, $\bar{x}_{\mathrm{n,H_2,out}}$, $x_{\mathrm{n,i}}$, and $x_{\mathrm{n,j}}$ are assumed constant.

The instantaneous values of current density (J_{l}), DC power ($P_{\mathrm{el,dc,l}}$), electric power density ($P_{\mathrm{el,d,l}}$), input power of hydrogen based on HHV ($P^{\mathrm{HHV}}_{\mathrm{H_2,in,l}}$), input power of hydrogen based on LHV ($P^{\mathrm{LHV}}_{\mathrm{H_2,in,l}}$), input thermal power ($P_{\mathrm{th,in,l}}$), input pneumatic power ($P_{\mathrm{p,in,l}}$), output thermal power ($P_{\mathrm{th,out,l}}$), output power of hydrogen based on HHV ($P^{\mathrm{HHV}}_{\mathrm{H_2,out,l}}$), and output power of hydrogen based on LHV ($P^{\mathrm{LHV}}_{\mathrm{H_2,out,l}}$) are calculated as follows:

$$J_{\mathrm{l}}\ (\mathrm{A/cm^2}) = \frac{I_{\mathrm{dc,l}}\ (\mathrm{A})}{A_{\mathrm{act}}\ (\mathrm{cm^2})}, \tag{E.2.2a}$$

$$P_{\mathrm{el,dc,l}}\ (\mathrm{kW}) = U_{\mathrm{dc,l}}\ (\mathrm{V}) \cdot I_{\mathrm{dc,l}}\ (\mathrm{A}) \cdot 10^{-3}\ (\mathrm{kW/W}), \tag{E.2.2b}$$

$$P_{\mathrm{el,d,l}}\ (\mathrm{W/cm^2}) = U_{\mathrm{dc,l}}\ (\mathrm{V}) \cdot J_{\mathrm{l}}\ (\mathrm{A/cm^2}), \tag{E.2.2c}$$

$$P^{\mathrm{HHV}}_{\mathrm{H_2,in,l}}\ (\mathrm{kW}) = q_{\mathrm{n,H_2,in,l}}\ (\mathrm{mol/s}) \cdot 79,4 \cdot 10^{-3}\ (\mathrm{kWh/mol}) \cdot 3600\ (\mathrm{s/h}), \tag{E.2.2d}$$

$$P^{\mathrm{LHV}}_{\mathrm{H_2,in,l}}\ (\mathrm{kW}) = q_{\mathrm{n,H_2,in,l}}\ (\mathrm{mol/s}) \cdot 67,2 \cdot 10^{-3}\ (\mathrm{kWh/mol}) \cdot 3600\ (\mathrm{s/h}), \tag{E.2.2e}$$

$$P_{\mathrm{th,in,l}}\ (\mathrm{kW}) = \sum_{\mathrm{i}} q^{\mathrm{i}}_{\mathrm{m,l}}\ (\mathrm{kg/s}) \cdot c^{\mathrm{i}}_{\mathrm{p}}\left(T^{\mathrm{i}}_{\mathrm{l}}\right)\ (\mathrm{kJ/(kg\ K)}) \cdot \left(T^{\mathrm{i}}_{\mathrm{l}}\ (\mathrm{K}) - T^{0}\ (\mathrm{K})\right), \tag{E.2.2f}$$

$$P_{\mathrm{p,in,l}}\ (\mathrm{kW}) = \sum_{\mathrm{j}} \left(\frac{\gamma^{\mathrm{j}}}{\gamma^{\mathrm{j}}-1}\right) \frac{\bar{Z}^{\mathrm{j}} \cdot R_{\mathrm{g}}\ (\mathrm{kJ/(mol\ K)}) \cdot T^{0}\ (\mathrm{K}) \cdot q^{\mathrm{j}}_{\mathrm{n,l}}\ (\mathrm{mol/h})}{3600\ (\mathrm{s/h})} \cdot \left(\left(\frac{p^{\mathrm{j}}_{\mathrm{l}}\ (\mathrm{kPa})}{p^{0}\ (\mathrm{kPa})}\right)^{\frac{\gamma^{\mathrm{j}}-1}{\gamma^{\mathrm{j}}}} - 1\right), \tag{E.2.2g}$$

$$P_{\mathrm{th,out,l}}\ (\mathrm{kW}) = \sum_{\mathrm{i}} q^{\mathrm{i}}_{\mathrm{m,l}}\ (\mathrm{kg/s}) \cdot c^{\mathrm{i}}_{\mathrm{p}}\left(T^{\mathrm{i}}_{\mathrm{l}}\right)\ (\mathrm{kJ/(kg\ K)}) \cdot \left(T^{\mathrm{i}}_{\mathrm{l}}\ (\mathrm{K}) - T^{0}\ (\mathrm{K})\right), \tag{E.2.2h}$$

$$P^{\mathrm{HHV}}_{\mathrm{H_2,out,l}}\ (\mathrm{kW}) = q_{\mathrm{n,H_2,out,l}}\ (\mathrm{mol/s}) \cdot 79,4 \cdot 10^{-3}\ (\mathrm{kWh/mol}) \cdot 3600\ (\mathrm{s/h}) \quad \text{and} \tag{E.2.2i}$$

$$P^{\mathrm{LHV}}_{\mathrm{H_2,out,l}}\ (\mathrm{kW}) = q_{\mathrm{n,H_2,out,l}}\ (\mathrm{mol/s}) \cdot 67,2 \cdot 10^{-3}\ (\mathrm{kWh/mol}) \cdot 3600\ (\mathrm{s/h}), \tag{E.2.2j}$$

respectively; $I_{\mathrm{dc,l}}$ is the instantaneous value of direct current, $U_{\mathrm{dc,l}}$ is the instantaneous value of DC voltage, $q^{\mathrm{i}}_{\mathrm{m,l}}$ is given by equation (E.2.1c), $T^{\mathrm{i}}_{\mathrm{l}}$ is the instantaneous value of temperature of fluid i, $q^{\mathrm{j}}_{\mathrm{n,l}}$ is given by equation (E.2.1d), $p^{\mathrm{j}}_{\mathrm{l}}$ is the instantaneous value of pressure of fluid j, $q_{\mathrm{n,H_2,in,l}}$ is given by equation (E.2.1a), and $q_{\mathrm{n,H_2,out,l}}$ is given by equation (E.2.1b). Note, the fluid properties $c^{\mathrm{i}}_{\mathrm{p}}$, $c^{\mathrm{j}}_{\mathrm{p}}$, $c^{\mathrm{j}}_{\mathrm{V}}$ and thus, γ^{j} as well as $\bar{Z}^{\mathrm{j}}$ which all are pressure and temperature dependent, are assumed constant. For simplicity, the average value of pressure of fluid i ($\bar{p}^{\mathrm{i}}$) given by equation (E.3.2i) and temperature of fluid i ($\bar{T}^{\mathrm{i}}$) given by equation (E.3.2j) may be used to determine $c^{\mathrm{i}}_{\mathrm{p}}$. Similarly, the average value of pressure of fluid j ($\bar{p}^{\mathrm{j}}$) given by equation (E.3.2k), and temperature of fluid j ($\bar{T}^{\mathrm{j}}$) given by equation (E.3.2l) may be used to determine γ^{j} and $\bar{Z}^{\mathrm{j}}$.

E.3 Computation of average values

The average repeating unit voltage ($\bar{U}_{\mathrm{RU}}$) of the cell/stack assembly unit is calculated as follows:

$$\bar{U}_{\mathrm{RU}}\ (\mathrm{V}) = \frac{\bar{U}_{\mathrm{dc}}\ (\mathrm{V})}{N_{\mathrm{cells}}}; \tag{E.3.1}$$

$\bar{U}_{\mathrm{dc}}$ is given by equation (E.3.3c).

The average values of stack temperature ($\bar{T}_{\mathrm{stack}}$), inlet volumetric flow rate ($\bar{q}_{\mathrm{V,in}}$), inlet molar flow rate of hydrogen ($\bar{q}_{\mathrm{n,H_2,in}}$), outlet molar concentration of hydrogen ($\bar{x}_{\mathrm{n,H_2,out}}$), product gas volumetric flow rate ($\bar{q}_{\mathrm{V,out,l}}$), outlet molar flow rate of hydrogen ($\bar{q}_{\mathrm{n,H_2,out}}$), mass flow rate of fluid i ($\bar{q}^{\mathrm{i}}_{\mathrm{m}}$), molar flow rate of fluid j ($\bar{q}^{\mathrm{j}}_{\mathrm{n}}$), pressure of fluid i ($\bar{p}^{\mathrm{i}}$), temperature of fluid i ($\bar{T}^{\mathrm{i}}$), pressure of fluid j ($\bar{p}^{\mathrm{j}}$), and temperature of fluid j ($\bar{T}^{\mathrm{j}}$) are calculated as follows:

$$\bar{T}_{\mathrm{stack}}\ (\mathrm{K}) = \frac{1}{L}\sum_{\mathrm{l}=1}^{L} T_{\mathrm{stack,l}}\ (\mathrm{K}), \tag{E.3.2a}$$

$$\bar{q}_{\mathrm{V,in}}\ (\mathrm{m^3/s}) = \frac{1}{L}\sum_{\mathrm{l}=1}^{L} q_{\mathrm{V,in,l}}\ (\mathrm{m^3/s}), \tag{E.3.2b}$$

$$\bar{q}_{\mathrm{n,H_2,in}}\ (\mathrm{mol/s}) = \frac{1}{L}\sum_{\mathrm{l}=1}^{L} q_{\mathrm{n,H_2,in,l}}\ (\mathrm{mol/s}), \tag{E.3.2c}$$

$$\bar{x}_{\mathrm{n,H_2,out}}\ (\mathrm{mol/mol}) = \frac{1}{L}\sum_{\mathrm{l}=1}^{L} x_{\mathrm{n,H_2,out,l}}\ (\mathrm{mol/mol}), \tag{E.3.2d}$$

$$\bar{q}_{\mathrm{V,out,l}}\ (\mathrm{m^3/s}) = \frac{1}{L}\sum_{\mathrm{l}=1}^{L} q_{\mathrm{V,out,l}}\ (\mathrm{m^3/s}), \tag{E.3.2e}$$

$$\bar{q}_{\mathrm{n,H_2,out}}\ (\mathrm{mol/s}) = \frac{1}{L}\sum_{\mathrm{l}=1}^{L} q_{\mathrm{n,H_2,out,l}}\ (\mathrm{mol/s}), \tag{E.3.2f}$$

$$\bar{q}^{\mathrm{i}}_{\mathrm{m}}\ (\mathrm{mol/s}) = \frac{1}{L}\sum_{\mathrm{l}=1}^{L} q^{\mathrm{i}}_{\mathrm{m,l}}\ (\mathrm{mol/s}), \tag{E.3.2g}$$

$$\bar{q}^{\mathrm{j}}_{\mathrm{n}}\ (\mathrm{mol/s}) = \frac{1}{L}\sum_{\mathrm{l}=1}^{L} q^{\mathrm{j}}_{\mathrm{n,l}}\ (\mathrm{mol/s}), \tag{E.3.2h}$$

$$\bar{p}^{\mathrm{i}}\ (\mathrm{kPa}) = \frac{1}{L}\sum_{\mathrm{l}=1}^{L} p^{\mathrm{i}}_{\mathrm{l}}\ (\mathrm{kPa}), \tag{E.3.2i}$$

$$\bar{T}^{\mathrm{i}}\ (\mathrm{K}) = \frac{1}{L}\sum_{\mathrm{l}=1}^{L} T^{\mathrm{i}}_{\mathrm{l}}\ (\mathrm{K}), \tag{E.3.2j}$$

$$\bar{p}^{\mathrm{j}}\ (\mathrm{kPa}) = \frac{1}{L}\sum_{\mathrm{l}=1}^{L} p^{\mathrm{j}}_{\mathrm{l}}\ (\mathrm{kPa})\ \text{ and} \tag{E.3.2k}$$

$$\bar{T}^{\mathrm{j}}\ (\mathrm{K}) = \frac{1}{L}\sum_{\mathrm{l}=1}^{L} T^{\mathrm{j}}_{\mathrm{l}}\ (\mathrm{K}), \tag{E.3.2l}$$

respectively; $T_{\mathrm{stack,l}}$ is the instantaneous value of stack temperature, $q_{\mathrm{V,in,l}}$ is the instantaneous value of inlet volumetric flow rate, $q_{\mathrm{n,H_2,in,l}}$ is given by equation (E.2.1a), $x_{\mathrm{n,H_2,out,l}}$ is the instantaneous value of outlet molar concentration of hydrogen, $q_{\mathrm{V,out,l}}$ is the instantaneous value of product gas volumetric flow rate, $q_{\mathrm{n,H_2,out,l}}$ is given by equation (E.2.1b), $q^{\mathrm{i}}_{\mathrm{m,l}}$ is given by equation (E.2.1c), $q^{\mathrm{j}}_{\mathrm{n,l}}$ is given by equation (E.2.1d), $p^{\mathrm{i}}_{\mathrm{l}}$ is the instantaneous value of pressure of fluid i, $T^{\mathrm{i}}_{\mathrm{l}}$ is the instantaneous value of temperature of fluid i, $p^{\mathrm{j}}_{\mathrm{l}}$ is the instantaneous value of pressure of fluid j, and $T^{\mathrm{j}}_{\mathrm{l}}$ is the instantaneous value of temperature of fluid j.

The average values of direct current ($\bar{I}_{\mathrm{dc}}$), current density ($\bar{J}$), DC voltage ($\bar{U}_{\mathrm{dc}}$), DC power ($\bar{P}_{\mathrm{el,dc}}$), electric power density ($\bar{P}_{\mathrm{el,d}}$), input thermal power ($\bar{P}_{\mathrm{th,in}}$), input pneumatic power ($\bar{P}_{\mathrm{p,in}}$), output thermal power ($\bar{P}_{\mathrm{th,out}}$), input power of hydrogen based on HHV ($\bar{P}^{\mathrm{HHV}}_{\mathrm{H_2,in}}$), input power of hydrogen based on LHV ($\bar{P}^{\mathrm{LHV}}_{\mathrm{H_2,in}}$), output power of hydrogen based on HHV ($\bar{P}^{\mathrm{HHV}}_{\mathrm{H_2,out}}$), and output power of hydrogen based on LHV ($\bar{P}^{\mathrm{LHV}}_{\mathrm{H_2,out}}$) are calculated as follows:

$$\bar{I}_{\mathrm{dc}}\ (\mathrm{A}) = \frac{1}{L}\sum_{\mathrm{l}=1}^{L} I_{\mathrm{dc,l}}\ (\mathrm{A}), \tag{E.3.3a}$$

$$\bar{J}\ (\mathrm{A/cm^2}) = \frac{1}{L}\sum_{\mathrm{l}=1}^{L} J_{\mathrm{l}}\ (\mathrm{A/cm^2}), \tag{E.3.3b}$$

$$\bar{U}_{\mathrm{dc}}\ (\mathrm{V}) = \frac{1}{L}\sum_{\mathrm{l}=1}^{L} U_{\mathrm{dc,l}}\ (\mathrm{V}), \tag{E.3.3c}$$

$$\bar{P}_{\mathrm{el,dc}}\ (\mathrm{kW}) = \frac{1}{L}\sum_{\mathrm{l}=1}^{L} P_{\mathrm{el,dc,l}}\ (\mathrm{kW}), \tag{E.3.3d}$$

$$\bar{P}_{\mathrm{el,d}}\ (\mathrm{W/cm^2}) = \frac{1}{L}\sum_{\mathrm{l}=1}^{L} P_{\mathrm{el,d,l}}\ (\mathrm{W/cm^2}), \tag{E.3.3e}$$

$$\bar{P}_{\mathrm{th,in}}\ (\mathrm{kW}) = \frac{1}{L}\sum_{\mathrm{l}=1}^{L} P_{\mathrm{th,in,l}}\ (\mathrm{kW}), \tag{E.3.3f}$$

$$\bar{P}_{\mathrm{p,in}}\ (\mathrm{kW}) = \frac{1}{L}\sum_{\mathrm{l}=1}^{L} P_{\mathrm{p,in,l}}\ (\mathrm{kW}), \tag{E.3.3g}$$

$$\bar{P}_{\mathrm{th,out}}\ (\mathrm{kW}) = \frac{1}{L}\sum_{\mathrm{l}=1}^{L} P_{\mathrm{th,out,l}}\ (\mathrm{kW}), \tag{E.3.3h}$$

$$\bar{P}^{\text{HHV}}_{\text{H}_2,\text{in}}\ (\text{kW}) = \frac{1}{L}\sum_{\text{l}=1}^{L} P^{\text{HHV}}_{\text{H}_2,\text{in,l}}\ (\text{kW}), \tag{E.3.3i}$$

$$\bar{P}^{\text{LHV}}_{\text{H}_2,\text{in}}\ (\text{kW}) = \frac{1}{L}\sum_{\text{l}=1}^{L} P^{\text{LHV}}_{\text{H}_2,\text{in,l}}\ (\text{kW}), \tag{E.3.3j}$$

$$\bar{P}^{\text{HHV}}_{\text{H}_2,\text{out}}\ (\text{kW}) = \frac{1}{L}\sum_{\text{l}=1}^{L} P^{\text{HHV}}_{\text{H}_2,\text{out,l}}\ (\text{kW}) \quad \text{and} \tag{E.3.3k}$$

$$\bar{P}^{\text{LHV}}_{\text{H}_2,\text{out}}\ (\text{kW}) = \frac{1}{L}\sum_{\text{l}=1}^{L} P^{\text{LHV}}_{\text{H}_2,\text{out,l}}\ (\text{kW}), \tag{E.3.3l}$$

respectively; J_{l} is given by equation (E.2.2a), $P_{\text{el,dc,l}}$ is given by equation (E.2.2b), $P_{\text{el,d,l}}$ is given by equation (E.2.2c), $P_{\text{th,in,l}}$ is given by equation (E.2.2f), $P_{\text{p,in,l}}$ is given by equation (E.2.2g), $P_{\text{th,out,l}}$ is given by equation (E.2.2h), $P^{\text{HHV}}_{\text{H}_2,\text{in,l}}$ is given by equation (E.2.2d), $P^{\text{LHV}}_{\text{H}_2,\text{in,l}}$ is given by equation (E.2.2e), $P^{\text{HHV}}_{\text{H}_2,\text{out,l}}$ is given by equation (E.2.2i), and $P^{\text{LHV}}_{\text{H}_2,\text{out,l}}$ is given by equation (E.2.2j).

The pseudo-averages of DC power ($\tilde{P}_{\text{el,dc}}$), electric power density ($\tilde{P}_{\text{el,d}}$), input thermal power ($\tilde{P}_{\text{th,in}}$), input pneumatic power ($\tilde{P}_{\text{p,in}}$), output thermal power ($\tilde{P}_{\text{th,out}}$), output thermal power ($\tilde{P}_{\text{th,out}}$), input power of hydrogen based on HHV ($\tilde{P}^{\text{HHV}}_{\text{H}_2,\text{in}}$), input power of hydrogen based on LHV ($\tilde{P}^{\text{LHV}}_{\text{H}_2,\text{in}}$), output power of hydrogen based on HHV ($\tilde{P}^{\text{HHV}}_{\text{H}_2,\text{out}}$), and output power of hydrogen based on LHV ($\tilde{P}^{\text{LHV}}_{\text{H}_2,\text{out}}$) are calculated as follows:

$$\tilde{P}_{\text{el,dc}}\ (\text{kW}) = \bar{U}_{\text{dc}}\ (\text{V}) \cdot \bar{I}_{\text{dc}}\ (\text{A}) \cdot 10^{-3}\ (\text{kW/W}), \tag{E.3.4a}$$

$$\tilde{P}_{\text{el,d}}\ (\text{W/cm}^2) = \bar{U}_{\text{dc}}\ (\text{V}) \cdot \bar{J}\ (\text{A/cm}^2), \tag{E.3.4b}$$

$$\tilde{P}_{\text{th,in}}\ (\text{kW}) = \sum_{i} \bar{q}^{\text{i}}_{\text{m}}\ (\text{kg/s}) \cdot c^{\text{i}}_{\text{p}}\ (\text{kJ/(kg K)}) \cdot \left(\bar{T}^{\text{i}}\ (\text{K}) - T^0\ (\text{K})\right), \tag{E.3.4c}$$

$$\tilde{P}_{\text{p,in}}\ (\text{kW}) = \sum_{j} \left(\frac{\gamma^{\text{j}}}{\gamma^{\text{j}}-1}\right) \frac{\bar{Z}^{\text{j}} \cdot R_{\text{g}}\ (\text{kJ/(mol K)}) \cdot T^0\ (\text{K}) \cdot \bar{q}^{\text{j}}_{\text{n}}\ (\text{mol/h})}{3600\ (\text{s/h})} \cdot \left(\left(\frac{\bar{p}^{\text{j}}\ (\text{kPa})}{p^0\ (\text{kPa})}\right)^{\frac{\gamma^{\text{j}}-1}{\gamma^{\text{j}}}} - 1\right), \tag{E.3.4d}$$

$$\tilde{P}_{\text{th,out}}\ (\text{kW}) = \sum_{i} \bar{q}^{\text{i}}_{\text{m}}\ (\text{kg/s}) \cdot c^{\text{i}}_{\text{p}}\ (\text{kJ/(kg K)}) \cdot \left(\bar{T}^{\text{i}}\ (\text{K}) - T^0\ (\text{K})\right), \tag{E.3.4e}$$

$$\tilde{P}^{\text{HHV}}_{\text{H}_2,\text{in}}\ (\text{kW}) = \bar{q}_{\text{n,H}_2,\text{in}}\ (\text{mol/s}) \cdot 79,4 \cdot 10^{-3}\ (\text{kWh/mol}) \cdot 3600\ (\text{s/h}), \tag{E.3.4f}$$

$$\tilde{P}^{\text{LHV}}_{\text{H}_2,\text{in}}\ (\text{kW}) = \bar{q}_{\text{n,H}_2,\text{in}}\ (\text{mol/s}) \cdot 67,4 \cdot 10^{-3}\ (\text{kWh/mol}) \cdot 3600\ (\text{s/h}), \tag{E.3.4g}$$

$$\tilde{P}^{\text{HHV}}_{\text{H}_2,\text{out}}\ (\text{kW}) = \bar{q}_{\text{n,H}_2,\text{out}}\ (\text{mol/s}) \cdot 79,2 \cdot 10^{-3}\ (\text{kWh/mol}) \cdot 3600\ (\text{s/h}) \quad \text{and} \tag{E.3.4h}$$

$$\tilde{P}^{\text{LHV}}_{\text{H}_2,\text{out}}\ (\text{kW}) = \bar{q}_{\text{n,H}_2,\text{out}}\ (\text{mol/s}) \cdot 67,2 \cdot 10^{-3}\ (\text{kWh/mol}) \cdot 3600\ (\text{s/h}), \tag{E.3.4i}$$

respectively; $\bar{U}_{\text{dc}}$ is given by equation (E.3.3c), $\bar{I}_{\text{dc}}$ is given by equation (E.3.3a), $\bar{J}$ is given by equation (E.3.3b), $\bar{q}^{\text{i}}_{\text{m}}$ is given by equation (E.3.2g), $\bar{T}^{\text{i}}$ is given by equation (E.3.2j), $\bar{p}^{\text{j}}$ is given by equation (E.3.2k), $\bar{q}^{\text{j}}_{\text{n}}$ is given by equation (E.3.2h), $\bar{q}_{\text{n,H}_2,\text{in}}$ is given by equation (E.3.2c), and $\bar{q}_{\text{n,H}_2,\text{out}}$ is given by equation (E.3.2f).

The average values of fuel cell electric efficiency based on HHV ($\bar{\eta}^{\text{HHV}}_{\text{el,FC}}$), fuel cell electric efficiency based on LHV ($\bar{\eta}^{\text{LHV}}_{\text{el,FC}}$), fuel cell thermal efficiency based on HHV ($\bar{\eta}^{\text{HHV}}_{\text{th,FC}}$), fuel cell thermal efficiency based on LHV ($\bar{\eta}^{\text{LHV}}_{\text{th,FC}}$), electrolyser energy efficiency based on HHV ($\bar{\eta}^{\text{HHV}}_{\text{e,EL}}$), and electrolyser energy efficiency based on LHV ($\bar{\eta}^{\text{LHV}}_{\text{e,EL}}$) are calculated as follows:

$$\bar{\eta}^{\text{HHV}}_{\text{el,FC}}\ (\%) = \frac{1}{L}\sum_{l=1}^{L} \frac{P_{\text{el,dc,l}}\ (\text{kW})}{P^{\text{HHV}}_{\text{H}_2,\text{in,l}}\ (\text{kW}) + P_{\text{th,in,l}}\ (\text{kW}) + P_{\text{p,in,l}}\ (\text{kW})} \cdot 100\ \%, \tag{E.3.5a}$$

$$\bar{\eta}^{\text{LHV}}_{\text{el,FC}}\ (\%) = \frac{1}{L}\sum_{l=1}^{L} \frac{P_{\text{el,dc,l}}\ (\text{kW})}{P^{\text{LHV}}_{\text{H}_2,\text{in,l}}\ (\text{kW}) + P_{\text{th,in,l}}\ (\text{kW}) + P_{\text{p,in,l}}\ (\text{kW})} \cdot 100\ \%, \tag{E.3.5b}$$

$$\bar{\eta}^{\text{HHV}}_{\text{th,FC}}\ (\%) = \frac{1}{L}\sum_{l=1}^{L} \frac{P_{\text{th,out,l}}\ (\text{kW})}{P^{\text{HHV}}_{\text{H}_2,\text{in,l}}\ (\text{kW}) + P_{\text{th,in,l}}\ (\text{kW}) + P_{\text{p,in,l}}\ (\text{kW})} \cdot 100\ \%, \tag{E.3.5c}$$

$$\bar{\eta}^{\text{LHV}}_{\text{th,FC}}\ (\%) = \frac{1}{L}\sum_{l=1}^{L} \frac{P_{\text{th,out,l}}\ (\text{kW})}{P^{\text{LHV}}_{\text{H}_2,\text{in,l}}\ (\text{kW}) + P_{\text{th,in,l}}\ (\text{kW}) + P_{\text{p,in,l}}\ (\text{kW})} \cdot 100\ \%, \tag{E.3.5d}$$

$$\bar{\eta}^{\mathrm{HHV}}_{\mathrm{e,EL}}\ (\%) = \frac{1}{L}\sum_{l=1}^{L}\frac{P^{\mathrm{HHV}}_{\mathrm{H_2,out,l}}\ (\mathrm{kW})}{P_{\mathrm{el,dc,l}}\ (\mathrm{kW}) + P_{\mathrm{th,in,l}}\ (\mathrm{kW}) + P_{\mathrm{p,in,l}}\ (\mathrm{kW})}\cdot 100\ \%\ \text{ and} \tag{E.3.5e}$$

$$\bar{\eta}^{\mathrm{LHV}}_{\mathrm{e,EL}}\ (\%) = \frac{1}{L}\sum_{l=1}^{L}\frac{P^{\mathrm{LHV}}_{\mathrm{H_2,out,l}}\ (\mathrm{kW})}{P_{\mathrm{el,dc,l}}\ (\mathrm{kW}) + P_{\mathrm{th,in,l}}\ (\mathrm{kW}) + P_{\mathrm{p,in,l}}\ (\mathrm{kW})}\cdot 100\ \%, \tag{E.3.5f}$$

respectively; $P_{\mathrm{el,dc,l}}$ is given by equation (E.2.2b), $P^{\mathrm{HHV}}_{\mathrm{H_2,in,l}}$ is given by equation (E.2.2d), $P^{\mathrm{LHV}}_{\mathrm{H_2,in,l}}$ is given by equation (E.2.2e), $P_{\mathrm{th,in,l}}$ is given by equation (E.2.2f), $P_{\mathrm{p,in,l}}$ is given by equation (E.2.2g), $P_{\mathrm{th,out,l}}$ is given by equation (E.2.2h), $P^{\mathrm{HHV}}_{\mathrm{H_2,out,l}}$ is given by equation (E.2.2i), and $P^{\mathrm{LHV}}_{\mathrm{H_2,out,l}}$ is given by equation (E.2.2j).

E.4 Computation of uncertainties

The standard variances of stack temperature ($s^2\left(T_{\mathrm{stack}}\right)$), inlet volumetric flow rate ($s^2\left(q_{\mathrm{V,in}}\right)$), inlet molar flow rate of hydrogen ($s^2\left(q_{\mathrm{n,H_2,in}}\right)$), outlet molar concentration of hydrogen ($s^2\left(x_{\mathrm{n,H_2,out}}\right)$), product gas volumetric flow rate ($s^2\left(q_{\mathrm{V,out}}\right)$), mass flow rate of fluid i ($s^2\left(q^{\mathrm{i}}_{\mathrm{m}}\right)$), molar flow rate of fluid j ($s^2\left(q^{\mathrm{j}}_{\mathrm{n}}\right)$), pressure of fluid i ($s^2\left(p^{\mathrm{i}}\right)$), temperature of fluid i ($s^2\left(T^{\mathrm{i}}\right)$), pressure of fluid j ($s^2\left(p^{\mathrm{j}}\right)$), and temperature of fluid j ($s^2\left(T^{\mathrm{j}}\right)$) are calculated as follows:

$$s^2\left(T_{\mathrm{stack}}\right)\ (\mathrm{K})^2 = \frac{1}{L-1}\sum_{l=1}^{L}\left(T_{\mathrm{stack,l}}\ (\mathrm{K}) - \bar{T}_{\mathrm{stack}}\ (\mathrm{K})\right)^2, \tag{E.4.1a}$$

$$s^2\left(q_{\mathrm{V,in}}\right)\ (\mathrm{m^3/s})^2 = \frac{1}{L-1}\sum_{l=1}^{L}\left(q_{\mathrm{V,in,l}}\ (\mathrm{m^3/s}) - \bar{q}_{\mathrm{V,in}}\ (\mathrm{m^3/s})\right)^2, \tag{E.4.1b}$$

$$s^2\left(q_{\mathrm{n,H_2,in}}\right)\ (\mathrm{mol/s})^2 = \frac{1}{L-1}\sum_{l=1}^{L}\left(q_{\mathrm{n,H_2,in,l}}\ (\mathrm{mol/s}) - \bar{q}_{\mathrm{n,H_2,in}}\ (\mathrm{mol/s})\right)^2, \tag{E.4.1c}$$

$$s^2\left(x_{\mathrm{n,H_2,out}}\right)\ (\mathrm{mol/s})^2 = \frac{1}{L-1}\sum_{l=1}^{L}\left(x_{\mathrm{n,H_2,out,l}}\ (\mathrm{mol/s}) - \bar{x}_{\mathrm{n,H_2,out}}\ (\mathrm{mol/s})\right)^2, \tag{E.4.1d}$$

$$s^2\left(q_{\mathrm{V,out}}\right)\ (\mathrm{m^3/s})^2 = \frac{1}{L-1}\sum_{l=1}^{L}\left(q_{\mathrm{V,out,l}}\ (\mathrm{m^3/s}) - \bar{q}_{\mathrm{V,out,l}}\ (\mathrm{m^3/s})\right)^2, \tag{E.4.1e}$$

$$s^2\left(q^{\mathrm{i}}_{\mathrm{m}}\right)\ (\mathrm{kg/s})^2 = \frac{1}{L-1}\sum_{l=1}^{L}\left(q^{\mathrm{i}}_{\mathrm{m,l}}\ (\mathrm{kg/s}) - \bar{q}^{\mathrm{i}}_{\mathrm{m}}\ (\mathrm{kg/s})\right)^2, \tag{E.4.1f}$$

$$s^2\left(q^{\mathrm{j}}_{\mathrm{n}}\right)\ (\mathrm{mol/s})^2 = \frac{1}{L-1}\sum_{l=1}^{L}\left(q^{\mathrm{j}}_{\mathrm{n,l}}\ (\mathrm{mol/s}) - \bar{q}^{\mathrm{j}}_{\mathrm{n}}\ (\mathrm{mol/s})\right)^2, \tag{E.4.1g}$$

$$s^2\left(p^{\mathrm{i}}\right)\ (\mathrm{kPa})^2 = \frac{1}{L-1}\sum_{l=1}^{L}\left(p^{\mathrm{i}}_{\mathrm{l}}\ (\mathrm{kPa}) - \bar{p}^{\mathrm{i}}\ (\mathrm{kPa})\right)^2, \tag{E.4.1h}$$

$$s^2\left(T^{\mathrm{i}}\right)\ (\mathrm{K})^2 = \frac{1}{L-1}\sum_{l=1}^{L}\left(T^{\mathrm{i}}_{\mathrm{l}}\ (\mathrm{K}) - \bar{T}^{\mathrm{i}}\ (\mathrm{K})\right)^2, \tag{E.4.1i}$$

$$s^2\left(p^{\mathrm{j}}\right)\ (\mathrm{kPa})^2 = \frac{1}{L-1}\sum_{l=1}^{L}\left(p^{\mathrm{j}}_{\mathrm{l}}\ (\mathrm{kPa}) - \bar{p}^{\mathrm{j}}\ (\mathrm{kPa})\right)^2 \text{ and} \tag{E.4.1j}$$

$$s^2\left(T^{\mathrm{j}}\right)\ (\mathrm{K})^2 = \frac{1}{L-1}\sum_{l=1}^{L}\left(T^{\mathrm{j}}_{\mathrm{l}}\ (\mathrm{K}) - \bar{T}^{\mathrm{j}}\ (\mathrm{K})\right)^2, \tag{E.4.1k}$$

respectively; $T_{\mathrm{stack,l}}$ is the instantaneous value of stack temperature, $\bar{T}_{\mathrm{stack}}$ is given by equation (E.3.2a), $q_{\mathrm{V,in,l}}$ is the instantaneous value of inlet volumetric flow rate, $\bar{q}_{\mathrm{V,in}}$ is given by equation (E.3.2b), $q_{\mathrm{n,H_2,in,l}}$ is the instantaneous value of inlet molar flow rate of hydrogen, $\bar{q}_{\mathrm{n,H_2,in}}$ is given by equation (E.3.2c), $x_{\mathrm{n,H_2,out,l}}$ is the instantaneous value of outlet molar concentration of hydrogen, $\bar{x}_{\mathrm{n,H_2,out}}$ is given by equation (E.3.2d), $q_{\mathrm{V,out,l}}$ is the instantaneous value of product gas volumetric flow rate, $\bar{q}_{\mathrm{V,out,l}}$ is given by equation (E.3.2e), $q^{\mathrm{i}}_{\mathrm{m,l}}$ is the instantaneous value of mass flow rate of fluid i, $\bar{q}^{\mathrm{i}}_{\mathrm{m}}$ is given by equation (E.3.2g), $q^{\mathrm{j}}_{\mathrm{n,l}}$ is the instantaneous value of molar flow rate of fluid j, $\bar{q}^{\mathrm{j}}_{\mathrm{n}}$ is given by equation (E.3.2h), $p^{\mathrm{i}}_{\mathrm{l}}$ is the instantaneous value of pressure of fluid i, $\bar{p}^{\mathrm{i}}$ is given by average value of pressure of fluid i, $T^{\mathrm{i}}_{\mathrm{l}}$ is the instantaneous value of temperature of fluid i, $\bar{T}^{\mathrm{i}}$ is given by average value of temperature of fluid i, $p^{\mathrm{j}}_{\mathrm{l}}$ is the instantaneous value of pressure of fluid j, $\bar{p}^{\mathrm{j}}$ is given

by average value of pressure of fluid j, $T_{\mathrm{l}}^{\mathrm{j}}$ is the instantaneous value of temperature of fluid j, and $\bar{T}^{\mathrm{j}}$ is given by average value of temperature of fluid j.

The relative standard uncertainties of stack temperature ($u_{\mathrm{r}}\left(T_{\mathrm{stack}}\right)$), inlet volumetric flow rate ($u_{\mathrm{r}}\left(q_{\mathrm{V,in}}\right)$), inlet molar flow rate of hydrogen ($u_{\mathrm{r}}\left(q_{\mathrm{n,H_2,in}}\right)$), outlet molar concentration of hydrogen ($u_{\mathrm{r}}\left(x_{\mathrm{n,H_2,out}}\right)$), product gas volumetric flow rate ($u_{\mathrm{r}}\left(q_{\mathrm{V,out}}\right)$), mass flow rate of fluid i ($u_{\mathrm{r}}\left(q_{\mathrm{m}}^{\mathrm{i}}\right)$), difference between temperature of fluid i and standard ambient temperature ($u_{\mathrm{r}}\left(\Delta T^{\mathrm{i}}\right)$), molar flow rate of fluid j ($u_{\mathrm{r}}\left(q_{\mathrm{n}}^{\mathrm{j}}\right)$), pressure of fluid i ($u_{\mathrm{r}}\left(p^{\mathrm{i}}\right)$), temperature of fluid i ($u_{\mathrm{r}}\left(T^{\mathrm{i}}\right)$), pressure of fluid j ($u_{\mathrm{r}}\left(p^{\mathrm{j}}\right)$), and temperature of fluid j ($u_{\mathrm{r}}\left(T^{\mathrm{j}}\right)$) are calculated as follows:

$$u_{\mathrm{r}}\left(T_{\mathrm{stack}}\right) = \frac{\sqrt{s^2\left(T_{\mathrm{stack}}\right)\ (\mathrm{K})^2}}{\bar{T}_{\mathrm{stack}}\ (\mathrm{K})}, \tag{E.4.2a}$$

$$u_{\mathrm{r}}\left(q_{\mathrm{V,in}}\right) = \frac{\sqrt{s^2\left(q_{\mathrm{V,in}}\right)\ (\mathrm{m^3/s})^2}}{\bar{q}_{\mathrm{V,in}}\ (\mathrm{m^3/s})}, \tag{E.4.2b}$$

$$u_{\mathrm{r}}\left(q_{\mathrm{n,H_2,in}}\right) = \frac{\sqrt{s^2\left(q_{\mathrm{n,H_2,in}}\right)\ (\mathrm{mol/s})^2}}{\bar{q}_{\mathrm{n,H_2,in}}\ (\mathrm{mol/s})}, \tag{E.4.2c}$$

$$u_{\mathrm{r}}\left(x_{\mathrm{n,H_2,out}}\right) = \frac{\sqrt{s^2\left(x_{\mathrm{n,H_2,out}}\right)\ (\mathrm{mol/mol})^2}}{\bar{x}_{\mathrm{n,H_2,out}}\ (\mathrm{mol/mol})}, \tag{E.4.2d}$$

$$u_{\mathrm{r}}\left(q_{\mathrm{V,out}}\right) = \frac{\sqrt{s^2\left(q_{\mathrm{V,out}}\right)\ (\mathrm{m^3/s})^2}}{\bar{q}_{\mathrm{V,out,l}}\ (\mathrm{m^3/s})}, \tag{E.4.2e}$$

$$u_{\mathrm{r}}\left(q_{\mathrm{m}}^{\mathrm{i}}\right) = \frac{\sqrt{s^2\left(q_{\mathrm{m}}^{\mathrm{i}}\right)\ (\mathrm{kg/s})^2}}{\bar{q}_{\mathrm{m}}^{\mathrm{i}}\ (\mathrm{kg/s})}, \tag{E.4.2f}$$

$$u_{\mathrm{r}}\left(\Delta T^{\mathrm{i}}\right) = \frac{\sqrt{s^2\left(T^{\mathrm{i}}\right)\ (\mathrm{K})^2}}{\bar{T}^{\mathrm{i}}\ (\mathrm{K}) - T^0\ (\mathrm{K})}, \tag{E.4.2g}$$

$$u_{\mathrm{r}}\left(q_{\mathrm{n}}^{\mathrm{j}}\right) = \frac{\sqrt{s^2\left(q_{\mathrm{n}}^{\mathrm{j}}\right)\ (\mathrm{mol/s})^2}}{\bar{q}_{\mathrm{n}}^{\mathrm{j}}\ (\mathrm{mol/s})}, \tag{E.4.2h}$$

$$u_{\mathrm{r}}\left(p^{\mathrm{i}}\right) = \frac{\sqrt{s^2\left(p^{\mathrm{i}}\right)\ (\mathrm{kPa})^2}}{\bar{p}^{\mathrm{i}}\ (\mathrm{kPa})}, \tag{E.4.2i}$$

$$u_{\mathrm{r}}\left(T^{\mathrm{i}}\right) = \frac{\sqrt{s^2\left(T^{\mathrm{i}}\right)\ (\mathrm{K})^2}}{\bar{T}^{\mathrm{i}}\ (\mathrm{K})}, \tag{E.4.2j}$$

$$u_{\mathrm{r}}\left(p^{\mathrm{j}}\right) = \frac{\sqrt{s^2\left(p^{\mathrm{j}}\right)\ (\mathrm{kPa})^2}}{\bar{p}^{\mathrm{j}}\ (\mathrm{kPa})}, \tag{E.4.2k}$$

$$u_{\mathrm{r}}\left(T^{\mathrm{j}}\right) = \frac{\sqrt{s^2\left(T^{\mathrm{j}}\right)\ (\mathrm{K})^2}}{\bar{T}^{\mathrm{j}}\ (\mathrm{K})}, \tag{E.4.2l}$$

respectively; $s^2\left(T_{\mathrm{stack}}\right)$ is given by equation (E.4.1a), $\bar{T}_{\mathrm{stack}}$ is given by equation (E.3.2a), $s^2\left(q_{\mathrm{V,in}}\right)$ is given by equation (E.4.1b), $\bar{q}_{\mathrm{V,in}}$ is given by equation (E.3.2b), $s^2\left(q_{\mathrm{n,H_2,in}}\right)$ is given by equation (E.4.1c), $\bar{q}_{\mathrm{n,H_2,in}}$ is given by equation (E.3.2c), $s^2\left(x_{\mathrm{n,H_2,out}}\right)$ is given by equation (E.4.1d), $\bar{x}_{\mathrm{n,H_2,out}}$ is given by equation (E.3.2d), $s^2\left(q_{\mathrm{V,out}}\right)$ is given by equation (E.4.1e), $\bar{q}_{\mathrm{V,out,l}}$ is given by equation (E.3.2e), $s^2\left(q_{\mathrm{m}}^{\mathrm{i}}\right)$ is given by equation (E.4.1f), $\bar{q}_{\mathrm{m}}^{\mathrm{i}}$ is given by equation (E.3.2g), $s^2\left(T^{\mathrm{i}}\right)$ is given by equation (E.4.1i), $\bar{T}^{\mathrm{i}}$ is given by equation (E.3.2j), $s^2\left(q_{\mathrm{n}}^{\mathrm{j}}\right)$ is given by equation (E.4.1g), $\bar{q}_{\mathrm{n}}^{\mathrm{j}}$ is given by equation (E.3.2h), $s^2\left(p^{\mathrm{i}}\right)$ is given by equation (E.4.1h), $\bar{p}^{\mathrm{i}}$ is given by equation (E.3.2i), $s^2\left(T^{\mathrm{i}}\right)$ is given by equation (E.4.1i), $\bar{T}^{\mathrm{i}}$ is given by equation (E.3.2j), $s^2\left(p^{\mathrm{j}}\right)$ is given by equation (E.4.1j), $\bar{p}^{\mathrm{j}}$ is given by equation (E.3.2k), $s^2\left(T^{\mathrm{j}}\right)$ is given by equation (E.4.1k), and $\bar{T}^{\mathrm{j}}$ is given by equation (E.3.2l).

The standard variances of DC voltage ($s^2\left(U_{\mathrm{dc}}\right)$), direct current ($s^2\left(I_{\mathrm{dc}}\right)$), current density ($s^2\left(J\right)$), input power of hydrogen based on HHV ($s^2\left(P_{\mathrm{H_2,in}}^{\mathrm{HHV}}\right)$), input power of hydrogen based on HHV ($s^2\left(P_{\mathrm{H_2,in}}^{\mathrm{HHV}}\right)$), output power of hydrogen based on LHV ($s^2\left(P_{\mathrm{H_2,out}}^{\mathrm{LHV}}\right)$), and output power of hydrogen based on LHV ($s^2\left(P_{\mathrm{H_2,out}}^{\mathrm{LHV}}\right)$) are calculated as follows:

$$s^2\left(U_{\mathrm{dc}}\right)\ (\mathrm{V})^2 = \frac{1}{L-1}\sum_{\mathrm{l}=1}^{L}\left(U_{\mathrm{dc,l}}\ (\mathrm{V}) - \bar{U}_{\mathrm{dc}}\ (\mathrm{V})\right)^2, \tag{E.4.3a}$$

$$s^2\left(I_{\mathrm{dc}}\right)\ (\mathrm{A})^2 = \frac{1}{L-1}\sum_{\mathrm{l}=1}^{L}\left(I_{\mathrm{dc,l}}\ (\mathrm{A}) - \bar{I}_{\mathrm{dc}}\ (\mathrm{A})\right)^2, \tag{E.4.3b}$$

$$s^2\left(J\right)\left(\mathrm{A/cm^2}\right)^2 = \frac{1}{L-1}\sum_{\mathrm{l}=1}^{L}\left(J_{\mathrm{l}}\left(\mathrm{A/cm^2}\right)-\bar{J}\left(\mathrm{A/cm^2}\right)\right)^2, \tag{E.4.3c}$$

$$s^2\left(P_{\mathrm{H_2,in}}^{\mathrm{HHV}}\right)\left(\mathrm{kW}\right)^2 = \frac{1}{L-1}\sum_{\mathrm{l}=1}^{L}\left(P_{\mathrm{H_2,in,l}}^{\mathrm{HHV}}\left(\mathrm{kW}\right)-\bar{P}_{\mathrm{H_2,in}}^{\mathrm{HHV}}\left(\mathrm{kW}\right)\right)^2, \tag{E.4.3d}$$

$$s^2\left(P_{\mathrm{H_2,in}}^{\mathrm{LHV}}\right)\left(\mathrm{kW}\right)^2 = \frac{1}{L-1}\sum_{\mathrm{l}=1}^{L}\left(P_{\mathrm{H_2,in,l}}^{\mathrm{LHV}}\left(\mathrm{kW}\right)-\bar{P}_{\mathrm{H_2,in}}^{\mathrm{LHV}}\left(\mathrm{kW}\right)\right)^2, \tag{E.4.3e}$$

$$s^2\left(P_{\mathrm{H_2,out}}^{\mathrm{HHV}}\right)\left(\mathrm{kW}\right)^2 = \frac{1}{L-1}\sum_{\mathrm{l}=1}^{L}\left(P_{\mathrm{H_2,out,l}}^{\mathrm{HHV}}\left(\mathrm{kW}\right)-\bar{P}_{\mathrm{H_2,out}}^{\mathrm{HHV}}\left(\mathrm{kW}\right)\right)^2 \quad \text{and} \tag{E.4.3f}$$

$$s^2\left(P_{\mathrm{H_2,out}}^{\mathrm{LHV}}\right)\left(\mathrm{kW}\right)^2 = \frac{1}{L-1}\sum_{\mathrm{l}=1}^{L}\left(P_{\mathrm{H_2,out,l}}^{\mathrm{LHV}}\left(\mathrm{kW}\right)-\bar{P}_{\mathrm{H_2,out}}^{\mathrm{LHV}}\left(\mathrm{kW}\right)\right)^2, \tag{E.4.3g}$$

respectively; $U_{\mathrm{dc,l}}$ is the instantaneous value of DC voltage, $\bar{U}_{\mathrm{dc}}$ is given by equation (E.3.3c), $I_{\mathrm{dc,l}}$ is the instantaneous value of direct current, $\bar{I}_{\mathrm{dc}}$ is given by equation (E.3.3a), J_{l} is given by equation (E.2.2a), $\bar{J}$ is given by equation (E.3.3b), $P_{\mathrm{H_2,in,l}}^{\mathrm{HHV}}$ is given by equation (E.2.2d), $\bar{P}_{\mathrm{H_2,in}}^{\mathrm{HHV}}$ is given by equation (E.3.3i), $P_{\mathrm{H_2,in,l}}^{\mathrm{LHV}}$ is given by equation (E.2.2e), $\bar{P}_{\mathrm{H_2,in}}^{\mathrm{LHV}}$ is given by equation (E.3.3j), $P_{\mathrm{H_2,out,l}}^{\mathrm{HHV}}$ is given by equation (E.2.2i), $\bar{P}_{\mathrm{H_2,out}}^{\mathrm{HHV}}$ is given by equation (E.3.3k), $P_{\mathrm{H_2,out,l}}^{\mathrm{LHV}}$ is given by equation (E.2.2j), and $\bar{P}_{\mathrm{H_2,out}}^{\mathrm{LHV}}$ is given by equation (E.3.3l).

The relative standard uncertainties of DC voltage ($u_{\mathrm{r}}\left(U_{\mathrm{dc}}\right)$), direct current ($u_{\mathrm{r}}\left(I_{\mathrm{dc}}\right)$), current density ($u_{\mathrm{r}}\left(J\right)$), input power of hydrogen based on HHV ($u_{\mathrm{r}}\left(P_{\mathrm{H_2,in}}^{\mathrm{HHV}}\right)$), input power of hydrogen based on LHV ($u_{\mathrm{r}}\left(P_{\mathrm{H_2,in}}^{\mathrm{LHV}}\right)$), output power of hydrogen based on HHV ($u_{\mathrm{r}}\left(P_{\mathrm{H_2,out}}^{\mathrm{HHV}}\right)$), and output power of hydrogen based on LHV ($u_{\mathrm{r}}\left(P_{\mathrm{H_2,out}}^{\mathrm{LHV}}\right)$) are calculated as follows:

$$u_{\mathrm{r}}\left(U_{\mathrm{dc}}\right) = \frac{\sqrt{s^2\left(U_{\mathrm{dc}}\right)\left(\mathrm{V}\right)^2}}{\bar{U}_{\mathrm{dc}}\left(\mathrm{V}\right)}, \tag{E.4.4a}$$

$$u_{\mathrm{r}}\left(I_{\mathrm{dc}}\right) = \frac{\sqrt{s^2\left(I_{\mathrm{dc}}\right)\left(\mathrm{A}\right)^2}}{\bar{I}_{\mathrm{dc}}\left(\mathrm{A}\right)}, \tag{E.4.4b}$$

$$u_{\mathrm{r}}\left(J\right) = \frac{\sqrt{s^2\left(J\right)\left(\mathrm{A/cm^2}\right)^2}}{\bar{J}\left(\mathrm{A/cm^2}\right)}, \tag{E.4.4c}$$

$$u_{\mathrm{r}}\left(P_{\mathrm{H_2,in}}^{\mathrm{HHV}}\right) = \frac{\sqrt{s^2\left(P_{\mathrm{H_2,in}}^{\mathrm{HHV}}\right)\left(\mathrm{kW}\right)^2}}{\bar{P}_{\mathrm{H_2,in}}^{\mathrm{HHV}}\left(\mathrm{kW}\right)}, \tag{E.4.4d}$$

$$u_{\mathrm{r}}\left(P_{\mathrm{H_2,in}}^{\mathrm{LHV}}\right) = \frac{\sqrt{s^2\left(P_{\mathrm{H_2,in}}^{\mathrm{LHV}}\right)\left(\mathrm{kW}\right)^2}}{\bar{P}_{\mathrm{H_2,in}}^{\mathrm{LHV}}\left(\mathrm{kW}\right)}, \tag{E.4.4e}$$

$$u_{\mathrm{r}}\left(P_{\mathrm{H_2,out}}^{\mathrm{HHV}}\right) = \frac{\sqrt{s^2\left(P_{\mathrm{H_2,out}}^{\mathrm{HHV}}\right)\left(\mathrm{kW}\right)^2}}{\bar{P}_{\mathrm{H_2,out}}^{\mathrm{HHV}}\left(\mathrm{kW}\right)} \quad \text{and} \tag{E.4.4f}$$

$$u_{\mathrm{r}}\left(P_{\mathrm{H_2,out}}^{\mathrm{LHV}}\right) = \frac{\sqrt{s^2\left(P_{\mathrm{H_2,out}}^{\mathrm{LHV}}\right)\left(\mathrm{kW}\right)^2}}{\bar{P}_{\mathrm{H_2,out}}^{\mathrm{LHV}}\left(\mathrm{kW}\right)}, \tag{E.4.4g}$$

respectively; $s^2\left(U_{\mathrm{dc}}\right)$ is given by equation (E.4.3a), $\bar{U}_{\mathrm{dc}}$ is given by equation (E.3.3c), $s^2\left(I_{\mathrm{dc}}\right)$ is given by equation (E.4.3b), $\bar{I}_{\mathrm{dc}}$ is given by equation (E.3.3a), $s^2\left(J\right)$ is given by equation (E.4.3c), $\bar{J}$ is given by equation (E.3.3b), $s^2\left(P_{\mathrm{H_2,in}}^{\mathrm{HHV}}\right)$ is given by equation (E.4.3d), $\bar{P}_{\mathrm{H_2,in}}^{\mathrm{HHV}}$ is given by equation (E.3.3i), $s^2\left(P_{\mathrm{H_2,in}}^{\mathrm{LHV}}\right)$ is given by equation (E.4.3e), $\bar{P}_{\mathrm{H_2,in}}^{\mathrm{LHV}}$ is given by equation (E.3.3j), $s^2\left(P_{\mathrm{H_2,out}}^{\mathrm{HHV}}\right)$ is given by equation (E.4.3f), $\bar{P}_{\mathrm{H_2,out}}^{\mathrm{HHV}}$ is given by equation (E.3.3k), $s^2\left(P_{\mathrm{H_2,out}}^{\mathrm{LHV}}\right)$ is given by equation (E.4.3g), and $\bar{P}_{\mathrm{H_2,out}}^{\mathrm{LHV}}$ is given by equation (E.3.3l).

The combined standard uncertainties of DC power ($u_{\mathrm{c}}\left(P_{\mathrm{el,dc}}\right)$) and electric power density ($u_{\mathrm{c}}\left(P_{\mathrm{el,d}}\right)$) are calculated as follows:

$$u_{\mathrm{c}}^2\left(P_{\mathrm{el,dc}}\right)\left(\mathrm{kW}\right)^2 = \left(\tilde{P}_{\mathrm{el,dc}}\left(\mathrm{kW}\right)\right)^2\cdot\left(u_{\mathrm{r}}^2\left(U_{\mathrm{dc}}\right)+u_{\mathrm{r}}^2\left(I_{\mathrm{dc}}\right)\right) \quad \text{and} \tag{E.4.5a}$$

$$u_{\mathrm{c}}^2\left(P_{\mathrm{el,d}}\right)\left(\mathrm{W/cm^2}\right)^2 = \left(\tilde{P}_{\mathrm{el,d}}\left(\mathrm{W/cm^2}\right)\right)^2\cdot\left(u_{\mathrm{r}}^2\left(U_{\mathrm{dc}}\right)+u_{\mathrm{r}}^2\left(J\right)\right), \tag{E.4.5b}$$

respectively; $\tilde{P}_{\mathrm{el,dc}}$ is given by equation (E.3.4a), $u_{\mathrm{r}}\left(U_{\mathrm{dc}}\right)$ is given by equation (E.4.4a), $u_{\mathrm{r}}\left(I_{\mathrm{dc}}\right)$ is given by equation (E.4.4b), $\tilde{P}_{\mathrm{el,d}}$ is given by equation (E.3.4b), and $u_{\mathrm{r}}\left(J\right)$ is given by equation (E.4.4c).

The relative standard uncertainties of relative standard uncertainty of DC power ($u_{\mathrm{r}}\left(P_{\mathrm{el,dc}}\right)$) and electric

power density ($u_{\mathrm{r}}\left(P_{\mathrm{el,d}}\right)$) are calculated as follows:

$$u_{\mathrm{r}}\left(P_{\mathrm{el,dc}}\right) = \frac{\sqrt{u_{\mathrm{c}}^2\left(P_{\mathrm{el,dc}}\right)\,(\mathrm{kW})^2}}{\bar{P}_{\mathrm{el,dc}}\,(\mathrm{kW})} = \frac{\tilde{P}_{\mathrm{el,dc}}\,(\mathrm{kW})}{\bar{P}_{\mathrm{el,dc}}\,(\mathrm{kW})} \cdot \sqrt{u_{\mathrm{r}}^2\left(U_{\mathrm{dc}}\right) + u_{\mathrm{r}}^2\left(I_{\mathrm{dc}}\right)} \text{ and} \tag{E.4.6a}$$

$$u_{\mathrm{r}}\left(P_{\mathrm{el,d}}\right) = \frac{\sqrt{u_{\mathrm{c}}^2\left(P_{\mathrm{el,d}}\right)\,(\mathrm{W/cm^2})^2}}{\bar{P}_{\mathrm{el,d}}\,(\mathrm{W/cm^2})} = \frac{\tilde{P}_{\mathrm{el,d}}\,(\mathrm{W/cm^2})}{\bar{P}_{\mathrm{el,d}}\,(\mathrm{W/cm^2})} \cdot \sqrt{u_{\mathrm{r}}^2\left(U_{\mathrm{dc}}\right) + u_{\mathrm{r}}^2\left(J\right)}, \tag{E.4.6b}$$

respectively; $u_{\mathrm{c}}^2\left(P_{\mathrm{el,dc}}\right)$ is given by equation (E.4.5a), $\bar{P}_{\mathrm{el,dc}}$ is given by equation (E.3.3d), $\tilde{P}_{\mathrm{el,dc}}$ is given by equation (E.3.4a), $\bar{U}_{\mathrm{dc}}$ is given by equation (E.3.3c), $\bar{I}_{\mathrm{dc}}$ is given by equation (E.3.3a), $u_{\mathrm{c}}^2\left(P_{\mathrm{el,d}}\right)$ is given by equation (E.4.5b), $\bar{P}_{\mathrm{el,d}}$ is given by equation (E.3.3e), $\tilde{P}_{\mathrm{el,d}}$ is given by equation (E.3.4b), and $\bar{J}$ is given by equation (E.3.3b).

The combined standard variances of square of combined standard uncertainty of fuel cell electrical efficiency based on HHV ($u_{\mathrm{c}}^2\left(\eta_{\mathrm{el,FC}}^{\mathrm{HHV}}\right)$), fuel cell electric efficiency based on LHV ($u_{\mathrm{c}}^2\left(\eta_{\mathrm{el,FC}}^{\mathrm{LHV}}\right)$), fuel cell thermal efficiency based on HHV ($u_{\mathrm{c}}^2\left(\eta_{\mathrm{th,FC}}^{\mathrm{HHV}}\right)$), fuel cell thermal efficiency based on LHV ($u_{\mathrm{c}}^2\left(\eta_{\mathrm{th,FC}}^{\mathrm{LHV}}\right)$), electrolyser energy efficiency based on HHV ($u_{\mathrm{c}}^2\left(\eta_{\mathrm{e,EL}}^{\mathrm{HHV}}\right)$), and electrolyser energy efficiency based on LHV ($u_{\mathrm{c}}^2\left(\eta_{\mathrm{e,EL}}^{\mathrm{LHV}}\right)$) are calculated as follows:

$$\begin{aligned} u_{\mathrm{c}}^2\left(\eta_{\mathrm{el,FC}}^{\mathrm{HHV}}\right)(\%)^2 = {} & \left(\bar{\eta}_{\mathrm{el,FC}}^{\mathrm{HHV}}\,(\%)\right)^2 \cdot \left[\left(\frac{\tilde{P}_{\mathrm{el,dc}}\,(\mathrm{kW})}{\bar{P}_{\mathrm{el,dc}}\,(\mathrm{kW})}\right)^2 \cdot \left[u_{\mathrm{r}}^2\left(U_{\mathrm{dc}}\right) + u_{\mathrm{r}}^2\left(I_{\mathrm{dc}}\right)\right] + \left(\bar{\eta}_{\mathrm{el,FC}}^{\mathrm{HHV}}\,(\%)\right)^2 \cdot \right. \\ & \left(\left(\frac{\tilde{P}_{\mathrm{H_2,in}}^{\mathrm{HHV}}\,(\mathrm{kW})}{\bar{P}_{\mathrm{el,dc}}\,(\mathrm{kW})}\right)^2 \cdot u_{\mathrm{r}}^2\left(q_{\mathrm{n,H_2,in}}\right) + \sum_{\mathrm{i}}\left(\frac{\tilde{P}_{\mathrm{th,in}}\,(\mathrm{kW})}{\bar{P}_{\mathrm{el,dc}}\,(\mathrm{kW})}\right)^2 \cdot \left[u_{\mathrm{r}}^2\left(q_{\mathrm{m}}^{\mathrm{i}}\right) + u_{\mathrm{r}}^2\left(\Delta T^{\mathrm{i}}\right)\right]\right. \\ & \left.\left. + \sum_{\mathrm{j}}\left(\frac{\tilde{P}_{\mathrm{p,in}}\,(\mathrm{kW})}{\bar{P}_{\mathrm{el,dc}}\,(\mathrm{kW})}\right)^2 \cdot \left[u_{\mathrm{r}}^2\left(q_{\mathrm{n}}^{\mathrm{j}}\right) + \left(\frac{\frac{\gamma^{\mathrm{j}}-1}{\gamma^{\mathrm{j}}}}{\frac{\bar{p}^{\mathrm{j}}}{p^0} - \left(\frac{\bar{p}^{\mathrm{j}}}{p^0}\right)^{\frac{1}{\gamma^{\mathrm{j}}}}}\right)^2 u_{\mathrm{r}}^2\left(p^{\mathrm{j}}\right)\right]\right)\right], \end{aligned} \tag{E.4.7a}$$

$$\begin{aligned} u_{\mathrm{c}}^2\left(\eta_{\mathrm{el,FC}}^{\mathrm{LHV}}\right)(\%)^2 = {} & \left(\bar{\eta}_{\mathrm{el,FC}}^{\mathrm{LHV}}\,(\%)\right)^2 \cdot \left[\left(\frac{\tilde{P}_{\mathrm{el,dc}}\,(\mathrm{kW})}{\bar{P}_{\mathrm{el,dc}}\,(\mathrm{kW})}\right)^2 \cdot \left[u_{\mathrm{r}}^2\left(U_{\mathrm{dc}}\right) + u_{\mathrm{r}}^2\left(I_{\mathrm{dc}}\right)\right] + \left(\bar{\eta}_{\mathrm{el,FC}}^{\mathrm{LHV}}\,(\%)\right)^2 \cdot \right. \\ & \left(\left(\frac{\tilde{P}_{\mathrm{H_2,in}}^{\mathrm{LHV}}\,(\mathrm{kW})}{\bar{P}_{\mathrm{el,dc}}\,(\mathrm{kW})}\right)^2 \cdot u_{\mathrm{r}}^2\left(q_{\mathrm{n,H_2,in}}\right) + \sum_{\mathrm{i}}\left(\frac{\tilde{P}_{\mathrm{th,in}}\,(\mathrm{kW})}{\bar{P}_{\mathrm{el,dc}}\,(\mathrm{kW})}\right)^2 \cdot \left[u_{\mathrm{r}}^2\left(q_{\mathrm{m}}^{\mathrm{i}}\right) + u_{\mathrm{r}}^2\left(\Delta T^{\mathrm{i}}\right)\right]\right. \\ & \left.\left. + \sum_{\mathrm{j}}\left(\frac{\tilde{P}_{\mathrm{p,in}}\,(\mathrm{kW})}{\bar{P}_{\mathrm{el,dc}}\,(\mathrm{kW})}\right)^2 \cdot \left[u_{\mathrm{r}}^2\left(q_{\mathrm{n}}^{\mathrm{j}}\right) + \left(\frac{\frac{\gamma^{\mathrm{j}}-1}{\gamma^{\mathrm{j}}}}{\frac{\bar{p}^{\mathrm{j}}}{p^0} - \left(\frac{\bar{p}^{\mathrm{j}}}{p^0}\right)^{\frac{1}{\gamma^{\mathrm{j}}}}}\right)^2 u_{\mathrm{r}}^2\left(p^{\mathrm{j}}\right)\right]\right)\right], \end{aligned} \tag{E.4.7b}$$

$$\begin{aligned} u_{\mathrm{c}}^2\left(\eta_{\mathrm{th,FC}}^{\mathrm{HHV}}\right)(\%)^2 = {} & \left(\bar{\eta}_{\mathrm{th,FC}}^{\mathrm{HHV}}\,(\%)\right)^2 \cdot \left[\left(\frac{\tilde{P}_{\mathrm{th,out}}\,(\mathrm{kW})}{\bar{P}_{\mathrm{th,out}}\,(\mathrm{kW})}\right)^2 \cdot \left[u_{\mathrm{r}}^2\left(q_{\mathrm{m}}^{\mathrm{i}}\right) + u_{\mathrm{r}}^2\left(\Delta T^{\mathrm{i}}\right)\right] + \left(\bar{\eta}_{\mathrm{el,FC}}^{\mathrm{HHV}}\,(\%)\right)^2 \cdot \right. \\ & \left(\left(\frac{\tilde{P}_{\mathrm{H_2,in}}^{\mathrm{HHV}}\,(\mathrm{kW})}{\bar{P}_{\mathrm{th,out}}\,(\mathrm{kW})}\right)^2 \cdot u_{\mathrm{r}}^2\left(q_{\mathrm{n,H_2,in}}\right) + \sum_{\mathrm{i}}\left(\frac{\tilde{P}_{\mathrm{th,in}}\,(\mathrm{kW})}{\bar{P}_{\mathrm{th,out}}\,(\mathrm{kW})}\right)^2 \cdot \left[u_{\mathrm{r}}^2\left(q_{\mathrm{m}}^{\mathrm{i}}\right) + u_{\mathrm{r}}^2\left(\Delta T^{\mathrm{i}}\right)\right]\right. \\ & \left.\left. + \sum_{\mathrm{j}}\left(\frac{\tilde{P}_{\mathrm{p,in}}\,(\mathrm{kW})}{\bar{P}_{\mathrm{th,out}}\,(\mathrm{kW})}\right)^2 \cdot \left[u_{\mathrm{r}}^2\left(q_{\mathrm{n}}^{\mathrm{j}}\right) + \left(\frac{\frac{\gamma^{\mathrm{j}}-1}{\gamma^{\mathrm{j}}}}{\frac{\bar{p}^{\mathrm{j}}}{p^0} - \left(\frac{\bar{p}^{\mathrm{j}}}{p^0}\right)^{\frac{1}{\gamma^{\mathrm{j}}}}}\right)^2 u_{\mathrm{r}}^2\left(p^{\mathrm{j}}\right)\right]\right)\right], \end{aligned} \tag{E.4.7c}$$

$$\begin{aligned} u_{\mathrm{c}}^2\left(\eta_{\mathrm{th,FC}}^{\mathrm{LHV}}\right)(\%)^2 = {} & \left(\bar{\eta}_{\mathrm{th,FC}}^{\mathrm{LHV}}\,(\%)\right)^2 \cdot \left[\left(\frac{\tilde{P}_{\mathrm{th,out}}\,(\mathrm{kW})}{\bar{P}_{\mathrm{th,out}}\,(\mathrm{kW})}\right)^2 \cdot \left[u_{\mathrm{r}}^2\left(q_{\mathrm{m}}^{\mathrm{i}}\right) + u_{\mathrm{r}}^2\left(\Delta T^{\mathrm{i}}\right)\right] + \left(\bar{\eta}_{\mathrm{el,FC}}^{\mathrm{LHV}}\,(\%)\right)^2 \cdot \right. \\ & \left(\left(\frac{\tilde{P}_{\mathrm{H_2,in}}^{\mathrm{LHV}}\,(\mathrm{kW})}{\bar{P}_{\mathrm{th,out}}\,(\mathrm{kW})}\right)^2 \cdot u_{\mathrm{r}}^2\left(q_{\mathrm{n,H_2,in}}\right) + \sum_{\mathrm{i}}\left(\frac{\tilde{P}_{\mathrm{th,in}}\,(\mathrm{kW})}{\bar{P}_{\mathrm{th,out}}\,(\mathrm{kW})}\right)^2 \cdot \left[u_{\mathrm{r}}^2\left(q_{\mathrm{m}}^{\mathrm{i}}\right) + u_{\mathrm{r}}^2\left(\Delta T^{\mathrm{i}}\right)\right]\right. \\ & \left.\left. + \sum_{\mathrm{j}}\left(\frac{\tilde{P}_{\mathrm{p,in}}\,(\mathrm{kW})}{\bar{P}_{\mathrm{th,out}}\,(\mathrm{kW})}\right)^2 \cdot \left[u_{\mathrm{r}}^2\left(q_{\mathrm{n}}^{\mathrm{j}}\right) + \left(\frac{\frac{\gamma^{\mathrm{j}}-1}{\gamma^{\mathrm{j}}}}{\frac{\bar{p}^{\mathrm{j}}}{p^0} - \left(\frac{\bar{p}^{\mathrm{j}}}{p^0}\right)^{\frac{1}{\gamma^{\mathrm{j}}}}}\right)^2 u_{\mathrm{r}}^2\left(p^{\mathrm{j}}\right)\right]\right)\right], \end{aligned} \tag{E.4.7d}$$

$$u_{\mathrm{c}}^2\left(\eta_{\mathrm{e,EL}}^{\mathrm{HHV}}\right)(\%)^2 = \left(\bar{\eta}_{\mathrm{e,EL}}^{\mathrm{HHV}}\,(\%)\right)^2 \cdot \left[\left(\frac{\tilde{P}_{\mathrm{H_2,out}}^{\mathrm{HHV}}\,(\mathrm{kW})}{\bar{P}_{\mathrm{H_2,out}}^{\mathrm{HHV}}\,(\mathrm{kW})}\right)^2 \cdot \left[u_{\mathrm{r}}^2\left(x_{\mathrm{n,H_2,out}}\right) + u_{\mathrm{r}}^2\left(q_{\mathrm{V,out}}\right)\right] + \left(\bar{\eta}_{\mathrm{e,EL}}^{\mathrm{HHV}}\,(\%)\right)^2 \cdot \right.$$

$$\left(\left(\frac{\tilde{P}_{\text{el,dc}}\ (\text{kW})}{\bar{P}^{\text{HHV}}_{\text{H}_2\text{,out}}\ (\text{kW})}\right)^2 \cdot \left[u_{\text{r}}^2\left(U_{\text{dc}}\right) + u_{\text{r}}^2\left(I_{\text{dc}}\right)\right] + \sum_{\text{i}}\left(\frac{\tilde{P}_{\text{th,in}}\ (\text{kW})}{\bar{P}^{\text{HHV}}_{\text{H}_2\text{,out}}\ (\text{kW})}\right)^2 \cdot \left[u_{\text{r}}^2\left(q^{\text{i}}_{\text{m}}\right) + u_{\text{r}}^2\left(\Delta T^{\text{i}}\right)\right] + \sum_{\text{j}}\left(\frac{\tilde{P}_{\text{p,in}}\ (\text{kW})}{\bar{P}^{\text{HHV}}_{\text{H}_2\text{,out}}\ (\text{kW})}\right)^2 \cdot \left[u_{\text{r}}^2\left(q^{\text{j}}_{\text{n}}\right) + \left(\frac{\frac{\gamma^{\text{j}}-1}{\gamma^{\text{j}}}}{\frac{\bar{p}^{\text{j}}}{p^0} - \left(\frac{\bar{p}^{\text{j}}}{p^0}\right)^{\frac{1}{\gamma^{\text{j}}}}}\right)^2 u_{\text{r}}^2\left(p^{\text{j}}\right)\right]\right] \quad \text{and} \tag{E.4.7e}$$

$$u_{\text{c}}^2\left(\eta^{\text{LHV}}_{\text{e,EL}}\right)(\%)^2 = \left(\bar{\eta}^{\text{LHV}}_{\text{e,EL}}\ (\%)\right)^2 \cdot \left[\left(\frac{\tilde{P}^{\text{LHV}}_{\text{H}_2\text{,out}}\ (\text{kW})}{\bar{P}^{\text{LHV}}_{\text{H}_2\text{,out}}\ (\text{kW})}\right)^2 \cdot \left[u_{\text{r}}^2\left(x_{\text{n,H}_2\text{,out}}\right) + u_{\text{r}}^2\left(q_{\text{V,out}}\right)\right] + \left(\bar{\eta}^{\text{LHV}}_{\text{e,EL}}\ (\%)\right)^2 \cdot \left(\left(\frac{\tilde{P}_{\text{el,dc}}\ (\text{kW})}{\bar{P}^{\text{LHV}}_{\text{H}_2\text{,out}}\ (\text{kW})}\right)^2 \cdot \left[u_{\text{r}}^2\left(U_{\text{dc}}\right) + u_{\text{r}}^2\left(I_{\text{dc}}\right)\right] + \sum_{\text{i}}\left(\frac{\tilde{P}_{\text{th,in}}\ (\text{kW})}{\bar{P}^{\text{LHV}}_{\text{H}_2\text{,out}}\ (\text{kW})}\right)^2 \cdot \left[u_{\text{r}}^2\left(q^{\text{i}}_{\text{m}}\right) + u_{\text{r}}^2\left(\Delta T^{\text{i}}\right)\right] + \sum_{\text{j}}\left(\frac{\tilde{P}_{\text{p,in}}\ (\text{kW})}{\bar{P}^{\text{LHV}}_{\text{H}_2\text{,out}}\ (\text{kW})}\right)^2 \cdot \left[u_{\text{r}}^2\left(q^{\text{j}}_{\text{n}}\right) + \left(\frac{\frac{\gamma^{\text{j}}-1}{\gamma^{\text{j}}}}{\frac{\bar{p}^{\text{j}}}{p^0} - \left(\frac{\bar{p}^{\text{j}}}{p^0}\right)^{\frac{1}{\gamma^{\text{j}}}}}\right)^2 u_{\text{r}}^2\left(p^{\text{j}}\right)\right]\right], \tag{E.4.7f}$$

respectively; $\bar{\eta}^{\text{HHV}}_{\text{el,FC}}$ is given by equation (E.3.5a), $\tilde{P}_{\text{el,dc}}$ is given by equation (E.3.4a), $\bar{P}_{\text{el,dc}}$ is given by equation (E.3.3d), $u_{\text{r}}\left(U_{\text{dc}}\right)$ is given by equation (E.4.4a), $u_{\text{r}}\left(I_{\text{dc}}\right)$ is given by equation (E.4.4b), $\tilde{P}^{\text{HHV}}_{\text{H}_2\text{,in}}$ is given by equation (E.3.4f), $u_{\text{r}}\left(q_{\text{n,H}_2\text{,in}}\right)$ is given by equation (E.4.2c), $\tilde{P}_{\text{th,in}}$ is given by equation (E.3.4c), $u_{\text{r}}\left(q^{\text{i}}_{\text{m}}\right)$ is given by equation (E.4.2f), $u_{\text{r}}\left(\Delta T^{\text{i}}\right)$ is given by equation (E.4.2g), $\tilde{P}_{\text{p,in}}$ is given by equation (E.3.4d), $u_{\text{r}}\left(q^{\text{j}}_{\text{n}}\right)$ is given by equation (E.4.2h), $\bar{p}^{\text{j}}$ is given by equation (E.3.2k), $u_{\text{r}}\left(p^{\text{j}}\right)$ is given by equation (E.4.2k), $\bar{\eta}^{\text{LHV}}_{\text{el,FC}}$ is given by equation (E.3.5b), $\tilde{P}^{\text{LHV}}_{\text{H}_2\text{,in}}$ is given by equation (E.3.4g), $\bar{\eta}^{\text{HHV}}_{\text{th,FC}}$ is given by equation (E.3.5c), $\tilde{P}_{\text{th,out}}$ is given by equation (E.3.4e), $\bar{\eta}^{\text{LHV}}_{\text{th,FC}}$ is given by equation (E.3.5d), $\bar{\eta}^{\text{HHV}}_{\text{e,EL}}$ is given by equation (E.3.5e), $\tilde{P}^{\text{HHV}}_{\text{H}_2\text{,out}}$ is given by equation (E.3.4h), $\bar{P}^{\text{HHV}}_{\text{H}_2\text{,out}}$ is given by equation (E.3.3k), $u_{\text{r}}\left(x_{\text{n,H}_2\text{,out}}\right)$ is given by equation (E.4.2d), $u_{\text{r}}\left(q_{\text{V,out}}\right)$ is given by equation (E.4.2e), $\bar{\eta}^{\text{LHV}}_{\text{e,EL}}$ is given by equation (E.3.5f), $\tilde{P}^{\text{LHV}}_{\text{H}_2\text{,out}}$ is given by equation (E.3.4i), and $\bar{P}^{\text{LHV}}_{\text{H}_2\text{,out}}$ is given by equation (E.3.3l).

The relative standard uncertainties of fuel cell electric efficiency based on HHV ($u_{\text{r}}\left(\eta^{\text{HHV}}_{\text{el,FC}}\right)$), fuel cell electric efficiency based on LHV ($u_{\text{r}}\left(\eta^{\text{LHV}}_{\text{el,FC}}\right)$), fuel cell thermal efficiency based on HHV ($u_{\text{r}}\left(\eta^{\text{HHV}}_{\text{th,FC}}\right)$), fuel cell thermal efficiency based on LHV ($u_{\text{r}}\left(\eta^{\text{LHV}}_{\text{th,FC}}\right)$), electrolyser energy efficiency based on HHV ($u_{\text{r}}\left(\eta^{\text{HHV}}_{\text{e,EL}}\right)$), and electrolyser energy efficiency based on LHV ($u_{\text{r}}\left(\eta^{\text{LHV}}_{\text{e,EL}}\right)$) are calculated as follows:

$$u_{\text{r}}\left(\eta^{\text{HHV}}_{\text{el,FC}}\right) = \frac{\sqrt{u_{\text{c}}^2\left(\eta^{\text{HHV}}_{\text{el,FC}}\right)(\%)^2}}{\bar{\eta}^{\text{HHV}}_{\text{el,FC}}\ (\%)}, \tag{E.4.8a}$$

$$u_{\text{r}}\left(\eta^{\text{LHV}}_{\text{el,FC}}\right) = \frac{\sqrt{u_{\text{c}}^2\left(\eta^{\text{LHV}}_{\text{el,FC}}\right)(\%)^2}}{\bar{\eta}^{\text{LHV}}_{\text{el,FC}}\ (\%)}, \tag{E.4.8b}$$

$$u_{\text{r}}\left(\eta^{\text{HHV}}_{\text{th,FC}}\right) = \frac{\sqrt{u_{\text{c}}^2\left(\eta^{\text{HHV}}_{\text{th,FC}}\right)(\%)^2}}{\bar{\eta}^{\text{HHV}}_{\text{th,FC}}\ (\%)}, \tag{E.4.8c}$$

$$u_{\text{r}}\left(\eta^{\text{LHV}}_{\text{th,FC}}\right) = \frac{\sqrt{u_{\text{c}}^2\left(\eta^{\text{LHV}}_{\text{th,FC}}\right)(\%)^2}}{\bar{\eta}^{\text{LHV}}_{\text{th,FC}}\ (\%)}, \tag{E.4.8d}$$

$$u_{\text{r}}\left(\eta^{\text{HHV}}_{\text{e,EL}}\right) = \frac{\sqrt{u_{\text{c}}^2\left(\eta^{\text{HHV}}_{\text{e,EL}}\right)(\%)^2}}{\bar{\eta}^{\text{HHV}}_{\text{e,EL}}\ (\%)} \quad \text{and} \tag{E.4.8e}$$

$$u_{\text{r}}\left(\eta^{\text{LHV}}_{\text{e,EL}}\right) = \frac{\sqrt{u_{\text{c}}^2\left(\eta^{\text{LHV}}_{\text{e,EL}}\right)(\%)^2}}{\bar{\eta}^{\text{LHV}}_{\text{e,EL}}\ (\%)}, \tag{E.4.8f}$$

respectively; $u_{\text{c}}^2\left(\eta^{\text{HHV}}_{\text{el,FC}}\right)$ is given by equation (E.4.7a), $\bar{\eta}^{\text{HHV}}_{\text{el,FC}}$ is given by equation (E.3.5a), $u_{\text{c}}^2\left(\eta^{\text{LHV}}_{\text{el,FC}}\right)$ is given by equation (E.4.7b), $\bar{\eta}^{\text{LHV}}_{\text{el,FC}}$ is given by equation (E.3.5b), $u_{\text{c}}^2\left(\eta^{\text{HHV}}_{\text{th,FC}}\right)$ is given by equation (E.4.7c), $\bar{\eta}^{\text{HHV}}_{\text{th,FC}}$ is given by equation (E.3.5c), $u_{\text{c}}^2\left(\eta^{\text{LHV}}_{\text{th,FC}}\right)$ is given by equation (E.4.7d), $\bar{\eta}^{\text{LHV}}_{\text{th,FC}}$ is given by equation (E.3.5d), $u_{\text{c}}^2\left(\eta^{\text{HHV}}_{\text{e,EL}}\right)$ is given by equation (E.4.7e), $\bar{\eta}^{\text{HHV}}_{\text{e,EL}}$ is given by equation (E.3.5e), $u_{\text{c}}^2\left(\eta^{\text{LHV}}_{\text{e,EL}}\right)$ is given by equation (E.4.7f), and $\bar{\eta}^{\text{LHV}}_{\text{e,EL}}$ is given

by equation (E.3.5f).

GETTING IN TOUCH WITH THE EU

In person

All over the European Union there are hundreds of Europe Direct centres. You can find the address of the centre nearest you online (european-union.europa.eu/contact-eu/meet-us_en).

On the phone or in writing

Europe Direct is a service that answers your questions about the European Union. You can contact this service:

— by freephone: 00 800 6 7 8 9 10 11 (certain operators may charge for these calls),

— at the following standard number: +32 22999696,

— via the following form: european-union.europa.eu/contact-eu/write-us_en.

FINDING INFORMATION ABOUT THE EU

Online

Information about the European Union in all the official languages of the EU is available on the Europa website (european-union.europa.eu).

EU publications

You can view or order EU publications at op.europa.eu/en/publications. Multiple copies of free publications can be obtained by contacting Europe Direct or your local documentation centre (european-union.europa.eu/contact-eu/meet-us_en).

EU law and related documents

For access to legal information from the EU, including all EU law since 1951 in all the official language versions, go to EUR-Lex (eur-lex.europa.eu).

Open data from the EU

The portal data.europa.eu provides access to open datasets from the EU institutions, bodies and agencies. These can be downloaded and reused for free, for both commercial and non-commercial purposes. The portal also provides access to a wealth of datasets from European countries.

Science for policy

The Joint Research Centre (JRC) provides independent, evidence-based knowledge and science, supporting EU policies to positively impact society

EU Science Hub
joint-research-centre.ec.europa.eu

Publications Office
of the European Union